CHARACTERIZING TREE SPECIES IN THE NORTHWEST TERRITORIES USING SPECTRAL MIXTURE ANALYSIS AND MULTI-TEMPORAL SATELLITE IMAGERY

Jurjen van der Sluijs
B.Sc., Brandon University, 2012

A Thesis
Submitted to the School of Graduate Studies
of the University of Lethbridge
in Partial Fulfilment of the
Requirements for the Degree

MASTER OF SCIENCE

Department of Geography

University of Lethbridge

LETHBRIDGE, ALBERTA, CANADA

CHARACTERIZING TREE SPECIES IN THE NORTHWEST TERRITORIES USING SPECTRAL MIXTURE ANALYSIS AND MULTI-TEMPORAL SATELLITE IMAGERY

JURJEN VAN DER SLUIJS

Approved:

* (Name)	(Signature)	(Rank)	(Highest Degree)	Date
* Supervisor				
* Committee Member				
* Committee Member				
* Committee Member				
* Chair, Thesis Examination Committee				

DEDICATION

I dedicate my thesis work to my parents, Peter and Elly van der Sluijs, whose words of encouragement and unquestioned support have helped me to make the most of the opportunities presented. Their sense of gratitude towards nature and ecological principles were instilled from a very young age, and I hope that this work reflects this. I thank you not only for your moral support, but also for continual interest in my work.

I also dedicate this work to my girlfriend Sarah, who has supported me throughout the process from one or two Provinces or Territories away. I thank you for your patience and understanding my long-term absence.

I hope that whatever merit derived from this thesis contributes to the welfare of all species and encourage further research and knowledge sharing that fosters an enlightened, sustainable human presence on Earth.

ABSTRACT

Natural resource management in northern boreal forests requires tree species identification for improved decision making. Satellite remote sensing provides a more cost-effective and time-efficient way to obtain this information in these large, remote, inaccessible areas. However, satellite signals are highly mixed due to increased tree shadows and visible understory vegetation in higher latitude, lower density open forests. Thus, methods used in southern forests are largely unsuitable. Therefore, spectral mixture analysis (SMA) was tested as it separates these signal components (trees, understory, shadow) at sub-pixel scales, allowing improved forest information. In this study, SMA was used to identify the dominant species near Fort Providence NWT using Landsat-5 Thematic Mapper imagery. An accuracy of 79 % was achieved for four species validated against 48 ground plots using multiple-date imagery acquired at different stages of the growing season. These positive results indicate SMA's capability to retrieve species information of highly mixed open stands.

ACKNOWLEDGEMENTS

I would like to thank Dr. Derek Peddle, my thesis supervisor. Derek encouraged me to pursue my graduate studies and provided me with an environment to make this work possible. Thanks to Derek I was able to work in an applied research setting with direct help and influence from a range of government stakeholders. My exposure to what Northern Canada has to offer could not have been realized without him, and I am very grateful to the opportunities of fieldwork and collaboration with project partners in Edmonton, Hay River, and Yellowknife. Figuratively, doors have opened because of this both career-wise and for further academic opportunities. Derek encouraged me to travel to academic and industry presentations to share research results, and become an Executive member of the Canadian Remote Sensing Society, which both have aided in an exciting academic experience.

I would also like to thank Dr. Ron Hall who provided essential ideas and guidance to establish the direction of my independent study and thesis, as well as an opportunity to spend 8 months at the Canadian Forest Service - Northern Forestry Centre in Edmonton. I would like to express my deepest gratitude for your patience in the teachings of boreal forest ecology and forest inventory methods, the countless hours reviewing drafts by e-mail, phone, or in person, and invaluable resources and knowledge provided during field work. Without your continual support and motivation this work would not have been possible. I would also like to thank my other thesis committee members, Dr. Karl Staenz and Dr. Nadia Rochdi, for their evaluations and suggestions along the way. Fieldwork was a key component to this research, whereby I am thankful for the forest inventory information acquired by the Canadian Forest Service and Government of the Northwest

Territories in 2005, which was supplied by Mr. Rob Skakun (Canadian Forest Service) along with QuickBird imagery and GIS datasets. In addition, I would like to thank Rob for his help with the collection of spectral field data in 2013.

I gratefully acknowledge financial support provided through a Natural Science and Engineering Research Council of Canada (NSERC) CREATE scholarship (Advanced Methods, Education and Training in Hyperspectral Science and Technology; AMETHYST) and additional funding and resources from the University of Lethbridge (Department of Geography, School of Graduate Studies), the Alberta Terrestrial Imaging Centre (ATIC), and Brandon University (John & Catherine Robbins Graduate Scholarship). This research was also supported by TECTERRA funding through their University Applied Research Funding Program.

A special thanks to Logan Pryor, Kyle Howard, Kevin Riddell, James Banting, and Peter Kennedy, for making my graduate program a very interesting time.

TABLE OF CONTENTS

LIST OF TABLES

LIST OF FIGURES

CHAPTER 1

Introduction

The world's boreal forests, which occupy large areas of the northern hemisphere, represent a major biogeoclimatic zone that regulates regional and global climates, cycles nutrients, and provide renewable resources, habitat, and recreational opportunities (Brandt, 2009). Despite the importance of this natural resource, boreal forests are under pressure from a variety of stressors, such as land-use conversions and climate change induced alterations to hydrological conditions as well as wildfire and insect disturbance patterns (Williamson et al., 2009; Natural Resources Canada, 2013). Current and future impacts of these stressors require accurate information on the spatial distribution, structure, and processes of forests for sustainable forest management. For example, government-based forest inventories produce detailed maps of species composition, defined as the relative proportion of tree species in a stand to the nearest 10 percent, that are important for forest resource reporting and the establishment of forest management plans (Gillis & Leckie, 1993; Leckie & Gillis, 1995).

1.1. Acquisition of Species Composition Information

Information about species composition can be difficult to collect on the ground due to site access challenges, budget limitations, and the large areas of forested land. Therefore, forest inventories are typically undertaken through the use of aerial photo-interpretation in combination with ground samples and have recently migrated to soft-copy digital stereo interpretation techniques (Power & Gillis, 2006). Despite these recent advancements, aerial photo-interpretation remains a technology whose limits are being challenged and is cost prohibitive over large, remote forests. A primary example of the

lack of spatial and temporal coverage of species composition information is in the Northwest Territories (NWT), Canada. Forests cover 33 million hectares in this territory (Government of Northwest Territories, 2011a), of which detailed forest inventories exist for less than 10 % of its forests (Hall et al., 2012). Yet in the last decade several territorial government policy initiatives such as the NWT Biomass Energy Strategy and Boreal Caribou Action Plan have identified a need for more detailed information regarding forest resources (Government of Northwest Territories, 2010b, 2010a). To alleviate information gaps, forest management agencies increasingly rely on spatial data of land cover derived through remote sensing due to its large area coverage (Franklin, 2001; Turner et al., 2003). While forest cover information exists for the NWT, these inventories characterize forested land to coniferous, deciduous, and mixed classes (Wulder et al., 2008), and therefore, a more specific characterization of tree species is desired.

1.2. Remote Sensing of Boreal Tree Species

Previous remote sensing approaches have been documented in the scientific literature to derive estimations of the spatial distribution of boreal tree species. This generally involves the discrete labeling of pixels that are based on the dominant or leading species within a stand (Franklin, 1994; Beaubien et al., 1999; Peddle et al., 2007), which is less detailed than the information acquired through aerial photo-interpretation. There is uncertainty in the degree to which the documented approaches can be integrated into current forest inventories, because the approach to determine the species composition of a stand (and therefore the leading species) differs among jurisdictions and in the literature. Resource management agencies may measure the species composition per percentage crown closure, basal area, stem density, or gross volume (Gillis & Leckie,

1993). The relative abundance estimations for each tree species present in a stand may not be the same among these metrics, and could influence which species is considered dominant. Differences in the definition used to estimate the leading species could therefore influence image classification results, yet in the remote sensing literature it is generally not determined whether an image is sensitive to how the leading species is characterized on the ground. It is therefore of particular interest to improve understanding of the sensitivity of satellite imagery to field-based descriptions of leading species.

It is important to note that the capabilities of the documented approaches are unknown for northern boreal forests due to the small number of studies in these regions (e.g., Gerylo et al., 2002; Franklin et al., 2003). Forest stands in northern boreal environments such as in the NWT vary widely in terms of their composition, structure, and spatial distribution, with a predominance of those with complex stand structures and open crown closures (Ecosystem Classification Group, 2007). The spectral response from these types of forests on 30-m Landsat Thematic Mapper (TM) images is mixed, and as a result conventional pixel-level approaches for species mapping are not considered suitable as the ground vegetation is a significant contributor to pixel-level reflectance. An image classification approach based on spectral mixture analysis (SMA) may be more suitable, as this technique decomposes mixed pixels into physically meaningful components (i.e., pure materials or so-called endmembers) of sunlit canopy, sunlit background, and shadow (Adams et al., 1993; Roberts et al., 1998) which can be related to tree species.

A key to successfully applying SMA is the appropriate specification of endmembers (Tompkins et al., 1997), which involves specifying the number and type of

endmembers and their corresponding spectral signatures. Endmember spectra are often measured in the field; however, this is not always possible because of technical and budgetary limitations (McCoy, 2005). As an alternative, endmember spectra can sometimes be derived directly from an image. Although considerable research has focused on image endmember extraction algorithms (Boardman, 1994; Winter, 1999; Plaza et al., 2012), the proper specification of image endmember spectra is not always possible. For example, for the background component there may be no suitable open areas that match or exceed the area of one single pixel. It is therefore of interest to determine whether endmember spectral impurity would influence the discrimination between tree species, and whether forest inventory information can be used to select meaningful image endmember spectra. As the degree to which tree species can be discriminated may be influenced by its stage of vegetative phenology, the use of multi-temporal imagery during the growing season was also deemed of interest for its potential to improve classification accuracies.

1.3. Thesis Research Objectives

The goal of this thesis is to obtain an improved understanding of the capabilities of SMA for mapping the leading tree species in northern boreal forests using Landsat TM by addressing four current unknowns: 1) the sensitivity to field-based descriptions of leading species, 2) the influence of the type of background endmember used for SMA, 3) the use of impure image endmember spectra selected using forest inventory information, and 4) the advantage of multi-temporal imagery. The objective of this thesis was to address these unknowns, and was achieved by answering five research questions for a representative study area in the Taiga Plains Ecozone as follows:

1. Is the determination of leading species from Landsat TM imagery influenced by its description from field-based inventory metrics?
2. Does the use of background endmembers defined by single species or mixed species spectra influence the discrimination of leading species?
3. Are there differences in classification performance between image-derived spectra and field-based spectra?
4. Is the performance of image-derived spectra dependent on the type of forest inventory information (e.g., by basal area or crown closure) used to select representative sunlit canopy and background components?
5. Would the use of multi-temporal Landsat TM imagery to represent different stages of vegetative phenology improve the determination of leading species?

1.4. Thesis Organisation

To address the five research questions, two studies were undertaken. The first study addressed the first and second research questions, and required three different sources of validation data and high-quality field spectra of the sunlit canopy and understory vegetation. Classification accuracy was estimated for a four-species classification scheme, and analyzed to identify patterns of highest agreement with the validation datasets. The second study compared the performance of the field spectra to image endmember spectra of the sunlit canopy and background components, which were selected using two different sets of selection criteria and detailed forest inventory information. Both single-date and multi-temporal imagery was evaluated to determine the performance of these spectra.

This thesis is written in a manuscript format with each Chapter representing a stand-alone, yet integrated part of the conducted research. Chapter 2 provides a literature overview of the potential and limitations of remote sensing to derive the spatial distribution of boreal tree species and highlights current challenges to derive this information for operational forest management. Chapter 3 presents the location of the

study area, and characterizes its abiotic and biotic components. Chapter 4 addresses the first and second research question by evaluating the sensitivity of Landsat TM imagery to multiple sources of validation data and its classification performance using various sets of understory spectra. Chapter 5 addresses the latter three research questions by evaluating the performance of image endmember spectra and multi-temporal imagery. Chapter 6 synthesizes the results, addresses the implications of this work for the remote sensing discipline and operational forest management in the NWT, and provides recommendations for future research. Chapter 7 concludes the findings of this research.

CHAPTER 2

Literature Review

The overall goal of this literature review is to provide an overview of the potential and limitations of remote sensing to derive the spatial distribution of tree species within a northern boreal forest context. The work described in this review represents a compilation and summary about the methods and data sources used to derive this information. This review is subdivided into multiple sections, whereby Section 2.1 introduces the boreal forests and emphasizes the importance of forest monitoring. Section 2.2 provides an overview of current forest inventory approaches and highlights current challenges. A review of the determinants of compositional and structural heterogeneity in boreal forests is provided in Section 2.3 to emphasize ecological considerations for mapping purposes. Section 2.4 assesses remote sensing methods to derive the spatial distribution of boreal tree species, while Section 2.5 synthesizes this literature and highlights current challenges to the derivation of this information, with the intent to identify future areas of research. Section 2.6 summarizes the findings.

2.1. The Boreal Forest and Importance of Forest Monitoring

The world's boreal forests occupy vast areas of the northern hemisphere and are mainly found in Canada, Russia, Alaska, and Scandinavia. These forests cover approximately 1,890 billion ha and represent one of the largest forest regions in the world (Brandt et al., 2013). This circumpolar forest represents a major biogeoclimatic zone, which regulates regional and global climates, cycles nutrients, acts at a reservoir for biological and genetic diversity, and provides renewable resources, habitat, and recreational opportunities (Brandt, 2009). By storing between 84-97 t/ha of carbon in its

aboveground and root biomass (Keith et al., 2009), as well as 116-343 t/ha in its soil due to the large peat stock (Malhi et al., 1999; Amundson, 2001), the boreal forest represents the world's second largest terrestrial carbon stock (384 Gt) after the tropical and subtropical forests (Trumper, 2009). Over North America, the boreal forest zone forms a broad uninterrupted crescent from Newfoundland to Alaska, covering approximately 6,270,000 km^2, and representing the most extensive forest-cover type on the continent (Brandt et al., 2013).

Given the importance of the North American boreal forest and its size relative to the entire circumpolar boreal zone (i.e., 25 % to 32 %; Brandt, 2009), an increased understanding of the distribution, composition, and structure of these forests is critical for sustainable forest management. This information is especially important with regards to the direct impacts of climate change on the boreal forest. Competitive relationships will change as a result of the gradual northward migration of species (Aitken et al., 2008; Walker et al., 2012), the increasing adaptational lags created by the shift in optimal climate (McKenney et al., 2011; Gray & Hamann, 2012), and the reduced productivity (Zhou et al., 2001) and increased mortality and forest dieback (Hogg et al., 2008; Michaelian et al., 2011; Peng et al., 2011) related to moisture stress.

Furthermore, the indirect impacts of climate change, such as the broadening and intensification of wildfire activity (Girardin & Mudelsee, 2008; Krawchuk & Cumming, 2010) and insect outbreaks (Berg et al., 2006; Safranyik et al., 2010), could introduce changes to the boreal landscape that could exceed the direct influence of climate change (Williamson et al., 2009). For example, with increasing fire frequency it is likely that more frequent shifts from coniferous to deciduous-dominated forests will occur

(Johnstone & Chapin III, 2006; Chen et al., 2009). Changes in the spatial distribution or depth of permafrost have altered drainage conditions that have led to subsequent changes to fire regimes and vegetation distribution (Hinzman et al., 2005; Jorgenson & Osterkamp, 2005). Unprecedented insect outbreaks, such as the recent attack of the mountain pine beetle in the boreal forests of north-western Alberta (Cullingham et al., 2011; de la Giroday et al., 2012), exemplify how climate change contributes to population range expansion towards previously unaffected forested environments (Carroll et al., 2003; Westfall & Ebata, 2011). Given the impacts of climate change, the acquisition of spatially referenced forest inventory information is therefore highly relevant to understand the rate of change, predict the outcome of these impacts on ecosystem function and diversity, and identify proper adaptation and mitigation strategies (Kurz & Apps, 2006; Lemprière et al., 2013; Price et al., 2013).

2.2. Forest Inventories

2.2.1. Terms and Definitions

In Canada, forest management is provincially regulated, whereby government agencies utilize inventory classification systems to extract and store spatially referenced information about forest characteristics, such as tree species, height, and density (Leckie & Gillis, 1995). Because of the compositional and structural complexity of forested areas, relatively homogenous units are established to reduce landscape complexity and to better understand attribute variations and determine the effects of management treatments (Bailey et al., 1978). Forest managers delineate homogenous forested areas for specific purposes of management and science, whereby they are primarily concerned with the forest stand as a spatial entity (Spies, 1997). A stand is a contiguous group of trees

sufficiently uniform in species composition, age distribution, and structure that can be identified as a distinguishable unit that fits the purposes of an intended use (Smith, 1986). Species composition is defined as the relevant proportion of tree species in a stand (Gillis & Leckie, 1993), and is the main variable of interest in this literature review. Mapping the species composition of tree species at a particular location is most relevant to operational forest management (Leckie, 1998) and is required to model stand volume and biomass (Boudewyn et al., 2007), net primary productivity (Tang et al., 2010), nutrient cycling (Prescott, 2002), carbon budgets (Kurz et al., 2013), stand dynamics (Cogbill, 1985), or successional pathways after disturbance (Amos-Binks et al., 2010).

2.2.2. Current Inventory Approaches

Forest inventories are carried out through an aerial-photo-interpretation process whose end goal is a forest inventory map (Hall, 2003). Aerial photographs record the radiance of features on the ground at the time of exposure, whereby this raw photographic data is subsequently processed through human interpretation (Leckie & Gillis, 1995). The fundamentals of aerial photo-acquisition and characteristics of both analog and digital sensors are well established in the literature (e.g., Lillesand & Kiefer, 1994; Wolf & DeWitt, 2000; Jensen, 2007), and thus the method of deriving species composition is of primary concern for this review. Forest species information can be extracted from photographs based on tonal, textural, pattern, size, shape, and shadow differences, along with spatial association (Lillesand and Kiefer, 1987). Polygons, representing areas of similar characteristics, are manually drawn using a stereo pair, whereby species composition is determined by dot grids to measure the relative abundance of a defined maximum number of most prevalent species to the nearest 10

percent (Leckie and Gillis, 1995). During the interpretation process, field checks may be performed for verification and calibration purposes. Field programs consisting of ground plot surveys are typically conducted as well to determine the agreement of the interpretation with field data and whether revisions are needed (Leckie and Gillis, 1995).

Because provincial forest inventories are not standardized across Canada, the variable used to measure and describe species composition varies between provinces and applications. For example, the relative proportion of a species can be given by percentage crown closure, stem density, or basal area (Table 1). It is important to note that forest inventory protocols are evolving with the need of an increasing number of variables at greater precision and accuracy (McRoberts & Tomppo, 2007). This means that the field-based description of species composition and the number of species reported change over time (e.g., British Columbia in Table 1).

Table 1: Definitions of species composition from forest inventory systems.

Metric	Number of species	Guidelines	Province	Source
% Crown closure	6	Minimum 10%, Sum = 100%	AB	Alberta Environmental Protection (1991)
% Crown closure	5	Minimum 10%, Sum = 100%	AB	Alberta Sustainable Resource Development (2005)
% Crown closure	3	Minimum 25%	NL	Gillis and Leckie (1993)
% Crown closure	4	Sum = 100%	NT	Government of Northwest Territories (2006a)
% Crown closure	10	Minimum 10%	ON	Gillis and Leckie (1993)
% Crown closure	3	$1^{st} + 2^{nd}$ minimum 75%	PEI	Gillis and Leckie (1993)
% Crown closure	n/a	Minimum 50% for species group	QB	Gillis and Leckie (1993)
% Crown closure	6	Sum = 100%	SK	Saskatchewan Environment (2004)
% Density stems	5	Minimum 6%, young stands	BC	Gillis and Leckie (1993)
% Density stems	6	Juvenile stands	BC	Sandvoss et al. (2005)
% GMV	3	Minimum 20%	NB	Gillis and Leckie (1993)
% GMV	4	Minimum 10%	NS	Gillis and Leckie (1993)
% Gross volume	5	Minimum 6%, old stands	BC	Gillis and Leckie (1993)
% Gross volume		Cover type specific	SK	Gillis and Leckie (1993)
% Gross volume	n/a	Not reported	SK	Lindenas (1985)
% Basal area	6	Older stands	BC	Sandvoss et al. (2005)
% Basal area	n/a	Not reported	MB	Gillis and Leckie (1993)
% Basal area	4	Sum = 100%	NT	Government of Northwest Territories (2006a)

* Crown closure is the percent of ground area covered by a vertical projection of foliage crowns on the ground (Alberta Environmental Protection, 1991).
* GMV: gross merchantable volume

Aerial photo-interpretation is regarded as the most accurate method to inventory forests (Hall, 2003; Falkowski et al., 2009). Nevertheless, differences in accuracy exist between stands and among inventory programs because the accuracy of a species composition classification is dependent on the complexity of the stand, the camera (and film) used to acquire the imagery, the skill of the photo-interpreter (Fent et al., 1995; Leckie & Gillis, 1995), as well as the data used for validation (Lillesand and Kiefer, 1987). In general, aerial photo-interpretation was expected to be accurate within 70 % and 85 % of the correct order or within ± 25 % of the true proportion of tree species (Leckie and Gillis, 1995). Because of the subjective nature of this inventory approach, forest inventories may contain significant misclassifications in relative proportion by volume in the majority of stands, as for example shown in northwestern Ontario (Thompson et al., 2007). While the aerial photo-interpretation approach is continually evolving and remains the most appropriate approach to inventory boreal forests, it remains a technology whose limits are being challenged, and it is cost prohibitive over large, remote forests.

2.2.3. Forest Inventories in the Northwest Territories – A Case Example

A primary example of the lack of spatial and temporal coverage of species composition information is in the Northwest Territories (NWT). Forests cover 33 million hectares in this territory (Government of Northwest Territories, 2011a), of which detailed forest inventories exist for less than 10 % of its forests (Hall et al., 2012). Where these data are available, they may be dated (Government of Northwest Territories, 2011b). The GNWT Department of Environment and Natural Resources requires this information to manage the forest resources sustainably (Smith, 2002), and multiple territorial

government policy initiatives (e.g., Northwest Territories Biomass Energy Strategy, Boreal Caribou Action Plan) have identified a need for detailed information regarding forest resources and wildlife habitat (Government of Northwest Territories, 2010b, 2010a). In the NWT, national-scale forest land-cover information is available from the Earth Observation for Sustainable Development of Forests (EOSD) project (Wulder et al., 2008), along with separate remote sensing -derived forest inventory products that include forest structure, stand volume, and above-ground biomass (Hall et al., 2012). While these remote sensing-based inventories characterize forest cover in coniferous, deciduous, and mixed classes, a more specific characterization of tree species is desired.

For the evaluation of remote sensing techniques that are capable of extracting information about species composition, it is important to recognize how the spectral reflectance of forest stands is influenced by ecological factors. Therefore, Section 2.3 provides a brief overview of the drivers of compositional and structural heterogeneity in boreal forests to develop an understanding of the various spatial and temporal aspects that must be considered from the perspective of using remote sensing for mapping forests.

2.3. Ecological Considerations for Mapping Boreal Forests

Although the boreal forest zone may appear uniform in its overall composition due to its relatively low-tree diversity, the physical, biological, and ecological factors controlling species distribution and stand structure have resulted in a broad range of different forest communities (Weber & Van Cleve, 2005). The high spatial heterogeneity can be explained by the wide distribution of tree species along environmental gradients according to individual genetic and physiologic adaptations and tolerances to soil, moisture, and light conditions (Beckingham & Archibald, 1996; Kimmins, 2003).

Besides micro-climatic and physiographic factors, the presence or absence of tree species may be partially explained by the disturbance history of the landscape. Disturbances are events that cause a significant change in the existing pattern in a system (Forman, 1987). In the boreal zone, natural disturbances such as wildfire (Brassard & Chen, 2006) and insect outbreaks (MacLean & MacKinnon, 1997) are key factors in maintaining landscape heterogeneity. The species composition and forest structure may be altered little (e.g., low intensity insect damage) or considerably (e.g., stand replacing crown fire) depending on the timing, frequency, and severity of a disturbance event (Johnstone & Chapin III, 2006; Johnstone et al., 2011). Because of spatial and temporal differences in disturbance regimes, boreal forests are highly diverse in terms of successional stage, stand structure, and forest health. Furthermore, differences in phenology (e.g., leaf flush; Brissette & Barnes, 1984) and morphology (Bond-Lamberty et al., 2002) are similarly influenced by abiotic and genetic factors, which add to the spatial complexity. With regards to the aforementioned factors, which influence the species composition and structure of stands, the boreal zone is relatively complex.

From the perspective of using remote sensing for mapping, the variation in forest composition, structure, as well as tree phenology and morphology, may cause challenges for accurate species identification due to larger intra-species spectral differences (e.g., Mora et al., 2010). Consequently, it is inappropriate to assume that a single value of an attribute (e.g., spectral response of a species), is representative over large regions (Peddle et al., 2007). Because age, morphology, stem density, crown closure, and species composition influence the spectral reflectance (Guyot et al., 1989; Spanner et al., 1990), failure to account for these factors may lower the accuracy of the mapping product when

these aspects of landscape heterogeneity are not accounted for. A proper stratification of field data ensures that most growing environments and forest types are accurately represented. As well, classification procedures that include additional spatial information (e.g., image texture, multi-temporal imagery, Digital Elevation Model; DEM) or that have expanded the classification scheme have been shown to be effective in accounting for environmental factors affecting the spectral response of a stand (Table 2). Such approaches allow appropriate inferences about the landscape to be made, and increases the confidence of labeling a species class to a spectral signature outside of the training and validation sites.

Table 2: Approaches to improve spectral discrimination between tree species.

Factor	Method	Source
Age	Image texture: spatial co-occurrence matrix Inclusion of "young" age classes (e.g., IGBP/GOFC*)	Franklin et al. (2001) Gamon et al. (2004)
Phenology	Multi-temporal image classification	Wolter et al. (1995) Dymond et al. (2002)
Topography	Inclusion of DEM variables (e.g., slope, aspect)	Franklin (1994) Bolstad and Lillesand (1992)
Density / Crown closure	Image texture: spatial co-occurrence matrix Inclusion of density labels (e.g., IGBP/GOFC)	Franklin et al. (2000) Franklin et al. (2002) Gamon et al. (2004)
Soil moisture	Inclusion of both dry and wet species labels	Bronge (1999)

IGBF: International Geosphere-Biosphere Programme, GOFC: Global Observation of Forest Cover.

2.4. Remote Sensing of Boreal Forests at the Species Level

To evaluate the capabilities of remote sensing techniques to extract information about species composition in northern boreal forests, the following section provides an overview of methods that have been used to classify boreal forests at the species level. To increase clarity in the evaluation, this section is subdivided according to the two main data types in which the distribution of vegetation can be depicted, mainly: 1) discrete classification schemes, and 2) continuous estimates of vegetation cover (DeFries et al., 1995). Discrete classification schemes characterize each image grid cell as a discrete

vegetation type, whereas continuous estimates of vegetation cover are typically expressed in percentages. Discrete land cover representations may be of relatively lower data volume and feature concise vegetation descriptions (Lambin, 1999), while continuous estimates of vegetation distribution may be better capable of capturing landscape heterogeneity (DeFries et al., 1995). Discrete image classifications based on the dominant or leading species (i.e., the species most abundant in a stand; Cumming & Vernier, 2002) may omit other species that are deemed of interest, and its accuracy statistics are not directly comparable with continuous estimates of tree species distributions (Plourde et al., 2007). Therefore, the distinction between the two information types is important from a literature review standpoint. The methods used to map the distribution of tree species in discrete classes (Section 2.4.1) and as continuous estimates (Section 2.4.2) are described separately to highlight differences in optical remote sensing approaches.

2.4.1. Discrete Image Classification at the Species Level

2.4.1.1. Medium Spatial Resolution Imagery

With respect to discrete image classifications of medium spatial resolution imagery (e.g., 30-m Landsat TM), numerous approaches have been used to obtain spatially referenced information regarding the distribution of boreal tree species. Commonly used supervised classification methods are the maximum likelihood classifier (e.g., Goodenough et al., 2003) and discriminant analysis (e.g., Franklin & Peddle, 1990; Franklin, 1994). In addition to its independent application, the maximum likelihood classifier can also be used in combination with topographic map data to mask regions in a stratified approach to increase the spectral separability between classes (Bronge, 1999). The unsupervised K-means clustering algorithm can be applied in combination with

NDVI thresholds to hypercluster Landsat TM imagery, whereby subsequent clusters were automatically labelled with the dominant tree species and structural class using randomly sampled photo-inventory pixels (Luther et al., 2006). Furthermore, classification methods that filter the imagery and enhance image contrast (Beaubien et al., 1999), or extract physical structure information through modeling radiative transfers in canopies (Peddle et al., 2004; Peddle et al., 2007) have also been applied. To overcome the limited discriminating power of the Landsat TM sensor between tree species (Luther et al., 2006), multi-temporal analysis or the inclusion of image texture, soil information, or Digital Elevation Model (DEM) derivatives, have been shown to increase the statistical separability of classes (Franklin, 1994; Wolter et al., 1995; Dymond et al., 2002). These studies highlight that numerous processing workflows have been developed to map the distribution of boreal tree species using medium-spatial resolution imagery.

Before outlining classification accuracies that have been achieved in the literature, it is important to note that classification accuracy is dependent on the classification method, number and type of assigned land-cover classes, the spatial heterogeneity of the forest, and the source data to assess the accuracy of the image classification (Lillesand & Kiefer, 1994). Thus, differences in accuracy can be contributed to a multitude of factors. When comparing inventory approaches, differences in accuracy should therefore be seen as the degree of similarity in classification performance between the evaluated remote sensing approach and the approach that represents the "true" stand characteristics.

Because the spectral response is affected by complex interactions between species composition, density, height, background vegetation, shadow, growing condition, and viewing and illumination geometry (Hall et al., 1997; Peddle et al., 2004), image

classification of a single variable may not be accurate if other biophysical characteristics of the stand are not accounted for. The majority of aforementioned studies have included additional biophysical information in the classification scheme, such as density, height, age, and moisture conditions (Table 3). The literature has reported a wide range of classification accuracies with no discernible patterns of accuracy in relation to the number of species related classes, total number of classes, or additional biophysical label separations (Table 3). In general, discriminant analysis (Franklin, 1994), the Enhanced-Classification method (Beaubien et al., 1999), and radiative transfer models (Peddle et al., 2004) have attained the highest similarities to reference data. However, because of differences in the classification method and detail, as well as quantity and quality of reference data between studies it is difficult to identify superior approaches.

Table 3: Overview of classification accuracies of medium spatial resolution imagery.

Data Source	Number of classes: species (overall) [1]	Biophysical Labels [2]	Inventory variable	Overall Accuracy	Source
ALI	5 (10)	D	n/a	75%	Goodenough et al. (2003)
Landsat MSS	20	-	% basal area	80%	Wolter et al. (1995)
Landsat MSS	5 (10)	M	n/a	74%	Wilson et al. (1994)
Landsat TM	9 (11)	D, H	n/a	81%	Franklin (1994)
Landsat TM + DEM	9 (11)	D, H	n/a	91%	Franklin (1994)
Landsat TM	5 (5)	D, H	% density stems	38%	Luther et al. (2006)
Landsat TM	10 (27)	A, M	n/a	71%	Bronge (1999)
Landsat TM	8 (13)	D, A	n/a	91%	Beaubien et al. (1999) in Peddle et al. (2004)
Landsat TM	8 (13)	D, A	n/a	85%	Peddle et al. (2004)
Landsat TM	16 (16)	D	n/a	60, 61%	Peddle et al. (2007)
Landsat TM	16 (16)	D	n/a	71%	Peddle et al. (2007)
Landsat TM	5 (19)	-	% crown closure	69%	Dymond et al. (2002)
Landsat TM	5 (19)	-	% crown closure	68%	Dymond et al. (2002)
Landsat ETM+	5 (10)	D	n/a	61%	Goodenough et al. (2003)
SPOT HRV	3 (7)	-	n/a	51%	Franklin and Peddle (1999)
SPOT HRV + texture	3 (7)	-	n/a	87%	Franklin and Peddle (1999)

[1] Only classes in reference to tree species are counted. Total number of classes reported in brackets (i.e., additional non-forest classes and cover type classes). Note: One species may be represented by multiple classes.

[2] Biophysical variables: Density (D), Height (H), Age (A), Moisture conditions (M).

2.4.1.2. High-Spatial Resolution Imagery

High-spatial resolution satellite-based (e.g., 1-m panchromatic, 4-m multispectral) or airborne-based sensors offer a spatial refinement of the forest objects to be mapped. Numerous methods have been developed to exploit this type of imagery to map forests at the species level. Because the spatial resolution is typically smaller than the object of interest (i.e., the individual tree), the imagery contains different spectral responses of tree parts due to the varying illumination, shading, and understory gaps. The application of high-spatial resolution imagery may not universally increase classification accuracies because any spatial refinement may reduce the statistical separability between classes (e.g., greater within-class variation) and skew the distribution of the spectral responses (Marceau et al., 1994; Quackenbush et al., 2000). In such cases, the assumption of normality that is required for parametric per-pixel classification algorithms will be invalidated (Lillesand and Kiefer, 1987). The unsuitability of the per-pixel classifications was highlighted by Gerylo et al. (1998) and Franklin et al. (2001), who used plot-level forest inventory codes as distinct classes and attributed the low performance to the constraints of using spectral signatures on a pixel basis to classify entire forest stands that often vary slightly in structure or composition. These studies highlight that although high-spatial resolution imagery offers a spatial refinement in mapping forest stands, per-pixel classifications may not be suitable to discriminate between stands of mixed species composition and structure due to high between-class variance and non-normality of spectral responses.

To address non-normality of datasets and reduce inter-class variance, numerous studies have aimed to subdivide the image into relatively homogenous regions through

image segmentation. In such instances, image objects instead of individual pixels become the carriers of image information and representatives of forest stands or individual trees (Chubey et al., 2006). For example, these authors used a region-based algorithm to segment IKONOS panchromatic and multispectral imagery into homogenous forest stand components, and characterized individual pine, spruce, and aspen-dominated stands by applying a decision tree using aggregative statistics of image and DEM values. Alternatively, individual trees can be delineated through local image maxima filters that represent crown apexes (Wulder et al., 2000), which are subsequently assigned a species label by using a maximum likelihood classifier of the sunlit side of the crowns (Gerylo et al., 1998). Instead of counting and classifying individual trees by finding the brightest pixel, Gougeon (1995b) and Gougeon and Leckie (2006) delineated entire individual tree crowns by using a valley-following algorithm that exploits the bands of shadow surrounding individual crowns. Once obtained, crowns can either be classified using spectral signatures and a maximum likelihood classifier (Gougeon, 1995a), or by using crown shape metrics derived from panchromatic imagery and a decision tree (Mora et al., 2010). Besides classification algorithms on a per-pixel basis, the aforementioned studies indicate that a variety of procedures exist to exploit high-spatial resolution imagery for tree species mapping.

A wide range of classification accuracies have been reported for high-spatial resolution imagery (Table 4), and with regards to per-pixel classifications, studies that used forest inventory plots to train the maximum likelihood classifier have achieved low similarities with reference data (Gerylo et al., 1998; Franklin et al., 2000). In contrast, the use of broader species classes in the classification scheme have obtained better results

(e.g., Franklin, 1994). The table highlights that image classifications at higher spatial resolutions do not automatically achieve greater similarities with reference data. Nevertheless, higher spatial resolution imagery allows for the generation of image texture at the stand and crown level, which has been shown in multiple studies to improve classification accuracies. To separate stands of different composition and density, a multi-scale texture approach has been shown to achieve the highest similarities with reference data (Coburn & Roberts, 2004). With respect to both stand and crown segmentation, it is apparent that favourable accuracies have been achieved in the classification of individual trees or stands (Table 4). Typical reported classification accuracies range between 59 % and 75 % for the classification of individual trees, and at the stand level, accuracies between 70 % and 93 % have been reported. Errors in the estimation of the relative abundance of tree species in a stand are generally less than 20 % in stems/ha^{-1} in comparison to reference data (Gerylo et al., 1998; Gougeon et al., 1999; Leckie et al., 2003), and as such fall within the expected range of errors of aerial photo-interpretation (Leckie and Gillis, 1995). Although favourable accuracies have been reported through image segmentation, the majority of studies fall short of the widely used 85-% overall accuracy suggested as a mapping standard (Anderson et al., 1976) or the 0.8 kappa threshold value of strong agreement with reference data (Landis & Koch, 1977). This suggests that spectral confusion between classes remains a considerable limitation to the ability for species discrimination.

Table 4: Classification types and reported accuracies of high spatial resolution imagery.

Type	Data Source	Spatial resolution	Number of classes: species (overall) [1]	Inventory variable	Overall Accuracy	Source
Per-pixel	MS Video	0.3 m	15 (15)	% stem density	26%	Gerylo et al. (1998)
	MS Video	0.3 m	17 (17)	% crown closure	15%	Franklin et al. (2000)
	MS Video	8.0 m	17 (17)	% crown closure	40%	Franklin et al. (2000)
	MS Video + texture	0.3 m	17 (17)	% crown closure	31%	Franklin et al. (2000)
	MS Video + texture	8.0 m	17 (17)	% crown closure	44%	Franklin et al. (2000)
	Sony XC-7500	4.0 m	3 (6)	n/a	61%	Coburn and Roberts (2004)
	Sony XC-7500 + texture	4.0 m	3 (6)	n/a	75%	Coburn and Roberts (2004)
	casi	2.5 m	9 (11)	n/a	81%	Franklin (1994)
	casi + DEM	2.5 m	9 (11)	n/a	90%	Franklin (1994)
	casi	1.0 m	17 (17)	% crown closure	42%	Franklin et al. (2000)
	casi + texture	1.0 m	17 (17)	% crown closure	42%	Franklin et al. (2000)
	casi	1.0 m	30 (30)	% crown closure	54%	Franklin et al. (2001)
	casi + texture	1.0 m	30 (30)	% crown closure	75%	Franklin et al. (2001)
Segmen-tation	IKONOS	4.0 m	3 (8)	% crown closure	93%	Chubey et al. (2006)
	MEIS	0.4 m	5	Individual trees	74%	Gougeon (1995a)
	IKONOS	4.0 m	7	Individual trees	59%	Gougeon and Leckie (2006)
	QuickBird (pan)	0.6 m	4 (4)	% basal area	73%	Mora et al. (2010)
	QuickBird	0.6 m	4 (4)	% basal area	67%	Mora et al. (2012)
	QuickBird + Landsat TM + DEM	0.6 m	4 (4)	% basal area	70%	Mora et al. (2012)

[1] Only classes in reference to tree species are counted. Total number of classes reported in brackets (i.e., additional non-forest classes). Note: One species may be represented by multiple classes.

2.4.1.3. Hyperspectral Imagery

Besides multispectral imagery, hyperspectral data can be used to derive the spatial distribution of tree species, and have been classified with a wide range of approaches. Spectral bands have typically been selected based on the sensitivity to leaf pigments, water absorption, or foliar chemistry (Martin et al., 1998). These spectral bands have been processed with supervised classifiers such as the minimum Euclidean distance, and maximum-likelihood, and spectral angle mapper (Martin et al., 1998; Sandmeier & Deering, 1999), or through the use of spectral mixture analysis and a maximum likelihood classifier (Ustin & Xiao, 2001). With respect to the aforementioned studies, it is evident that some hyperspectral approaches have been conducted in boreal forests with regards to tree species mapping. However, the number of studies are limited relative to multispectral imagery due to the smaller number of hyperspectral satellite sensors

available (Shippert, 2004) and its high costs associated with airborne data collection (Youngentob et al., 2011).

In comparison to the classification accuracies reported in the literature that used multispectral airborne imagery, studies involving airborne hyperspectral sensors achieved a similar range of classification results for a similar number of tree species (Table 5). This is most likely due to the spatial and spectral complexity of surface reflectance values of forest canopies and the inherent spectral and spatial limitations of the sensors (Hu et al., 2008). With respect to spaceborne sensors, Goodenough et al. (2003) indicated that the classification of hyperspectral data (EO-1 Hyperion) can obtain greater similarities to reference data than Landsat ETM+ (61 % compared to 81 %). Thus, although higher classification accuracies are generally expected due to greater dimensionality of hyperspectral data, the current literature indicates that this may only be the case with spaceborne sensors.

Table 5: Classification types and reported accuracies of hyperspectral imagery.

Sensor	Classification Method [1]	Number of classes: species (overall) [2]	Inventory variable	Overall Accuracy	Source
AVIRIS	MLC	7 (11)	% crown closure	75%	Martin et al. (1998)
AVIRIS	SMA → MLC	5 (10)	n/a	74%	Ustin and Xiao (2001)
ASAS	MLC	4 (6)	% volume	43%	Sandmeier and Deering (1999)
ASAS	MLC + CA	4 (6)	% volume	49%	Sandmeier and Deering (1999)
ASAS	MED	4 (6)	% volume	31%	Sandmeier and Deering (1999)
ASAS	MED + CA	4 (6)	% volume	44%	Sandmeier and Deering (1999)
ASAS	SAM	4 (6)	% volume	54%	Sandmeier and Deering (1999)
ASAS	SAM + CA	4 (6)	% volume	64%	Sandmeier and Deering (1999)
Hyperion	MLC	5 (10)	n/a	81%	Goodenough et al. (2003)

[1] Classification method acronyms: MLC: Maximum likelihood classifier, CA: Canopy anisotropy information, MED: Minimum Euclidian Distance, SAM: Spectral Angle Mapper, SMA: Spectral Mixture Analysis.

[2] Only classes in reference to tree species are counted. Total number of classes reported in brackets (i.e., additional non-forest classes). Note: One species may be represented by multiple classes.

2.4.2. Continuous Estimation of Species Coverage

2.4.2.1. Regression Models

Regression models use individual image bands and other raster-based information (e.g., digital elevation models) as independent variables to estimate the spatial distribution of tree species in percentage of crown closure or basal area. Although these models may be ideally suited to address the heterogeneity of forests (DeFries et al., 1995), only one study located within the boreal forest was found. Through the integration of different combinations of Landsat, Radarsat-1, PALSAR, and SPOT-5 sensor data, Wolter and Townsend (2011) derived 147 variables to estimate the relative basal area of 12 tree species using partial least squares regression. For remote sensing, partial least squares regression combines features of principal component analysis (Byrne et al., 1980) and multiple linear regression to predict the response (e.g., abundance per basal area) using a greater number of collinear independent variables than there are field observations (Wolter et al., 2008). Because each data type discriminates the structural and compositional properties of the forest stand differently, combining the discriminative power of independent variables increases the separability of classes. As a result, Wolter and Townsend (2011) achieved relatively low root mean square errors (RMSE) in relative basal area, ranging between a low 2.5 % and high 10.3 % for jack pine (*Pinus banksiana*) and white cedar (*Thuja occidentalis*), respectively. Because the study has reported errors within the expected error of inventories through aerial photo-interpretation (Leckie and Gillis, 1995), it appears that regression models may be a viable alternative in deriving the relative abundance of tree species of a forested environment. However, due to the lack of studies in the boreal forest the capabilities of regression models remain to be investigated.

2.4.2.2. Spectral Mixture Analysis

Similar to partial least squares regression, spectral mixture analysis (SMA) can be used to determine the relative abundance of features in an image, whereby the spectral signal of a pixel can be represented as a mixture of signals contributed by "pure" features within the instantaneous field-of-view (IFOV) of the sensor (Adams et al., 1993). SMA quantifies the proportion of each pixel that is occupied by a single set of the pure features occurring in an image (i.e., endmembers), whereby the output is a fraction image for each endmember along with the error of fit. For each pixel, this model can be derived as follows:

$$R'_i = \sum_{k=1}^{N} f_k \, R_{ik} + \varepsilon_i \, , \quad (1)$$

where the spectral mixture R'_i is the encoded reflectance in band i for each pixel, and modeled as the sum of the reflectance in band i for N image endmembers k, whereby each endmember is weighted by fraction f_k. The ε_i term represents the remainder between the measured and modelled reflectance, and is expressed as a band residual. The fractions of endmembers that are allowed during spectral mixture analysis can be set to unconstrained (from $-\infty$ to ∞) or fully constrained (i.e., between 0 and 1). The condition that the fractions of endmembers must be summed to 1 for each pixel (i.e., fully constrained), or not (i.e., unconstrained) can also be set, whereby weakly constrained unmixing (i.e., sum of fractions ≤ 1) have been shown to improve unmixing results when not all endmembers are known (Shang et al., 2008). Model fit can be assessed either by using this residual term, or via the root mean square error (RMSE; Roberts et al., 1998) over the total number of bands (ν):

$$RMSE_{(\lambda)} = \sqrt{\sum_{i=1}^{\nu} (\varepsilon_i)^2 / N} \, . \quad (2)$$

Because SMA is a model that converts reflectance values to physical variables, its output can be directly incorporated into models to estimate biophysical parameters (Peddle et al., 1999). A major obstacle to accurately use SMA is its assumption that the mixed pixel is a combination of all of the image-wide endmembers without accounting for the spatial heterogeneity of the imaged surface (Roberts et al., 1998). For example, the number of features within a pixel and the spectral characteristics of endmembers vary across an image. As SMA is limited to a single set of endmembers, studies involving vegetation generally extract the abundance of sunlit canopy, sunlit background, and shade (e.g., Hall et al., 1996; Peddle et al., 1999). Using these fractional abundances, Ustin and Xiao (2001) employed a maximum likelihood classifier to classify six boreal forest cover types by species with 74 % accuracy.

If only a single endmember of interest is known (e.g., one particular tree species), approaches such as Mixture Tuned Matched Filtering (MTMF; Boardman, 1998) have been developed to determine the fractional abundance of a single cover type when all other endmembers are not known. The MTMF approach appears to be a suitable alternative to partial least squares regression to map the spatial distribution of deciduous tree species, as Plourde et al. (2007) achieved sugar maple (*Acer saccharum*) and American beech (*Fagus grandifolia*) abundance estimates with RMSEs of 9 - 15 % and 16 - 18 % using AVIRIS and Hyperion data, respectively. SMA could thus be used to detect gradual shifts in land cover and provide a robust estimation of the distribution of land-cover features. However, the highlighted study only modeled two species across a landscape, irrespective of other tree species and landscape features, and without accounting for phenological and stand structure differences. Additional research

concerning the estimation of the relative abundance of tree species using SMA is thus warranted, but due to the inherent limitations of this approach a method capable of dealing with a larger variety of tree species and greater landscape heterogeneity will be more relevant to forest management.

2.4.2.3. Multiple Endmember Spectral Mixture Analysis

To address the challenges concerning endmember variability in SMA, a Multiple Endmember SMA (MESMA; Roberts et al., 1998) has been developed that is not constrained by a single set of endmembers and allows the number and types of endmembers to vary on a per-pixel basis to account for spatial heterogeneity. Because MESMA is not constricted by the number of spectral bands, it has been successfully applied to obtain species abundance maps of a variety of different species in vegetated areas such California (Dennison & Roberts, 2003b) and Australia (Youngentob et al., 2011). In the boreal zone, however, this approach has only been used to improve the estimation of leaf area index of peatlands (Sonnentag et al., 2007) and insofar has not been quantitatively assessed in its capability to extract information about tree species. Although Roberts et al. (1999) introduced MESMA in a preliminary study and indicated some level of discrimination between boreal species, no quantitative evaluation was conducted.

Even though MESMA is capable of addressing endmember variability, tree species with a high degree of spectral similarity remain a challenge for accurate class discrimination due to the effects of illumination, canopy structure, and the spatial resolution of the sensor (Roberts et al., 2004), as well as tree phenology (Dennison & Roberts, 2003a). The majority of studies involving MESMA have employed

hyperspectral imagery to improve the discriminating ability between species (e.g., Roberts et al., 1998; Dennison and Roberts, 2003a,b). The small number of hyperspectral satellite sensors and its high costs associated with airborne data collection, however, has resulted in limited operational applications of this approach in northern Canada.

2.5. Synthesis of Literature

Through this review it became apparent that numerous remote sensing approaches have been used to derive discrete and continues estimations of the spatial distribution of boreal tree species under a wide range of forest conditions. Nevertheless, uncertainty exists in the application of these approaches in a northern boreal forest context, and three main drivers of uncertainty are identified in this review.

Firstly, the remote sensing approaches have generally been tested in the southern boreal forest and forests in British Columbia (Figure 1). Northern boreal forests, such as in the Taiga Plains and Taiga Shield Ecozones, are considered heterogeneous in both species composition and structure (Ecosystem Classification Group, 2007), where mixed pixels occur as a result of open forest canopies (Franklin et al., 2003; Chasmer et al., 2011). With respect to mapping the spatial distribution of tree species, the absence of remote sensing studies in northern boreal environments introduces uncertainty in the identification of appropriate approaches from the aforementioned studies. Conventional pixel-level approaches for species mapping using digital satellite imagery are likely not suitable for the open stands of northern boreal forests because understory ground vegetation is a significant contributor to pixel-level reflectance. Future research in northern boreal forests is thus warranted to obtain new insights in the capabilities of remote sensing approaches to map the spatial distribution of tree species.

Figure 1: Location of aforementioned remote sensing studies. Shapefile from Brandt (2009) and Ecological Stratification Working Group (1995).

Second, a wide range of accuracies have been reported in the literature as a result of the numerous data sources and processing procedures that have been used in a variety of compositional and structural forest settings (Figure 2). Although high accuracies up to 93 % have been achieved for each image type, on average, remote sensing approaches have had only moderate success in approximating the information derived through ground inventories or aerial photo-interpretation. This level of success can be attributed to two counteracting challenges with regards to image classification: 1) the similarity of reflectance spectra between even widely differing tree species, and 2) the large intra-species variation in reflectance spectra due to the influences of stand structure, morphology, health, as well as viewing and illumination angles. These challenges are not easily overcome, and given the wide range of classification accuracies reported, data processing procedures are at least of similar importance as the data source itself.

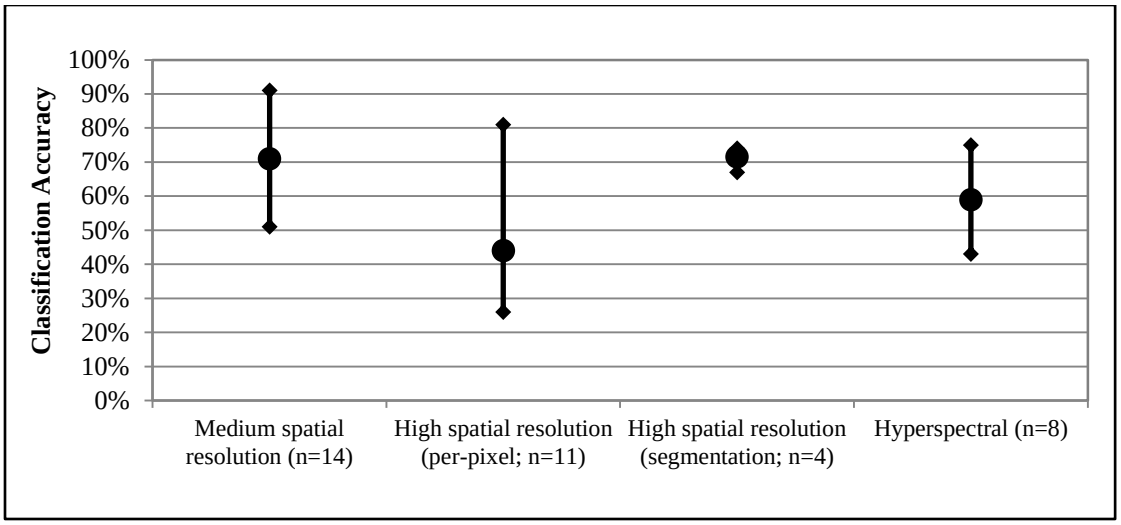

Figure 2: Median, minimum, and maximum reported accuracies per imagery type. Note: Worst and best reported accuracies for each image type deleted to remove outliers. (Source: calculated statistics from Tables 3, 4, and 5).

Another uncertainty is the degree to which information derived through remote sensing approaches can be integrated into current forest inventories. Image classifications at the species level generally involve the discrete labeling of pixels that constitute the greatest proportion within a stand (i.e., the dominant or leading species). Current forest inventories derive the relative abundance of tree species in a stand to the nearest 10 percent, which is of much greater level of detail than what has been achieved with image classifications. The approach used to determine species composition (and thus the leading species) differs among jurisdictions and in the literature. Resource management agencies may measure the composition of tree species per percentage crown closure, basal area, stem density, or gross volume (Gillis and Leckie, 1995), which may not provide the same relative abundance estimations. Therefore, the definition used to estimate the relative proportion of tree species and identify the leading species is an important consideration. Distinct patterns of classification accuracy can be highlighted when the results of the studies are stratified by field-based description of leading species (Figure 3).

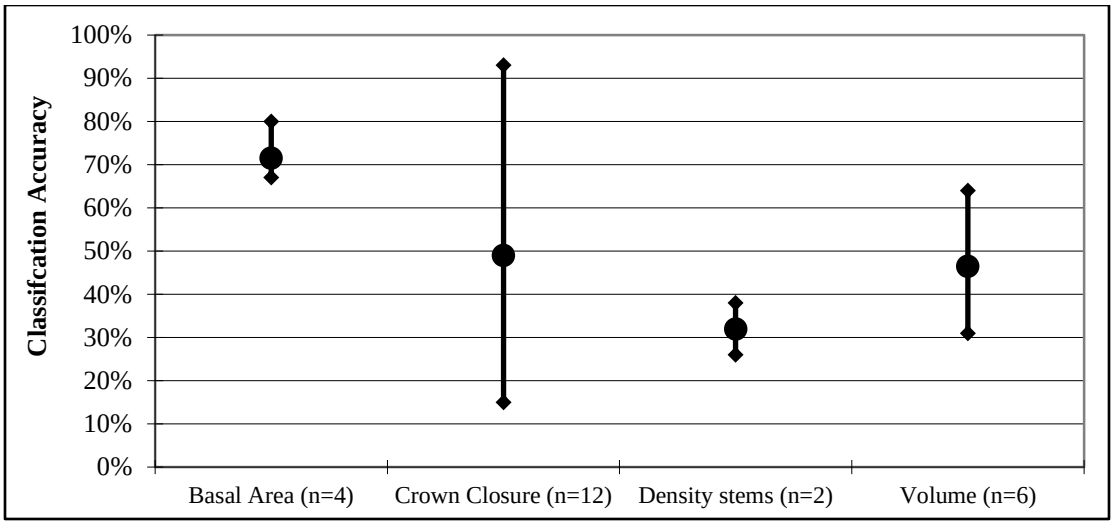

Figure 3: Median, minimum, and maximum reported accuracies per leading species indicator.

Half of the referenced studies in this review have not provided information regarding the definition of species composition used in the training and validation of the classified imagery, and no study was found that discussed if the imagery may be sensitive to differences in field-based descriptions of species composition. Both Pontius et al. (2005) and Plourde et al. (2007) briefly noted that remote sensing validation data based on basal area measurements may be imperfect to determine the relative abundance of tree species in temperate and hemi-boreal forests, because the radiance recorded from the top of the canopy may not be influenced by sub-canopy individuals for which basal measurements are included. However, this observation is likely not valid in all North American forest types, as the background reflectance of open canopies characteristic of northern boreal forests may contribute considerably to the spectral response. For example, differences in Landsat TM spectral signatures can be observed within mixed jack pine/black spruce stands (Figure 4a and 4b) and compared to mixed jack pine/white spruce stands (Figure 4c and 4d) as a result of differences in tree species composition and background vegetation types, even though stand structural characteristics are relatively

similar (e.g., stand height: 8 m – 12 m, crown closure: 30 % - 38 %, stem density: 525 - 750 stems/ha). The complexity with respect to differences in background vegetation communities challenge, current remote sensing approaches for northern boreal forest applications, and the slight variations in species composition (e.g., Pj_9Sw_1 versus Pj_7Sw_3) are relevant to operational forest management but have not yet been detected through remote sensing in a robust and accurate approach. Evidently, differences in paradigms exist in terms of data capture and the representation of information between remote sensing approaches and forest inventories for an operational forest management level.

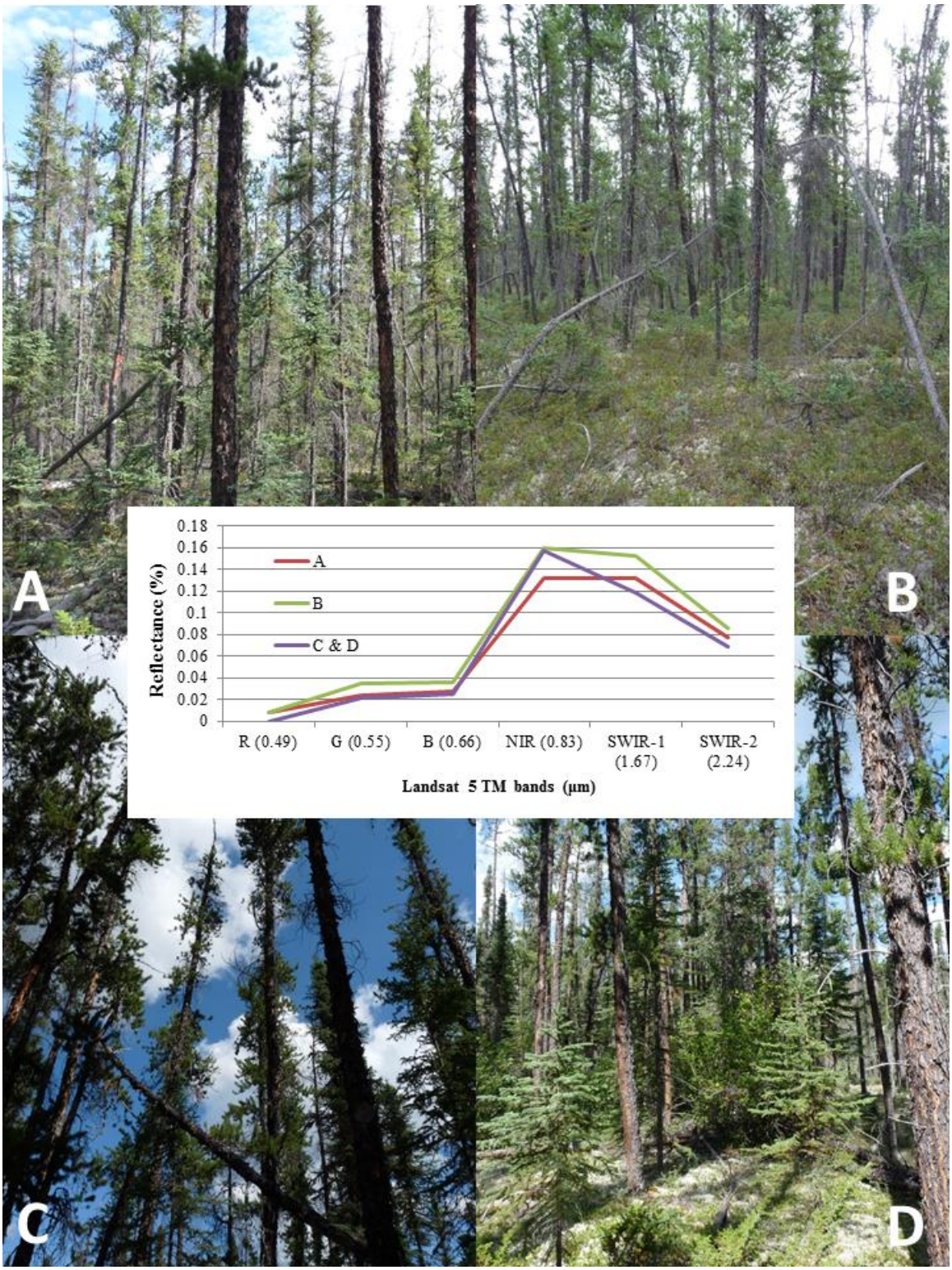

Figure 4: Plate highlighting the diversity of stand types and understory compositions. A: Mixed jack pine and black spruce stand (overstory: Pj_9Sb_1, understory: Pj_7Sb_3). B: Mixed jack pine and black spruce stand (overstory: Pj_7Sb_3, understory Sb_8Pj_2). C and D: Mixed jack pine and white spruce stand (overstory: Pj_9Sw_1, understory: $Sw_6Pj_3Bw_1$). Species composition labels based on Alberta Vegetation Inventory Standards. Note the complexity of the background vegetation.

2.6. Summary

Regarding the direct and indirect impacts of climate change on the North American boreal forests, an increased understanding of the factors that influence its composition and structure is critical for the protection of social, environmental, and economic forest values. Although aerial photo-interpretation is regarded as the most accurate method to inventory forests, it is cost prohibitive over large, remote forests, such as in the Northwest Territories. Because remote sensing may be used to supplement current forest inventory data, the overall goal of this review was to provide an overview of the potential and limitations of remote sensing to derive the spatial distribution of tree species within a northern boreal forest context. This review focused on techniques, which depict the distribution of tree species through discrete classification approaches and continuous estimates of vegetation cover.

A wide range of sensors and data processing methods have been used to discretely estimate the distribution of tree species, with varying degrees of success. With regards to Landsat TM/ETM+ imagery, the highest similarities with reference data have been obtained through discriminant analysis, the Enhanced-Classification method, and radiative transfer models. Although high-spatial resolution sensors allow individual trees to be mapped, only through image segmentation at the stand or crown level can this spatial refinement be effectively exploited. Similar classification accuracies have been reported for both multispectral and hyperspectral airborne imagery, while hyperspectral spaceborne sensors of the latter type do appear to perform better than multispectral sensors. In general, remote sensing techniques have had only moderate success in approximating the information derived through current forest inventory methods. This is

due to the spectral similarities between tree species and the large intra-species variation in spectral response.

To derive continuous estimates of the relative proportion of tree species a limited number of processing methods have been described, namely: 1) partial least squares regression and 2) spectral mixture analysis. Both methods have derived estimations with relatively low RMS errors (i.e., < 20 %), which fall within the expected error of inventories through aerial photo-interpretation. However, due to the lack of studies elsewhere in the boreal forest the capabilities of these methods remain to be investigated. Particularly the abilities of MESMA to account for background reflectance and shade may be exploited to discriminate between tree species. Its potential has not yet been evaluated in boreal forests. The assessment of MESMA's capabilities in northern boreal forest conditions may thus bring considerable knowledge gains.

Uncertainty exists in the capabilities of remote sensing techniques to derive the distribution of tree species in a northern boreal forest context. Due to the absence of remote sensing studies conducted in this setting the results presented in this review may not be representative of what can be achieved in a northern boreal forest setting. The lower availability of hyperspectral and multi-source data in northern Canada and the possible sensitivity of imagery to the various field descriptions of species composition further increases the uncertainty in the role these approaches may play in the derivation of information at an operational forest management level. The robustness of the highlighted approaches to greater understory reflectance and stand structural variation remains to be investigated.

CHAPTER 3

Study Area

The purpose of this Chapter is to describe the characteristics of the study area, including its location and both abiotic (e.g., climate, geomorphology, soils) and biotic components of the landscape (e.g., forest vegetation, non-forest cover types). To place to study area in context with the circumpolar boreal zone, a brief description of the boreal zone at an international, national, and Ecozone scale is provided.

3.1. The Boreal Zone

The boreal zone is a circumpolar vegetation zone located at high northern latitudes in countries including Canada, Russia, United States of America (Alaska), and Scandinavia, and covers approximately 1,890 billion ha (Brandt et al., 2013). The land cover in this zone can be characterized primarily by forests and other wooded land, as well as lakes, rivers, and wetlands. The trees within the boreal zone belong to cold-tolerant coniferous and deciduous species, and include the genera *Abies* (firs), *Larix* (larches), *Picea* (spruces), *Pinus* (pines), *Populus* (poplars), and *Betula* (birches) (Weber & Van Cleve, 2005). Over North America, the boreal forest forms a broad uninterrupted crescent from Newfoundland to Alaska, which covers approximately 627 million ha and represents the most extensive forest-cover type on the continent (Brandt et al., 2013).

The Canadian boreal forest constitutes approximately 88 % of the North American boreal forests, and 28 % of the entire circumpolar boreal zone (Brandt et al., 2013). The boreal forest in Canada covers an estimated 552 million ha, of which forests and other wooded land are the predominant land-cover types (270 million ha and 39 million ha, respectively) (Brandt et al., 2013). Its distribution ranges from Newfoundland

to the Arctic coast, extends into British Columbia, and includes the Atlantic Provinces, Quebec, Ontario, Manitoba, Saskatchewan, Alberta, British Columbia, as well as the Yukon, Nunavut, and Northwest Territories (Figure 5). Eight ecological zones can be identified in the boreal region based on landform and climate, major soil orders, and broad vegetation types, and include the Cordillera (Boreal, Taiga, Montane), Shield (Boreal and Taiga), and the Plains (Boreal, Taiga, Hudson) (Ecological Stratification Working Group, 1995). The Cordilleran Ecozones are typical of vegetative mountainous regions, the Shield Ecozones cover the continental Precambrian Shield, and the Plains Ecozones are characterized by gently rolling lowland regions. The distinction between the Boreal and Taiga Ecozones is related to the length of the growing season, climate, and soil productivity, whereby the latter Ecozones have a shorter growing season, colder winter temperatures, lower soil productivity, and contain more open canopy forest with thinner trees (Ecological Stratification Working Group, 1995).

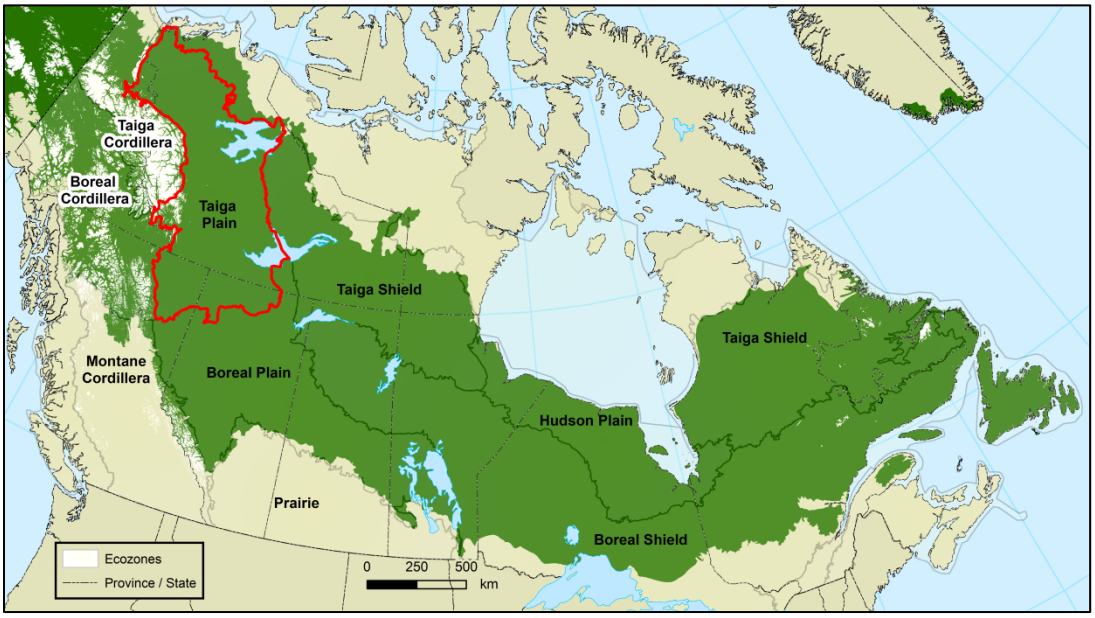

Figure 5: Distribution of the Canadian boreal zone (Brandt, 2009) with Ecozones.

The Taiga Plains Ecozone, which consists of the Mackenzie River and its tributaries, is bordered by Great Slave Lake and Great Bear Lake to the west, Cordilleran Mountains to the east, the Boreal Plains Ecozone to the south, and the Mackenzie Delta to the north (Ecological Stratification Working Group, 1995). This Ecozone covers over 480,000 km^2, drains in the Arctic Ocean, contains over 100,000 water bodies as well as extensive peatlands and permafrost (Ecosystem Classification Group, 2007).

3.2. Location of the Study Area

Most of the timber productive forests occur within the southern portion of the Taiga Plains Ecozone, which is referred to as the Taiga Plains Mid-Boreal Ecoregion (Ecosystem Classification Group, 2007). In this Ecoregion an 18-km by 19-km region of interest was selected based on the presence of representative tree species and forest stands, accessibility of the terrain, availability of suitable, cloud-free satellite imagery, and the availability of ground reference data. The study area is located 20 km south of Fort Providence, NWT in the Deh Cho Region (Figure 6), within the Universal Transverse Mercator (UTM) Zone 11N, and is bounded by 458,353 mE and 6,773,736 mN on the southwest to 476,148 mE and 6,792,690 mN on the northeast. The study area can be found on the eastern half of the National Topographic System (NTS) 1:50,000 map sheet 85F/04, and can be characterized as the Great Slave Lowland Mid-Boreal Ecoregion according to the Ecosystem Classification Group (2007).

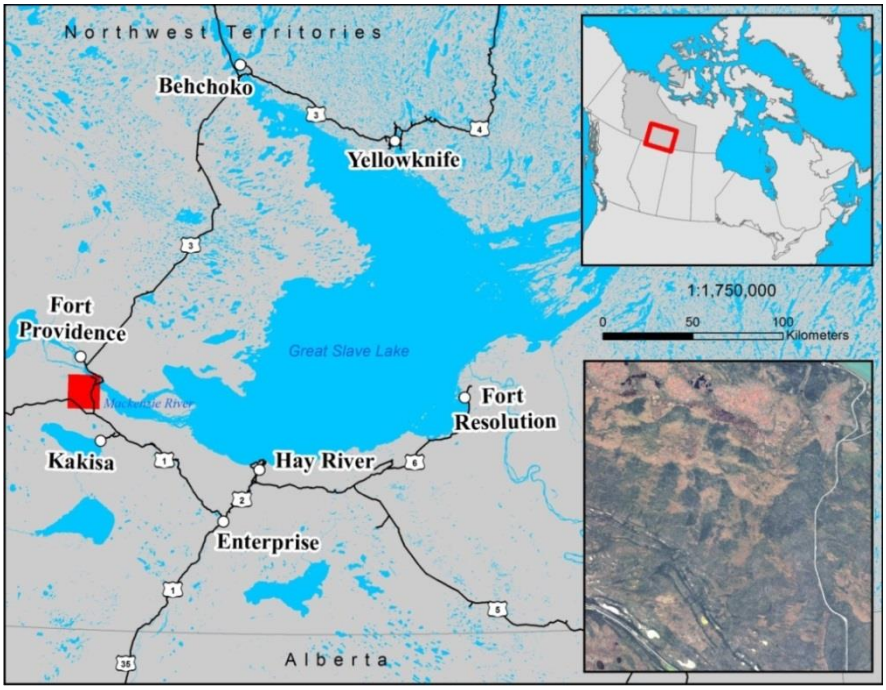

Figure 6: Location of the study area with QuickBird extent inset.

3.3. Climate

The Taiga Plains Mid-Boreal Ecoregion is characterized by the mildest climatic conditions in the Northwest Territories with short, cool summers, and long, cold winters. Average temperatures generally range from -28 °C in January to 16.5 °C in July, with a mean annual temperature ranging between -2.0 °C to -5.5 °C (Ecosystem Classification Group, 2007). The mean annual precipitation ranges between 310 mm and 410 mm, whereby the wettest period occurs between June and August. With regards to long-term climatic trends in the Mackenzie District, an increase of 2.4 °C in annual mean temperature has been documented between 1948 and 2011 (Environment Canada, 2011), whereby in a similar period the maximum temperature of the hottest month and minimum temperature of the coldest month increased by 0.7 °C and 5.5 °C, respectively (Lemprière et al., 2008). A trend of increasing annual precipitation (+ 23 mm) has also been documented (Lemprière et al., 2008).

3.4. Geomorphology and Soils

The study area is located in a region primarily composed of Upper Devonian bedrock, including shale and calcareous sandstone and siltstone (Day, 1968), and whereby the surficial geology is predominantly influenced by glacial activity. The entire study area was once covered by the Laurentide ice sheet during the last glaciation period, which formed Glacial Lake McConnell upon deglaciation. Both the ice sheet and glacial lake left fine- to coarse-textured glaciolacustrine and glacial till materials on upland areas (Day, 1968). Wave-generated beach ridge features can also be observed in the southern portion of the study area (Figure 7), which typically consist of course-textured alluvial and wave-washed till deposits (Ecosystem Classification Group, 2007). The soils of the upland regions consists of the Brunisolic (e.g., beach deposits) and Luvisolic (well-drained wooded areas) Orders, while poorly drained lowland areas consists of various Gleysolic (e.g., adjacent to wetlands), Organic (e.g., peat), and Crysolic (e.g., permafrost) soil orders (Day, 1968; Ecosystem Classification Group, 2007). The distribution of permafrost in the region is patchy and largely confined to organic terrain, and no observable trend in permafrost temperature and melting increase has been detected since 1984 (Smith, 2011). In general, the study area can be characterized by gently rolling glaciolacustrine plains overlaid by peatlands (Figure 8; Ecosystem Classification Group, 2007).

Figure 7: Beach-ridge landscape features (Government of Northwest Territories, 2005).

Figure 8: Gently rolling plains with peatlands (Government of Northwest Territories, 2006b).

3.5. Vegetation and Wetlands

The tree species considered in this study are distributed across the landscape in response of micro-topographical effects (Ecosystem Classification Group, 2007). Early to mid-successional mixed-wood forests consisting of white spruce *(Picea glauca*), balsam poplar *(Populus balsamifera*) and trembling aspen *(Populus tremuloides*) are dominant along the alluvial flats adjacent to rivers and contain diverse herb and shrub understories (Figure 9a). In these locations, late successional stands are characterized by white spruce and herb-feathermoss understories (Figure 9b). Stands consisting of jack pine (*Pinus banksiana*) and trembling aspen are generally found in dry, coarse-textured soils typical of beach ridges, and have sparse shrub, forb, and reindeer lichen (*Cladina mitis*) understories (Figure 10a) . Poorly drained stands are populated by black spruce *(Picea mariana*), tamarack *(Larix laricina*) and white birch *(Betula papyrifera*). The understory of these sites typically consists of Labrador tea (*Ledum groenlandicum*), mosses (*Sphagnum* spp., *Drepanocladus* spp.), leatherleaf (*Chamaedaphne calyculata*), and sedges (*Carex* spp.) (Figure 10b). Wildfire initiated by lightning strikes is the primary forest disturbance agent in the region whereby it alters the successional pathways of stands (Government of Northwest Territories, 2011b). However, no forest fire has been recorded in the study area since monitoring began in 1965, and the majority of forest stands are estimated to be at least 90 years old (GNWT Forest inventory, 1994; Canadian Forest Service 2005 ground inventory plots). Besides forests, the region is covered by thermokarst lakes and extensive fen complexes that are either treed, shrub, or sedge dominated (Ecosystem Classification Group, 2007).


A: White spruce and aspen stand with dwarf birch, juniper, willow, buffalo berry understory.


B: White and black spruce stand with feather moss, prickly rose, green alder, juniper understory.

Figure 9: White spruce mid-succession (A) and late successional (B) overstory and understory compositions.


A: Well-drained jack pine stand with black spruce, reindeer lichen, juniper, bearberry understory.


B: Poorly drained black spruce stand with sphagnum moss, Labrador tea, lichen understory.

Figure 10: Jack pine (A) and black spruce (B) overstory and understory compositions.

CHAPTER 4

Classification Using Reference Endmembers

4.1. Introduction

Boreal forests in North America represent a major biogeoclimatic zone, which regulates regional and global climates, cycles nutrients, acts as a reservoir for biological and genetic diversity and provides renewable resources, habitat, and recreational opportunities (Brandt, 2009). Given the importance of the North American boreal forest and its size relative to the entire circumpolar boreal zone (i.e., 25 % to 32 %; Brandt, 2009), an increased understanding of the distribution, composition, and structure of these forests is critical for sustainable forest management. This information is especially important with regards to long-term changes in temperature and precipitation patterns (Williamson et al., 2009; Environment Canada, 2011; Price et al., 2013) and the expansion and intensification of natural disturbances in the boreal zone (e.g., Krawchuk & Cumming, 2010; Safranyik et al., 2010; Peng et al., 2011). Because of these impacts, the acquisition of spatially referenced forest information is highly relevant to understand the rate of change, predict the outcome of these impacts on ecosystem function and diversity, and identify proper adaptation and mitigation strategies (Kurz et al., 2013; Lemprière et al., 2013).

Natural resource management agencies utilize spatially referenced inventory systems that result in the delineation of forest stands by polygons of similar species composition, height, and crown closure (Leckie & Gillis, 1995; Tomppo et al., 2010). Species composition, defined as the relevant proportion of tree species in a stand (Gillis & Leckie, 1993), is typically derived through an aerial photo-interpretation process

whose end goal is a forest inventory map (Hall, 2003). Mapping the species composition at a particular location is most relevant to operational forest management (Leckie, 1998), and is required to model stand volume and biomass (Boudewyn et al., 2007), net primary productivity (Tang et al., 2010), nutrient cycling (Prescott, 2002), carbon budgets (Kurz et al., 2013), and stand dynamics (Cogbill, 1985; Amos-Binks et al., 2010). While the aerial photo-interpretation approach has been changing with softcopy methods now being applied to digital photography, it remains a technology whose limits are being challenged, and it is cost prohibitive over large, remote forests such as those in northern boreal regions (Falkowski et al., 2009). The distance from major urban areas and general lack of infrastructure in northern boreal regions has resulted in very limited forest inventories. Therefore, it is partially in these regions that forest inventories must improve for regional and global carbon sink modeling (Pan et al., 2011; Chen et al., 2012).

To alleviate information gaps, forest management agencies increasingly rely on spatial data of land cover derived from remote sensing data (Franklin, 2001; Turner et al., 2003), as it allows frequent measurements of forests over a large geographic area. A recent review of the literature (Tables 3, 4, and 5) found that numerous remote sensing approaches have been documented to classify forest land cover at the tree species level in the North American boreal region and noted that a wide range of accuracies has been reported as a result of the numerous data sources and processing procedures that have been used in a variety of compositional and structural forest settings. With regards to Landsat TM/ETM+ imagery, the highest agreements between tree-species classifications and reference data have been obtained through discriminant analysis, the Enhanced-Classification method, and radiative transfer models (Franklin, 1994; Beaubien et al.,

1999; Peddle et al., 2004). Although high-spatial resolution sensors allow individual trees to be detected, only through image segmentation at the stand or crown level can this spatial refinement be effectively exploited (Gougeon, 1995a; Chubey et al., 2006; Mora et al., 2010). The range of accuracies reported for multispectral airborne imagery (e.g., 61 - 91 %; Franklin, 1994; Gougeon, 1995a; Coburn & Roberts, 2004) is similar to those reported from analysis of hyperspectral airborne imagery (e.g., 64 - 75 %; Martin et al., 1998; Sandmeier & Deering, 1999; Ustin & Xiao, 2001) for the same number of tree species classes (Chapter 2). However, direct comparisons between spaceborne multispectral sensors (e.g., Landsat ETM+) and hyperspectral sensors (e.g., EO-1 Hyperion) indicate that hyperspectral sensors outperform multispectral sensors (Goodenough et al., 2003; Staenz & Held, 2012). In general, optical remote sensing techniques have had only moderate success in mapping the distribution of tree species due to the spectral similarities between tree species and the large intra-species variation in spectral response as a result of complex forest canopies.

The literature review highlighted that remote sensing capabilities to derive tree species information of northern boreal forests are unknown due to the absence of studies in these regions (Chapter 2, Figure 1). The performance of the documented remote sensing approaches remains to be investigated in forests characterized by lower density, open stands where understory ground vegetation is a significant component of pixel-level reflectance and where stand structural variation is high. A classification approach based on spectral mixture analysis (SMA; Adams et al., 1993; Roberts et al., 1998), whereby mixed pixels are decomposed to physically meaningful components of sunlit canopy, background, and shadow (i.e., endmembers), may be suited to obtain species information

about northern boreal forests. The selection of appropriate endmembers, however, is important for successful spectral mixture analysis (Tompkins et al., 1997). With respect to the background component of northern boreal forests it is yet to be determined whether this can be represented by endmember spectra of the most dominant understory species in a stand or if the endmember spectra must consider the heterogeneity of the understory (Figures 9 and 10). Because the fractional cover of understory species is often not known, requires field observation, and is difficult to estimate consistently. Therefore, it was of interest whether endmember spectra require this information to approximate the background heterogeneity.

Another uncertainty is the degree to which information derived through remote sensing approaches can be integrated into current forest inventories, as image classifications of boreal forests at the species level generally involve the discrete labeling of pixels that constitute the greatest proportion within a stand (i.e., the leading species). This indicator is different than what professional foresters refer to as species composition, which indicates the relative proportion of most or all tree species in a stand to the nearest 10 percent (Gillis & Leckie, 1993). The definition and approach used to determine species composition (and thus the leading species) differ among jurisdictions and in the literature, whereby it can be measured per percentage crown closure, basal area, stem density, or gross volume (Gillis and Leckie, 1995). These definitions may not provide the same relative abundance estimates and identify the same tree species as dominant in a stand. It is therefore important to determine whether remotely sensed imagery is sensitive to how the leading species is characterized on the ground. Although Congalton and Biging (1992) found a strong agreement between visual calls of the

leading species based on stand volume and basal area field measurements, no further research has been conducted regarding this matter. To address unknowns regarding the sensitivity of remotely sensed imagery to field-based description of leading species and the influence of the type of background endmember used for SMA, this study addressed the following two research questions:

1. Is the determination of leading species from Landsat TM imagery influenced by its description from field-based inventory metrics?
2. Does the use of background endmembers defined by single species or mixed species spectra influence the discrimination of leading species?

4.2. Methods

4.2.1. Study Area

A study area within the Northwest Territories, Canada was selected based on the presence of representative northern boreal tree species, accessibility of the terrain, availability of suitable, cloud-free satellite imagery, and the availability of ground-reference datasets. The study area is located within the Taiga Plains Ecozone, an Ecozone which covers the western Northwest Territories, the northeast corner of British Columbia, and northern Alberta (Ecological Stratification Working Group, 1995). Most of the timber productive forests occur within the southern portion from which an 18-km x 19-km study area was located 20 km south of Fort Providence, NWT (Figure 6). This region belongs to the Great Slave Lowland Mid-Boreal Ecoregion according to the Ecosystem Classification Group (2007).

The tree species considered in this study are distributed along environmental gradients of soil conditions, drainage, micro-topographical effects, and disturbance histories (Fowells & Means, 1990; Ecosystem Classification Group, 2007). Early to mid-

successional mixed-wood forests, consisting of white spruce *(Picea glauca*), balsam poplar *(Populus balsamifera*) and trembling aspen *(Populus tremuloides*), are dominant along the alluvial flats adjacent to rivers, and contain diverse herb and shrub understories (Figure 9a; Ecosystem Classification Group, 2007). In these locations, late successional stands are characterized by white spruce and herb-feather moss understories (Figure 9b). Dense to open stands consisting of jack pine (*Pinus banksiana*) and trembling aspen are found in dry, coarse-textured soils associated with beach ridges, and typically have sparse shrub, forb, and reindeer lichen (*Cladina mitis*) understories (Figure 10a). Colder, poorly drained sites are populated by black spruce *(Picea mariana*), tamarack *(Larix laricina*) and white birch *(Betula papyrifera*), whereby the understories typically consist of Labrador tea (*Ledum groenlandicum*) and mosses (*Sphagnum* spp., *Drepanocladus* spp.) (Figure 10b).

4.2.2. Data Collection

4.2.2.1. Imagery

For this study, imagery was needed which can be used cost-effectively at an operational forest-management level. Therefore, a Landsat-5 TM (Table 6) scene acquired on July 8, 2004 was downloaded from the United States Geological Survey data archive using the GLOVIS interface (Path/Row: 48/17). This scene was the most appropriate with respect to the timing of the forest inventory data (July 2005) and the phenological stage of the spectral field data (July 16-22, 2013). Landsat-5 TM radiance data were atmospherically corrected to surface reflectance using Fast Line-of-sight Atmospheric Analysis of Spectral Hypercubes (FLAASH) in ENVI 4.8 with a Sub-Arctic

Summer atmospheric model and rural aerosol model. Band 1 and 2 were excluded to reduce the influence of atmospheric haze (Chavez, 1988).

Table 6: Landsat-5 TM sensor characteristics.

Sensor Specifications		**TM Bands**		
Launch	March 1, 1984	Band number		Wavelengths (µm)
Number of bands	7	1	Blue*	0.45 - 0.52
Spectral range	0.45 – 12.5 µm	2	Green*	0.52 - 0.60
Revisit time	16 days	3	Red	0.63 - 0.69
Image size	185 km x 172 km	4	Near-IR	0.76 - 0.90
Orbit	Sun-synchronous (705 km)	5	Near-IR	1.55 - 1.75
Orbit period	98.9 min	6	Thermal*	10.4 - 12.5
Status	Decommissioned (2013)	7	Mid-IR	2.08 - 2.35

Source: United States Geological Service (2013). * Bands were not included in the analysis.

4.2.2.2. Forest Inventory Data

Forest inventory data were collected in July 2005, whereby 20-m x 20-m plots were distributed in stands of jack pine, white spruce, black spruce, trembling aspen, and various mixed-woods (Hall & Skakun, 2007). Forest plots were located at least 100 m away from roads, cut lines, water bodies, and non-forested areas, and were generally within 500 m of the nearest road for ease of accessibility. Plot centres were established using a pigtail with flagging tape, after which the locations were recorded using a Trimble differentially corrected GPS system (UTM Zone 11, NAD83). Measuring tape and a compass were used to mark the cardinal (i.e., N, W, S, E) and intercardinal (i.e., NW, SW, SE, NE) points of the plot with flagging tape and to determine plot boundaries. The species, diameter at breast height, and height were recorded for every tree that was at least 1.3 m in height and 5 cm in diameter breast height. Because northern boreal forest stands typically contain a very large number of small trees, the same measurements were recorded for a selection of small trees (i.e., diameter breast height less than 5 cm, and a height of 1.3 m or greater) albeit within a smaller 10-m x 10-m quadrant. The stand attribute estimations of small trees were subsequently multiplied by 4 to represent the

entire contribution of the small trees within the plot. Crown-closure estimates were obtained at the intercardinal corners of the plot (n = 4) and within the plot at mid-corner locations (n = 5) using a spherical densitometer. Fractional cover of understory species was visually estimated for the six most dominant species in 5-% increments for each plot.

Using these data, the species composition of each plot was determined using two field-descriptions: 1) per fraction of total basal area of all trees >1.3 m in height, 5 cm in diameter, i.e., "*All trees*", 2) per fraction of total basal area of the dominant/co-dominant trees, i.e., "*Dom/Co-dom*". Lorey height was selected as the threshold to identify the dominant and co-dominant trees, and is defined as the basal area weighted average tree height at plot scales (Naesset, 1997). An ocular stand call of the overstory ("*Ocular AVI Call*") was also made to record the species composition, height, and crown closure of the stand following the Alberta Vegetation Inventory Interpretation (AVI) Standards (Alberta Sustainable Resource Development, 2005). AVI is an inventory method by which forest inventory data is collected on the ground or from aerial imagery. Lastly, species composition information for each stand was also extracted from a photo interpretation of a 1:20,000 black/white aerial photo (1994), which was conducted by a third-party contractor and on file at the GNWT Forest Management Division ("*GNWT Photo*").

A total of four different field-based descriptions of species composition were acquired, which were used to identify the leading species. Because stands are inherently open from a spaceborne sensor perspective, of interest was to which field-based description the imagery was most sensitive to. The "*All trees*" field-based description represents the leading species when basal measurements of all trees above a minimum threshold were included in the determination of species dominance. Spaceborne sensors

may not receive photons from shaded individuals in the lower canopy and, therefore, the "*Dom/Co-dom*" indicator includes a minimum height threshold to limit the determination of species dominance to only those individuals that were present in the upper canopy. As basal measurements are time consuming, the "*Ocular AVI call*" description identified the leading species through a faster visual estimation of the overstory. The "*GNWT Photo*" indicator expressed the leading species derived through an aerial photo interpretation, and enabled the comparison with the conventional method of large-area forest inventories.

4.2.2.3. Spectral Field Data

Spectral endmember data were collected within the forest inventory plots from July 16 to 22, 2013, which coincided with the same phenological stage of the Landsat-5 TM imagery. An Analytical Spectral Devices (ASD) Field Spec Pro spectroradiometer was used to record the spectral properties of vegetation samples between 350 – 2,500 nm within three hours of local solar noon. Sunlit-background endmember spectra were measured in-situ at ground-level, with sunlit-canopy endmember spectra obtained from samples extracted from the tree canopy that were arranged in 30-cm diameter optically thick stacks to ensure sufficient target coverage given the sensor field-of-view (FOV) (McCoy, 2005). Optically thick stacks allow for consistent sampling of vegetation, albeit that the natural structure and geometry of branches is not preserved and that reflectance is overestimated (Peddle, 1998; Peddle & Smith, 2005). Instrument calibration was performed using a levelled Spectralon panel (Labsphere Inc.), after which multiple measurements were taken in reflectance mode at various FOV by raising or lowering the pointed fore-optic lens (25°) between 15 cm and 40 cm. At these heights, the FOV ranged between 7 cm and 19 cm in diameter. Whenever possible, measurements were taken

when direct solar flux was the dominant incident radiation, and instrument calibration was performed for each vegetation target (< 5 minutes) to avoid differences in illumination conditions (Goetz, 2012). The dense understories typical of northern boreal forests did not permit the pistol grip to be mounted on a tripod. However, it remained handheld in a near-nadir orientation for each sample (Figure 11). The operator was positioned behind the Spectralon panel and target directly in line with the solar irradiance to maintain a consistent viewing geometry relative to the solar azimuth throughout the sampling period (McCoy, 2005). Besides measurements of individual understory species, integrated spectra were collected whereby multiple understory species were included in the FOV to approximate the heterogeneity of the background component when individual cover fractions were not known (Figure 12).

Figure 11: White reference measurement (left) and target measurement (right).

Figure 12: Optically thick stack of jack pine branches (left) and the area of an integrated measurement of orange moss and Labrador tea (right). Spectralon panel included for reference.

4.2.3. Data Processing

4.2.3.1. Field Spectral Data

Post-processing of spectral data was necessary to evaluate the quality of individual spectra and to prepare the data for spectral mixture analysis. Using metadata about the illumination conditions during spectral measurements, the consistency of all collected spectra (n = 559) were assessed. Spectra were deemed to be of sufficient quality when acquired during: 1) clear sky conditions, 2) or when clouds present did not obstruct direct sunlight, 3) or when no atmospheric noise could be seen in the spectra collected when the sun was obstructed. A total of 383 spectra were collected under such conditions, belonging to 7 tree species identified during the fieldwork campaign as well as 16 individual understory species and 12 mixed understory species groups (Table 7). A total of 129 tree species spectra, 134 individual background spectra, and 120 integrated background spectra, were further post-processed and represent many replications for each species. To account for the small percentage of incident irradiation not reflected by the Spectralon panel (Peddle et al., 2001), a second panel with known reflectance properties was used to obtain calibration coefficients using an integrating sphere with an illumination source angle of 8° to produce a hemispherical geometry[1]. These calibration coefficients were multiplied by the measured reflectance of each acquired spectra. Jumps in the spectra between the bordering regions of the three ASD sensors was resolved

[1] C. Coburn, personal communication, August 8, 2013

through a multiplicative correction (Dorigo et al., 2006), after which the spectra were resampled to Landsat-5 TM spectral bands using the corresponding spectral response functions in ENVI 4.8.

Table 7: Number of endmember spectra for the sunlit canopy and background components.

Sunlit canopy [1] **(n = 129)**	**Sunlit background**	
	Single Species (n = 134)	**Integrated Species (n = 120)**
White spruce	Green moss	Reindeer lichen + Moss
Black spruce	Leather lichen	Reindeer lichen + Rose + Common bearberry
Jack pine	Reindeer lichen	Graminoid species + Litter
Aspen	Sphagnum moss	Reindeer lichen + Graminoid species
Larch	Labrador tea	Brown moss + Leather lichen
White birch	Yellow moss	Reindeer lichen + Red bearberry + Northern toadflax
Poplar	Crowberry	Yellow moss + Common bearberry + Graminoid species
	Brown moss	Rose + Yellow moss + Juniper
	Willow	Reindeer lichen + Rose + Common bearberry + Toadflax
	Juniper	Reindeer lichen + Juniper + Common bearberry
	Black moss	Reindeer lichen + Yellow moss + Common bearberry
	Red bearberry	Sphagnum moss + Labrador tea
	Green alder	
	Snowberry	
	Yellow-marsh saxifrage	
	Buffaloberry	

4.2.3.2. Spectral Mixture Analysis

Spectral mixture analysis (SMA) quantifies the proportion of each pixel that is occupied by a single set of the pure features occurring on the ground (i.e., endmembers), whereby the output is a fraction image for each endmember along with the error of fit (Adams et al., 1993). For each pixel, this model can be derived as follows:

$$R'_i = \sum_{k=1}^{N} f_k \, R_{ik} + \varepsilon_i \quad , \tag{1}$$

where the spectral mixture R'_i is the encoded reflectance in band i for each pixel, and modeled as the sum of the reflectance in band i for N image endmembers k, whereby each endmember is weighted by fraction f_k. The ε_i term represents the remainder between

the measured and modelled reflectance, and is expressed as a band residual. The fractions of endmembers that are allowed during SMA can be set to unconstrained (from $-\infty$ to ∞) or fully constrained (i.e., between 0 and 1). The condition that the fractions of endmembers must be summed to 1 for each pixel (i.e., fully constrained), or not (unconstrained) can also be set, whereby weakly constrained unmixing (i.e., sum of fractions ≤ 1) have been shown to improve unmixing results when not all endmembers are known (Shang et al., 2008). Model fitness can be assessed either by using the residual term or via the root mean square error (RMSE; Roberts et al., 1998) over the total number of bands (v):

$$RMSE_{(\lambda)} = \sqrt{\sum_{i=1}^{v} (\varepsilon_i)^2 / N} \quad (2)$$

For this study, Multiple Endmember Spectral Mixture Analysis (MESMA; Roberts et al., 1998) was chosen as an alternative to conventional SMA, as MESMA is not constrained by a single set of endmembers and allows the number and types of endmembers to vary on a per-pixel basis to account for spatial heterogeneity. Because MESMA is not constricted by the number of spectral bands, it has been successfully applied to obtain species abundance maps of a variety of different species in vegetated areas such as California (Dennison & Roberts, 2003b), Australia (Youngentob et al., 2011), and Hawaii (Somers & Asner, 2012). MESMA was facilitated by the open-source software plugin VIPER Tools available for ENVI (Roberts et al., 2007). It estimates sub-pixel fractions of endmembers and provides a raster image of the endmember models of best fit that represents a per-pixel land-cover classification image. MESMA shares characteristics of both fully constrained and unconstrained unmixing, whereby the sum of the fractions must equal 1.00, but where the individual endmember fractions are allowed

to be less than 0.00 and greater than 1.00 (i.e., partially constrained unmixing). A fraction criteria of -10 % and 110 % was empirically determined to optimize vegetation class accuracies by permitting MESMA to consider models that fit the measured reflectance of a pixel despite slightly physically unrealistic endmember fractions (Dennison & Roberts, 2003a; Thorp et al., 2013). A maximum RMSE criterion of 2.5 % was used to ensure that a candidate model was selected for the majority of pixels and to guarantee reasonable confidence in the accuracy of the candidate model selected (Roberts et al., 1998).

The Landsat TM imagery was unmixed using three-endmember models, whereby all possible combinations of sunlit canopy spectra of the four most dominant tree species (n = 93) and individual species background spectra (n = 134) were iteratively computed, and whereby the best model based on RMSE was selected as a combination of sunlit canopy, background, and shadow components. Because understories characteristic of northern boreal forests are typically dominated by more than one species, the imagery was also unmixed using combinations of sunlit canopy spectra (n = 93), integrated background spectra (n = 120), and shadow. To model the average background reflectance of the forest stands, the weighted average of individual understory spectra was calculated for each plot based on 2013 ocular field estimations of ground cover. Changes in understory diversity and relative abundance of species between 2005 and 2013 were expected, but due to the slow growth and absence of wildfire and other large forest disturbances in the study area (Hart & Chen, 2006), relative differences are assumed to be minor and within the expected error envelope of visual estimations. These weighted-average sunlit-background spectra were used in combination with all possible sunlit-canopy spectra and shadow in the third unmixing model. The rationale for the

development of three different understory spectral libraries was to determine whether the endmember spectra should consider the heterogeneity of the understory (i.e., single spectra versus spectra of mixed species), and if cover proportions of understory species must be known to approximate this diversity (integrated library versus weighted average library). After unmixing, the classification images produced by MESMA were regrouped to the four dominant species in the ground-reference dataset (i.e., white spruce, black spruce, jack pine, and aspen).

4.2.4. Accuracy Assessment

To assess the accuracy of the per-pixel image classification produced by MESMA, the shapefile of the inventory plots were converted to a point shapefile using the centroid function in ESRI ArcMap. To test whether differences exist in classification accuracy among field-based descriptions of leading species, the four ground-reference indicators of leading species were entered in the attribute table of the shapefile. This shapefile was used in the contingency matrix to determine the overall accuracy, the producer and user accuracy, and the Kappa estimate using the ground-reference plots. The overall accuracy of each classified image is the sum of the correctly classified plots divided by the total number of plots assessed (Congalton & Green, 2009). Individual class accuracies are represented by the producer accuracy (errors of omission) and user accuracy (errors of commission). The Kappa statistic is an estimate derived through Kappa analysis (Cohen, 1960), which is a measure of the proportional improvement by the image classifier over a purely random assignment of pixels to classes (Congalton & Green, 2009). The Kappa estimate is recognized as a powerful accuracy measure, because it takes non-diagonal elements of the contingency matrix into account and

addresses the probability of chance agreement. It can be used along with its variance to compare the accuracy of two classified images and determines if the contingency matrices are significantly different at a particular confidence level (CL) using the standard normal deviate (e.g., 95-% CL; Z-critical value = 1.96; Congalton & Green, 2009). Accuracy estimates were compared at a global level (i.e., all ground-reference plots combined) and for plots grouped by crown closure using ground observations of crown closure and range definitions from the Alberta Vegetation Inventory (Table 8).

Table 8: Crown closure classes of the Alberta Vegetation Inventory.

Crown Closure (%)	Stand call class	Authors' Interpretation
6 - 30	A	Very open forest
31 - 50	B	Open forest
51 - 70	C	Medium dense forest
71 - 100	D	Dense forest

Source: Alberta Sustainable Resource Development (2005)

4.3. Results

4.3.1. Field Inventory Data

A total of 48 field-inventory plots were established whereby their distribution highlight site access challenges typical of northern boreal forests (Figure 13). Plots were located in both compositionally pure (> 80 % abundance of one species) and mixed stands to take into account the heterogeneity of the forests in the study area (Table 9). The plots further reflect a wide range of stand structural characteristics common in the region. The majority were established in very open (n = 14) to open stands (n = 27) with crown closure estimates ranging between 16 % and 61 % (mean = 35 %). The average stand height of the inventoried stands was 12 m, with a range between 6 m and 21 m. Stem density estimates also indicated that the field inventory plots were selected over a wide variety of stands, ranging between 875 stems/ha and 3,600 stems/ha.

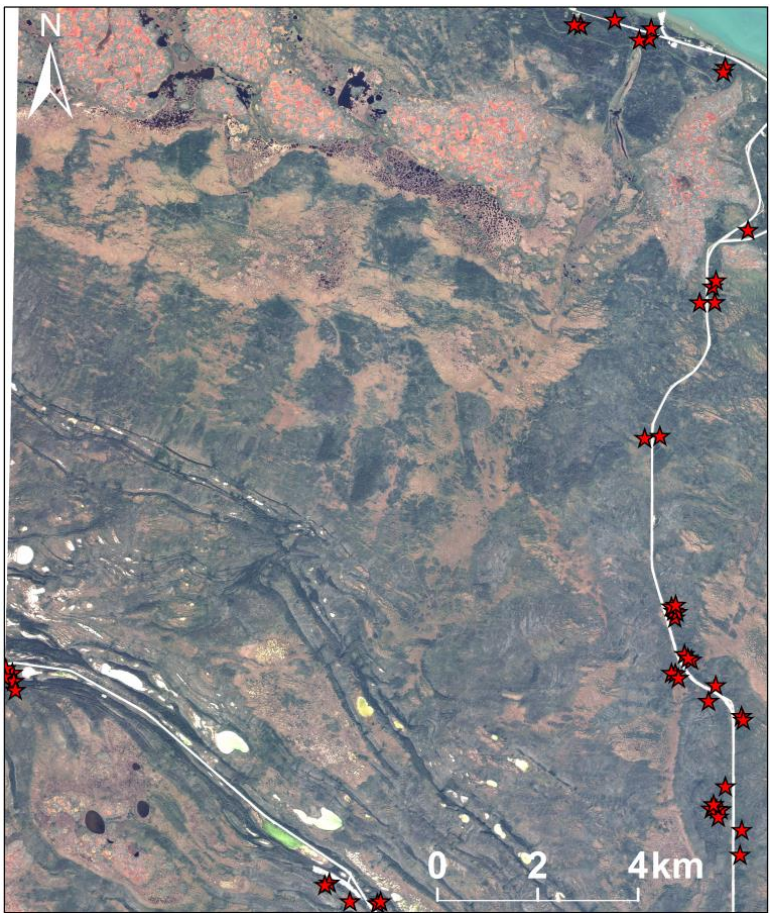

Figure 13: Distribution of field-inventory plots.

Table 9: Species composition and stand structure estimates for field inventory plots.

	Species composition [1]				Stand structure [2]		
Plot	***All trees***	***Dom/Co-dom***	***Ocular call***	***GNWT Photo***	**Stand Height**	**Crown closure**	**Stem Density**
01	Sw9A1	Sw9A1	Sw7Aw2Sb1	Sw7Sb3	15	60	2875
02	Sw9A1	Sw10	Sw9Aw1	Sb9Sw1	19	59	1075
03	Sw10	Sw10	Sw10	Sb9Sw1	16	56	2525
18	Pj5Sb5	Pj8Sb2	Pj10	Sb9La1	7	23	1975
19	Sb6Pj4	Pj8Sb2	Pj10	Sb9La1	6	21	2675
25	Pj5Sw5	Pj6Sw4	Pj8Sb2	Sb9La1	9	40	2750
26	Sb5Pj5	Pj7Sb3	Pj10	Sb9La1	8	39	3550
27	Sb9La1	Sb8La2	Sb9Lt1	Sb8Sw1L1	7	17	2800
48	Sw9Po1	Sw10	Sw8Aw2	Sw8Po2	18	61	2075
49	Sw9A1	Sw9A1	Sw9Aw1	Sw8Po2	19	57	1700
50	Sw10	Sw10	Sw9Aw1	Sw8Po2	18	53	2000
51	Sb10	Sb10	Sb10	Sb8La2	8	16	1025
52	Sb5Sw5	Sw5Sb5	Sb10	Sb10	10	23	1825
53	Sw10	Sw10	Sb10	Sb10	9	24	2025
54	Sb7Sw3	Sw8Sb2	Sb10	Sb9La1	9	22	1375
55	Sb9Pj1	Sb9Pj1	Sb10	Sb9La1	9	27	1700
56	Sb10	Sb9La8	Sb10	Sb8Sw1La1	10	18	1675
59	Sw6Sb4	Sw8Sb2	Sb10	Sb9La1	11	32	1575
60	Pj7Sw3	Pj9Sw1	Pj9Sb1	Pj7Sb2L1	12	27	1850
62	Pj9Sb1	Pj10	Pj9Sb1	Sb8Pj2	14	31	1950
63	Pj8Sb2	Pj8Sb2	Pj6Sb4	Pj9Sb1	15	27	1050
64	Pj10	Pj10	Pj10	Sb8Pj2	15	34	1700
65	Sb7Pj3	Pj6Sb4	Pj7Sb3	Sb7La2Pj1	8	30	2525
66	Sb8Pj2	Sb6Pj4	Pj6Sb4	Pj9Sb1	8	30	3600
67	Pj8Sb2	Pj10	Pj9Sb1	Sb8Pj2	13	34	1625
68	Sb5Pj5	Pj7Sb3	Pj6Sb4	Sb7La2Pj1	8	31	2575
69	Sb6Pj4	Pj5Sb5	Pj6Sb4	Sb7La2Pj1	8	25	2675
70	Sb8Pj2	Sb6Pj4	Pj6Sb4	Sb7La2Pj1	7	28	2825
71	Sb7Pj3	Sb7Pj3	Pj8Sb2	Sb7La2Pj1	10	32	1650
72	Sb6Pj4	Pj7Sb3	Pj8Sb2	Pj9Sb1	11	38	2100
73	Sb9La1	Sb9La1	Sb10Lt1	Sb8Sw1L1	8	24	2450
74	Pj8Sb2	Pj9Sb1	Pj9Sb1	Pj5Sb3Sw1L1	13	42	2200
75	Sb8Pj1Sw1	Sb5Pj3Sw2	Sb9Pj3	Sb7L1Sw1Pj1	9	38	2700
76	Pj10	Pj10	Pj9Sb1	Pj5Sb3Sw1L1	16	37	1075
77	Pj8Sb2	Pj9Sb1	Pj9Sb1	Pj5Sb3Sw1L1	13	38	2000
80	Pj6Sw4	Pj5Sw5	Pj8Sw2	Pj5Sb3Sw1L1	14	34	975
81	Pj8Sw2	Pj8Sw2	Pj7Sb3	Pj5Sb3Sw1L1	16	31	1450
82	Pj10	Pj10	Pj10	Pj5Sb3Sw1L1	15	31	1525
83	Pj8Sw2	Pj9Sw1	Pj9Sw1	Pj9Sw1	12	35	1825
84	Pj10	Pj10	Pj9Sw1	Pj9Sw1	14	34	1375
85	Pj9Sw1	Pj10	Pj10	Pj10	13	33	1850
86	Pj8Sb2	Pj8Sb2	Pj9Sb1	Sb6Pj3Sw1	10	34	2600
87	Pj7Sb3	Pj8Sb2	Pj8Sb2	Sb6Pj3Sw1	10	32	2100
88	Sw8Pj1A1	Sw8Pj2	Sw8Pj2	Sb8Pj2	17	33	875
89	A5Sw5	A6Sw3Pj1	Sw6Aw4	Sb8Pj2	18	53	1825
90	Sw10	Sw10	Sw10	Sw9Sb1	21	44	1275
91	Sw5Pj5	Pj7Sw3	Sw6Pj4	Sb8Pj2	12	45	2325
92	Pj6Sw4	Pj7Sw3	Sw6Pj4	Sw9Sb1	15	32	900

[1] Refer to Chapter 4.2.2.2. for species composition descriptions.

[2] Stand height (Lorey height) in metres, Crown closure in percentages, and stem density in stems per hectare.

The species composition estimates for each of the field-based descriptions were used to derive the leading species of stands. The results indicate that the descriptions do not provide the same relative abundance estimations nor identify the same tree species as dominant in a stand (Table 9). Considerable differences exist in the total number of plots belonging to each species (Figure 14), and although the *Dom/Co-dom* and *Ocular AVI call* indicators appear similar, a total of 10 plots were not labelled the same. These observed differences in leading species estimations therefore warrant the objectives of this study, and indicate that it was important to determine whether remotely sensed imagery was sensitive to how the leading species is characterized on the ground.

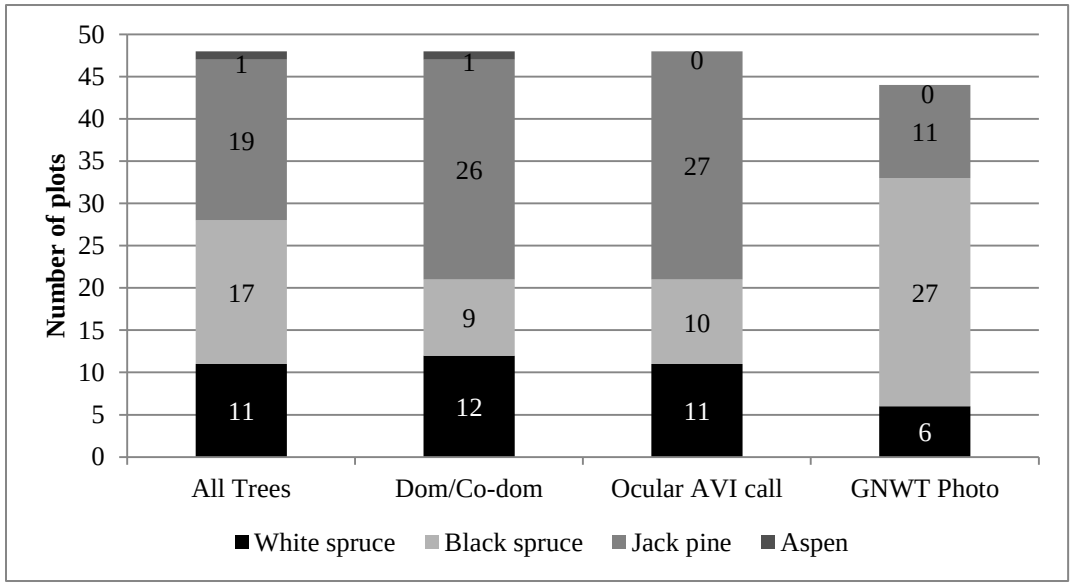

Figure 14: Number of plots belonging to each species for the four field-based descriptions.

4.3.2. Classification Accuracies for Entire Ground-Reference Dataset

The classification accuracies achieved in this study were relatively low, with overall accuracies ranging between 20 % and 50 %, and Kappa ranging from 0.00 to 0.31 (Table 10), and indicate the considerable challenges to which the leading species can be

identified in northern boreal forests using field reflectance spectra. Despite the low accuracies, clear patterns of classification results can be highlighted regarding the research objectives. Among the different field-based descriptions of leading species, the Landsat TM imagery was most sensitive to the indicator of leading species per fraction of total basal area of the *Dominant/Co-dominant* trees. This observation was consistent regardless of which understory library was used, which highlighted that consistent results can be obtained and that the use of this field-based description warrants adoption in subsequent studies.

As the leading species identified by the *ocular AVI call* of the overstory was the same as the *Dominant/Co-dominant* indicator in 38 of the 48 inventory plots, this field-based description performed second best among the field-based descriptions of leading species. The difference between these two indicators was only significant (80-% confidence level, Z-score = 1.332, Z-critical = 1.282) for the single understory spectral library. This significant difference was primarily due the improved agreement with black spruce leading stands, although those stands were highly mixed with jack pine. The differences in accuracy between the *All Trees* and *Dom/Co-dom* indicators ranged between 7 % and 19 % in overall accuracy and 0.09 and 0.26 in Kappa for all understory spectral libraries, yet was only significant for the weighted understory spectral library (90-% confidence level, Z-score = 1.716, Z-critical = 1.64). These differences were a result of a better discrimination of stands where jack pine was dominant in the overstory and black spruce was dominant in the understory. As the classification images consistently labelled such stands as jack pine dominant, it indicated that Landsat TM is most sensitive to trees present in the overstory. The results also highlighted that the

image classification show a low agreement with the *GNWT Photo* indicator of leading species (16 % - 34 % overall accuracy).

Table 10: Classification accuracies per field-based description and understory spectral library.

Understory library	***AVI Call*** [1]		***All trees*** [1]		***Dom/Co-dom*** [1]		***GNWT Photo*** [1]	
	OA (%)	Kappa	OA (%)	Kappa	OA (%)	Kappa	OA (%)	Kappa
Single	27	-0.03	35	0.09	42	0.18	27	-0.04
Integrated	33	0.04	23	-0.12	33	0.04	16	-0.32
Weighted	40	0.15	33	0.05	**52**	**0.31**	34	0.10

[1] Refer to Chapter 4.2.2.2. for leading species descriptions.
OA: Overall accuracy

The development of three different understory spectral libraries was to determine whether the endmember spectra should consider the heterogeneity of the understory and if cover proportions of understory species must be known to approximate this diversity. Interpretation of the results suggested that the weighted understory library performed the best in terms of overall accuracy and Kappa regardless if which field-based description of leading species was used (Table 9). For the *ocular AVI call* reference dataset, a gradual but consistent improvement in classification accuracy was observed when the understory spectra used for unmixing represent a greater diversity of vegetation components. Although this general pattern was not present for the other field-based descriptions of leading species, the best results achieved with the weighted spectra highlighted that approximated the complex understory vegetation better than the other two libraries, and that cover fractions must be known to generate representative spectra. The library containing spectra of individual vegetation components mapped the aspen stand correctly, but the lack of aspen dominated stands in the study area precludes any investigations as to why this is the case.

4.3.3. Classification Accuracies of Plots Grouped by Crown Closure

To determine whether the field-based description of leading species was dependent on crown closure, overall accuracy estimates were stratified by crown closure ranges using ground observations of crown closure and range definitions from the Alberta Vegetation Inventory. The results highlighted that Landsat TM imagery was most sensitive to the indicator of leading species per fraction of total basal area of the *Dominant/Co-dominant* trees regardless of crown closure range, and that this observation is consistent among understory libraries (Table 11). The image classification had the second highest correspondence to the leading species identified by the *ocular AVI call* of the overstory, yet only for very open (A) and open (B) stands. No differences in overall accuracy existed between the *All Trees* and *Dom/Co-dom* descriptions of leading species for medium dense stands because they identified the same species as dominant. Although some differences existed on a case-by-case basis, no apparent pattern of accuracy as influenced by crown closure can be highlighted regardless of approach used to characterize understory spectra (Table 11).

Table 11: Overall classification accuracy grouped by crown closure class.

Understory library	**Crown closure** [1, 2]	**Overall accuracy for field-based descriptions (%)**			
		AVI Call	*All trees*	*Dom/Co-dom*	*GNWT Photo*
Single background	A	21	29	36	29
	B	26	33	41	22
	C	43	57	57	29
Integrated background	A	50	36	57	29
	B	30	19	26	11
	C	14	14	14	0
Weighted background	A	43	43	71	29
	B	33	22	41	22
	C	57	57	57	71

[1] Crown closure classes: A: 6 % to 30 %, B: 31 % to 50 %, C: 51 % to 70 %.

[2] Sample size: A (n = 14), B (n = 27), C (n = 7).

4.3.4. Fitness Metrics

Besides estimations of classification accuracy, the performance of the understory libraries can also be measured through fitness metrics that are indicative of how well the modeled reflectance derived through MESMA matches the measured reflectance of the pixels. The RMSEs for the single and integrated spectral library were less than 0.00025 of the original pixel reflectance when all inventory plots were grouped together as well as for individual crown closure classes (Figure 15). The RMSEs for the weighted spectral library were substantially larger (0.001), but remains small relative to the overall pixel reflectance. In general, the RMSE of open stands (B) was twice as large as the RMSE of very open (A) and medium dense stands (C). These reported RMSEs were much smaller than the established threshold and accepted norm of good results (i.e., 0.025; Roberts et al., 2007), and indicate the appropriate use of spectral endmembers in this study. It is evident that the higher RMSE for the weighted spectral library is primarily due to the larger band residuals in TM band 5 (1.67 μm centre wavelength) and band 7 (2.24 μm centre wavelength) located in the shortwave-infrared spectrum (Figure 16).

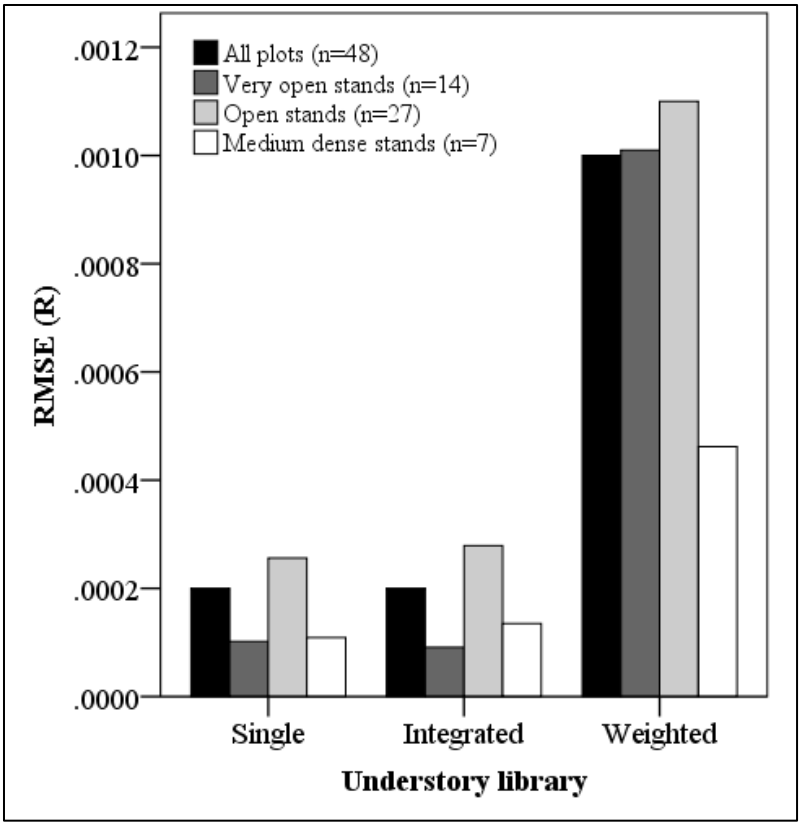

Figure 15: Fitness (in RMSE) of SMA for each understory spectral library.

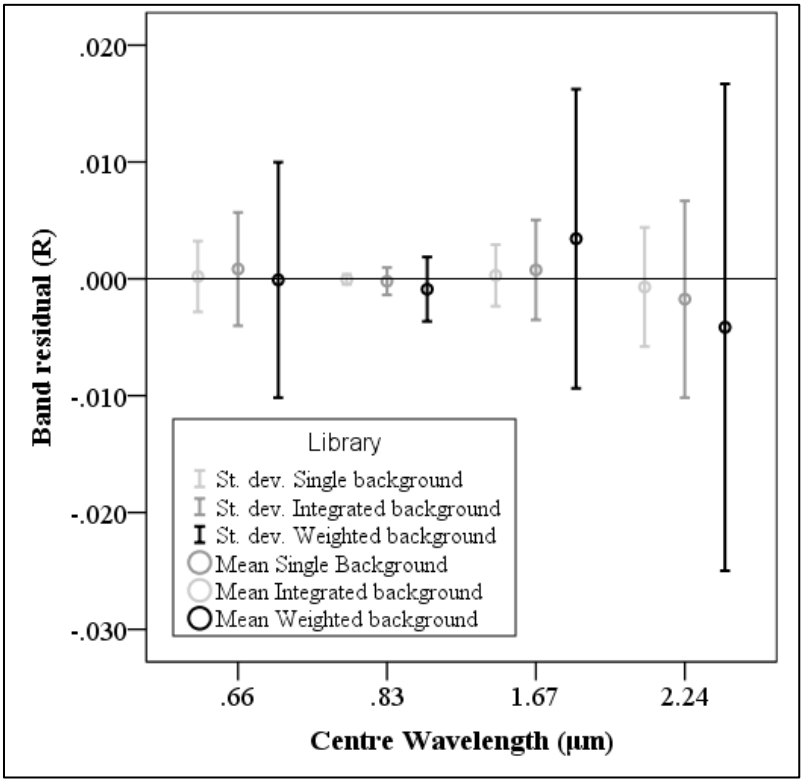

Figure 16: Mean and standard deviation of band residuals for each spectral library.

4.3.5. Distribution of Tree Species

Because each individual pixel was classified according to the endmember model with lowest RMSE, noticeable pixelation is present in the species distribution maps (Figure 17). This pixelation was expected given the complexity of stand structure and species composition typical of northern boreal forests, and is not necessarily a mapping error. When the single understory spectral library was used for MESMA (Figure 17a), no noticeable spatial patterns of tree species can be observed. Figure 17b depicts the image classification produced when the integrated spectra of the understory was used, and shows the over-representation of black spruce (user accuracy = 17 %) and the under-representation of white spruce (reduction in producer accuracy from 50 % to 25 % between Figures 17a and 17b). In comparison, the image classification generated using the weighted understory spectra (Figure 17c) shows more distinct patterns for white spruce, black spruce, and jack pine.

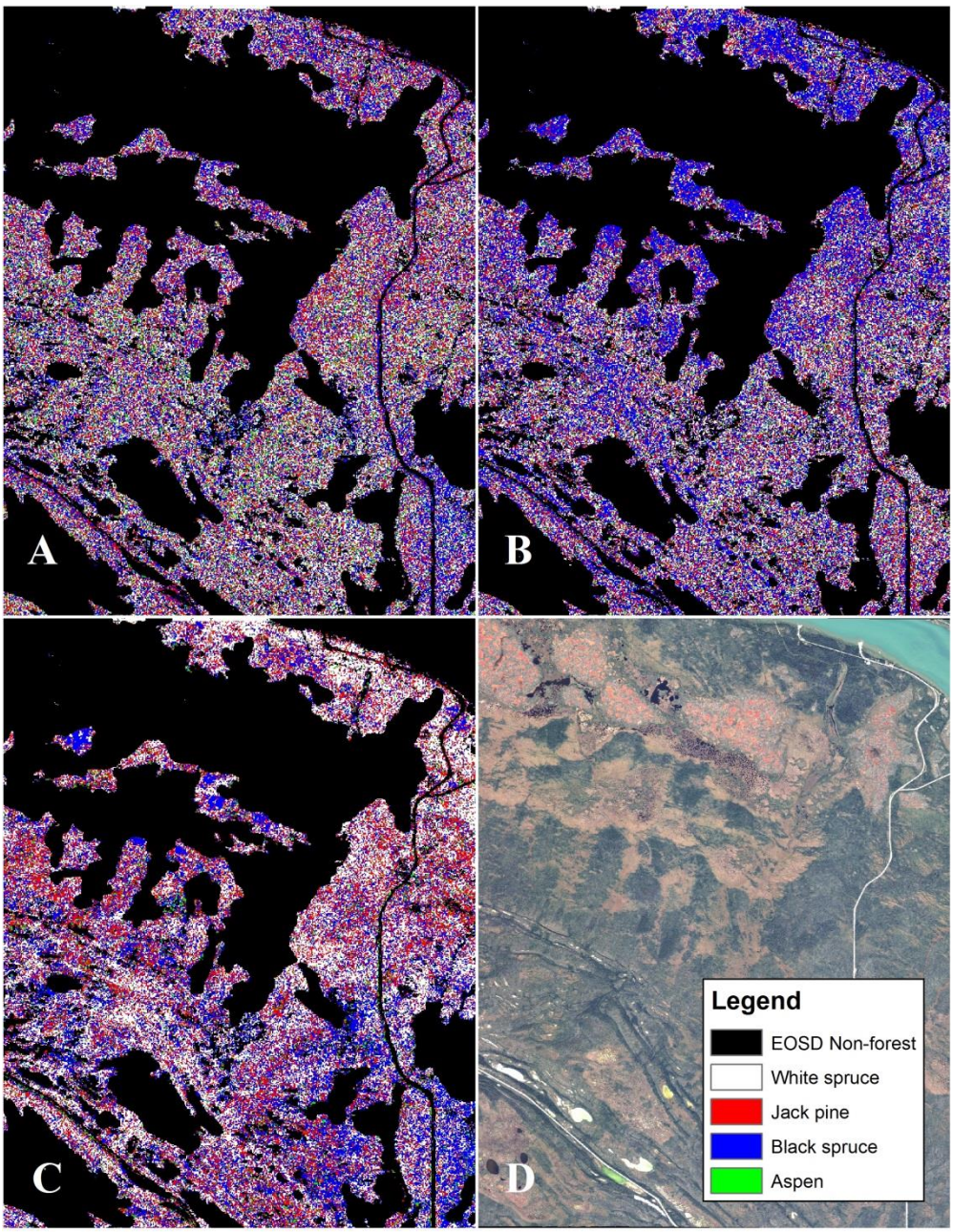

Figure 17: Tree species distribution maps using field-based spectra. Spectral libraries of the understory for: (A) single spectra, (B) integrated spectra, and (C) weighted spectra. A multispectral QuickBird image is provided for spatial reference (D).

To highlight the challenges regarding the discrimination between tree species, a contingency matrix for the image classification results was generated based on the weighted understory spectra and the *Dominant/Co-dominant* indicator of leading species as this combination was most successful of those evaluated (Tables 10 and 11; See

Appendix 1 for other matrices). Spectral confusion occurred to varying degrees depending upon tree species. The producer accuracy highlights the number of field plots that were classified to their known value. The low producer accuracy of jack pine is a result of confusion with black spruce and white spruce (Table 12). The confusion with black spruce was expected given that upland black spruce and jack pine often occur on the same well-drained sites with reindeer lichen understories (Figure 18). Among the field plots sampled for example, varying amounts of jack pine and black spruce was observed in 11 of the 26 jack pine dominant stands (Table 9). Jack pine dominated stands were also confused with white spruce, affecting 7 of the 26 jack pine stands (Table 9). Black spruce dominated stands were also confused with white spruce to a lesser degree. The confusion among these three species was expected as productive, well-drained sites often support all three species. The user accuracies, which indicate the reliability of the derived tree species map, show that the greatest confidence exists in the distribution of jack pine (i.e., 11 of the 14 jack pine labelled stands were actually jack pine dominant). Lower user accuracies exist for white and black spruce because of the predominant spectral confusion with jack pine. For example, even though 75 % of white spruce dominated stands were correctly classified, only 47 % of the pixels labelled as white spruce were actually white spruce dominant.

Table 12: Contingency matrix of the weighted understory image classification.

	Ground reference (# of stands)					**User**
Map prediction	Aspen	Jack pine	Black spruce	White spruce	Total	**accuracy**
Aspen	**0**	2	0	1	3	0 %
Jack pine	1	**11**	1	1	14	79 %
Black spruce	0	6	**5**	1	12	42 %
White spruce	0	7	3	**9**	19	47 %
Total	1	26	9	12	**48**	
Producer accuracy	0 %	42 %	56 %	75 %		
Overall accuracy = (25/48) 52 %						
Kappa = 0.31						

Figure 18: Well-drained upland mixed jack pine and black spruce stand (Plot 68).

4.4. Discussion

Three advancements were reported in this study. This study represented one of the first documented cases of tree-species classification using medium spatial resolution imagery in a northern boreal forest context. Second, it was determined that remotely sensed imagery was sensitive to how the leading species was characterized on the ground. Third, the degree to which the background endmember should approximate the complexity of northern boreal forest understories was assessed.

4.4.1. Field-based Descriptions of Leading Species

In this study, Landsat TM imagery was most sensitive to the indicator of leading species per fraction of total basal area of the *Dominant/Co-dominant* trees, whereby this observation was consistent among understory libraries and crown closure ranges. The

radiant energy received by the Landsat TM sensor was therefore mainly influenced by the upper forest canopy level and the highly reflective background vegetation at the expense of sub-canopy individuals. A total of 8 plots were labelled differently between the *All Trees* and *Dominant/Co-dominant* indicators of leading species, whereby a greater correspondence between the image classification and the latter indicator was achieved for plots of both very open (n = 3) and open (n = 5) stands. These results compared well with trends reported by other published studies (Chen et al., 2012), and expand upon general comments made by Pontius et al. (2005) and Plourde et al. (2007) who discarded basal-area related indicators of species composition as sub-canopy individuals were included in those accuracy assessments. The findings of this study also indicate that the Landsat TM image classification is consistent with, and meets the compliance for, forest inventories for operational-forest management which focus on the dominant/co-dominant trees in a stand (Government of Northwest Territories, 2006a).

Image classifications had the second highest agreement with the *ocular AVI call* indicator of leading species. When the results of the basal field measurements and ocular AVI call were expressed in a contingency matrix, an overall accuracy of 79 % and Kappa of 0.69 was obtained (i.e., 38 out of 48 plots were labelled the same). The strong agreement between the ocular call of the overstory and the basal-area indicator of leading species and their similarity in respective accuracy estimations suggests that Landsat TM is sensitive to both indicators of leading species. The majority of plots that were labelled differently were highly mixed in terms of species composition, which clarified the discrepancies between the two ground-reference indicators (e.g., a Sw_6Pj_4 *ocular AVI call* for a Pj_7Sw_3 plot by basal area of the *Dominant/Co-dominant* species). These results are

similar to preliminary work conducted by Congalton and Biging (1992), who reported an 85 % correspondence between field measurements and ocular calls.

This study further emphasized caution in the assumption that the results of the *GNWT aerial photo-interpretation* were sufficient for use as reference data. The lowest agreement between the Landsat TM image classifications was obtained with this indicator of leading species. When the leading species defined by *ocular AVI calls* and *Dom/Co-dom* are compared to the photo-interpreted map, overall accuracies were 60 % and 56 %, respectively. Similar accuracies (64 %) were obtained when a subset of 25 pure plots (> 80-% relative abundance for one species) were compared. These comparisons assume that the ground inventory plots were representative of the forest inventory polygons (e.g., species composition, structure), and that no micro-type or scaling differences occurred. The low user accuracies of black spruce (32 % – 34 %) suggests that the disagreements were predominantly a factor of the over-representation of black spruce in the photo-interpreted map as a result of its misidentification (e.g., black spruce label in a stand with a Sw_9Aw_{10} overstory and Sw_{10} understory) and over-estimation of its contribution to the overstory. The accuracy to which boreal tree species have been successfully mapped using aerial photo-interpretation generally ranges between 60 % and 80 % (Fent et al., 1995; Leckie & Gillis, 1995; Luther et al., 2006), whereby significant differences in relative proportions of tree species (by volume) can occur (e.g., in Ontario; Thompson et al., 2007). Although sufficient correspondence between aerial photo-interpreted maps and image classifications of tree species have been achieved in boreal forests in southern Canada (e.g., Peddle et al., 2004), the results of this study suggest that the forest inventory derived through aerial photo-interpretation was not

sufficient to assess the accuracy of image classifications in this study area. The low correspondence to field observations can to a certain degree be attributed to the time difference between the photo interpretation (1994) and the field measurements (2005) wherein stands have encountered structural and compositional changes through succession. However, from a tree species point-of-view, a 10-year difference would be minimal in areas of slow growth.

4.4.2. Understory Complexity

Considerable increases in classification accuracy and more distinct patterns of leading species were obtained when the weighted spectra were used for the background endmember. It is evident that good knowledge of the understory leads to a better characterization of the spectral response of this endmember and thereby improved classification results. The weighted spectral library outperformed the integrated spectral library, which suggests that field estimations of ground cover are necessary for improved species discrimination. Although field estimations of ground cover are time consuming and neither practical nor representative for large-scale forest mapping, it may be possible to link overstory compositions with understory compositions whereby a range of representative understory spectra can be generated using sets of slightly different relative abundances. Such weighted spectra could more easily accommodate the greater variation in understory compositions and relative abundances found at increased mapping extents. However, the performance of these spectra would be an area worthy of further investigation.

4.4.3. Challenges

The achieved classification accuracies were lower than average in the context of other studies conducted in the southern boreal forests using Landsat TM or similar sensors (e.g., Franklin, 1994; Dymond et al., 2002; Peddle et al., 2004). Due to the frequency of cloud cover at high latitudes (Rees et al., 2002), it was difficult to obtain cloud or haze free imagery for the phenological stage in which the spectral field data were acquired (e.g., one appropriate scene within a 10-year window). The imagery used in this study contained considerable haze over much of the study area that could not be reduced through atmospheric correction. Although the vegetation samples used for the collection of endmember spectra were controlled, they may have not matched the tree species in the image because of differences in atmospheric conditions (Song & Woodcock, 2003). Furthermore, reflectance spectra were acquired at a branch scale while image classification was conducted at the stand scale. This difference in scale causes spectral confusion among tree species, as it has been shown that the separability of coniferous tree species at the branch scale is greater than at the stand scale (Roberts et al., 2004). Because of scaling differences and atmospheric influences, the application of image endmembers is worthy to investigate further.

Stand structure also influenced the classification performance of MESMA. In this study area, stand height is inversely related to stem density ($R = -0.55$, $P < 0.001$), similar to other forests in the Northwest Territories and elsewhere in the boreal whereby older stands are taller and at lower densities than younger, shorter, and more dense stands (Gerylo et al., 2002; Brassard & Chen, 2006). The distribution of stand height between correctly and incorrectly classified was significantly different for very open stands (Table

13), whereby challenges with successful species discrimination were encountered in stands taller than 8 m (Figure 19). Taller stands often exhibit greater multiple scattering of photons between the canopy and forest background, which causes non-linear mixing of scene components which affects spectral mixture models (Borel & Gerstl, 1994; Gemmell, 2000; Chen et al., 2012). MESMA cannot accommodate multiple scattering as it assumes that photons interact with a single component within the FOV (Roberts et al., 1998). Multiple scattering may have led to fractional abundance errors or higher RMSEs in these very open stands, which when exceeded beyond user-defined thresholds could have caused MESMA to model a particular pixel with an incorrect sunlit canopy endmember. Therefore, when stands become more structurally complex, multiple scattering complicates the radiant energy received by the Landsat TM sensor and influences MESMA's ability to label plots according to its most dominant species. Non-linear spectral mixture models may lead to some incremental improvements in classification accuracy as such approaches typically improve endmember fraction estimations (Somers et al., 2009a; Quintano et al., 2012).

Table 13: Strength (p-values) of Independent Samples Mann-Whitney U-test for equal distributions between correctly and incorrectly classified stands.

		Field-based description of leading species			
Crown closure	**Variable**	***AVI call*** [1]	***All trees*** [1]	***Dom/Co-dom*** [1]	***B/W Photo*** [1]
A (6%-30%)	Stem density	0.23	0.23	0.11	0.30
	Stand height	**0.01**	**0.08**	**0.03**	0.14
	Crown closure	0.11	0.57	0.24	0.64
B (31%-50%)	Stem density	0.22	0.49	0.22	0.93
	Stand height	0.15	0.79	0.10	0.44
	Crown closure	0.36	0.38	0.64	0.98
C (51%-70%)	Stem density	0.63	0.63	0.63	0.86
	Stand height	0.86	0.86	0.86	0.57
	Crown closure	0.63	0.63	0.63	0.38

[1] Refer to Chapter 4.2.2.2. for leading species descriptions.

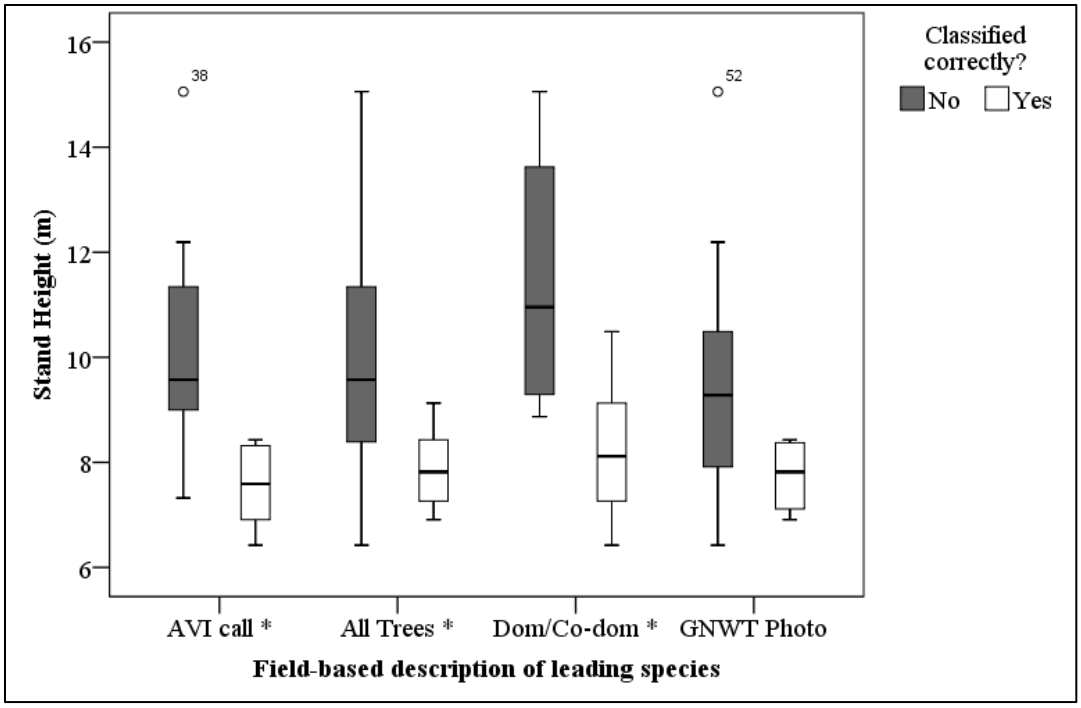

Figure 19: Distribution of stand height for correctly classified and incorrectly classified very open stands. * Indicates a significant difference at a 90-% confidence level.

4.5. Conclusions and Future Research

Satellite-based remote sensing is increasingly used to derive information products of forests over large areas. However, documented approaches are either untested or not suitable for the open forest stands of northern boreal forests. Due to the open and complex character of forest stands at higher latitudes, of interest was whether Landsat TM was sensitive to how the leading species of a stand can be described on the ground, and whether the endmember spectra representing the background component in MESMA should approximate the heterogeneity of the background vegetation. Interpretation of the results suggested that Landsat TM imagery was most sensitive to the indicator of leading species per fraction of total basal area of the dominant/co-dominant trees, and that this observation was consistent among crown-closure ranges. Inclusion of all the trees in the determination of leading species was not necessary. This finding indicated that the image

classification was consistent with forest inventories for operational-forest management, as they typically focus on the dominant/co-dominant trees in a stand. As well, the highest similarities with ground-reference data were obtained when the full heterogeneity of the understory was approximated through the calculation of a weighted average of individual spectra with ground-cover abundances known. Knowledge of understory compositions and relative abundances led to a better characterization of the spectral response of the background endmember and thereby improved classification results to 71 %, 41 %, and 57 % for very open, open, and medium dense forest stands, respectively (overall accuracy = 52 %, Kappa = 0.32).

The identified atmospheric and scaling issues associated with the use of reference endmembers warrant an investigation in the application of image spectral endmembers. The use of image spectral endmember avoids these challenges, and could leverage multi-temporal imagery to exploit phenological differences among tree species early and late in the growing season as a means of improving the image classification results reported in this study.

CHAPTER 5

Classifications Using Image Endmembers

5.1. Introduction

Forests are key ecosystems that host high levels of biodiversity, influence biogeochemical cycles, and provide ecosystem services (Kimmins, 2003). Forest management decisions often require information about species composition as an important component of government-based forest inventories (Leckie & Gillis, 1995), where species composition is defined as the relevant proportion of tree species in a stand (Gillis & Leckie, 1993). In the boreal forest zone, this information is especially relevant given the susceptibility of particular tree species to large-scale insect disturbances (Cullingham et al., 2011; de la Giroday et al., 2012), moisture stress (Michaelian et al., 2011; Griesbauer & Green, 2012), and climate-induced alterations to the wildfire regime which have the potential to introduce changes to the boreal landscape that could exceed the direct influence of climate change on species composition and structure (Williamson et al., 2009; Price et al., 2013). Information about species composition can be difficult to collect on the ground due to site access challenges and budget limitations. The use of aerial photo-interpretation techniques for forest inventory purposes is common for large-area forest inventories (Michalak et al., 2002; Hall, 2003), and despite recent transitions to softcopy methods being applied to digital photography, it remains a technology whose limits are being challenged and is cost prohibitive over large, remote forests (Falkowski et al., 2009). This lack of complete and up-to-date forest inventories is especially apparent in northern boreal forests (Government of Northwest Territories, 2011b; Pan et al., 2011), which subsequently drives the need to alleviate information gaps using remote sensing.

Northern boreal forests can be characterized by lower density, open forest stands (i.e., crown closure generally less than 60 %) where understory ground vegetation is a significant component of pixel-level reflectance and where stand structural variation is high (Franklin et al., 2003; Ecosystem Classification Group, 2007). Given the small crowns typical of tree species in the northern boreal zone, the canopy, understory, and shadow components mix together spectrally and create mixed pixels at both high- and medium- spatial resolution (e.g., 2-m, 30-m). Therefore, conventional pixel-level approaches for image classification at the tree species level (e.g., Franklin, 1994; Dymond et al., 2002; Dalponte et al., 2008) are not considered suitable for the open stands. Instead, a classification approach based on spectral mixture analysis (SMA; Adams et al., 1993), whereby mixed pixels are decomposed to physically meaningful components of sunlit canopy, background, and shadow (i.e., endmembers), may be suited to derive information about tree species in northern boreal forests (Roberts et al., 1999).

A key to successful spectral mixture analysis is the appropriate selection of endmembers (Tompkins et al., 1997), which involves identifying the number and type of endmembers and their corresponding spectral signatures. An endmember is an idealized pure signature of a class, and should represent a fundamental spectral component to the image analysis process (Adams et al., 1993). Endmembers may be derived through field measurements with a spectroradiometer (i.e., reference endmembers), directly from the image data (i.e., image endmembers), or through canopy reflectance models (Peddle et al., 1999). While endmember spectra are often measured in the field, this is not always possible because of technical and budgetary limitations. Because of differences in atmospheric conditions between the reference endmembers and the image and the scale at

which the endmember spectra are applied (Chapter 4; Drake et al., 1999), the use of reference endmembers may not be suitable to discriminate among coniferous tree species at the stand scale (Roberts et al., 2004). As an alternative, endmember spectra can sometimes be derived directly from an image, which avoids these challenges.

Although numerous endmember extraction algorithms (EEA) exist to find pure image endmembers, such as N-FINDR (Winter, 1999), pixel purity index (Boardman, 1994), orthogonal subspace projection (Harsanyi & Chein, 1994), principal component analysis (Bateson & Curtiss, 1996), vertex component analysis (Nascimento & Bioucas Dias, 2005), and iterative error analysis (Neville et al., 1999), the proper specification of image endmember spectra is not always possible. As an example, for the background component there may be no suitable open areas that match or exceed the pixel area (spatial resolution). The inherent wide variability in the diversity and composition of understory vegetation (Figures 9 and 10) would challenge the selection of homogenous spectra for both the sunlit canopy and background endmembers. Therefore, an important question was whether endmember spectral impurity would influence image classifications at the tree species level?

Within a forest context, pixels at almost any spatial resolution are inherently mixed at the branch, crown, and stand scale due to the three-dimensional architecture of foliage and non-photosynthetic tissue, which subsequently creates variations in radiation regime (Asner, 1998). With respect to image endmembers, because they can be "expressed as mixtures of spectra of meaningful scene components, defined by the field scientist" (Smith et al., 1990, p. 7), they may not be spectrally pure. Other EEA methods do not assume the presence of pure endmembers in the imagery, and generate virtual

endmembers which are not necessarily present in the imagery itself (Tompkins et al., 1997; Plaza et al., 2012). While considerable research has been undertaken to automatically extract pure image endmembers using EEAs, little is known about the application of meaningful image endmembers identified using forest inventory information, and how the performance of these endmember spectra compare with field-based spectral measurements for image classifications at the leading species level (i.e., the tree species most dominant in a stand). Furthermore, as the degree to which tree species can be discriminated may be influenced by the stage of vegetative phenology at the time of image data collection (Schriever & Congalton, 1995; Mickelson et al., 1998; Wolter & Townsend, 2011), of interest was whether multi-temporal imagery acquired during the growing season improves discrimination of leading species in northern boreal forests. The objective of this study was to investigate these unknowns, and was achieved by answering the following research questions:

- Are there differences in classification performance between SMA-based image classifications using image-derived spectra and field-based spectra?
- Is the performance of image-derived spectra dependent on the type of forest inventory information (e.g., by basal area or crown closure) used to select representative sunlit canopy and background components?
- Would the use of multi-temporal Landsat TM imagery to represent different stages of vegetative phenology improve the determination of leading species?

5.2. Methods

5.2.1. Study Area

A study area within the Northwest Territories, Canada was selected based on the presence of representative tree species, accessibility of the terrain, availability of suitable, cloud-free satellite imagery, and the availability of ground-reference data. The study area is located within the Taiga Plains Ecozone, an Ecozone that covers the western Northwest Territories, the northeast corner of British Columbia, and northern Alberta (Ecological Stratification Working Group, 1995). Most of the timber productive forests occur within the southern portion of the Ecozone from which an 18-km x 19-km study area was located 20 km south of Fort Providence, NWT (Figure 6). This region belongs to the Great Slave Lowland Mid-Boreal Ecoregion (Ecosystem Classification Group, 2007).

The tree species considered in this study are distributed across the landscape in response of micro-topographical effects (Ecosystem Classification Group, 2007). Early to mid-successional mixed-wood forests, consisting of white spruce *(Picea glauca*), balsam poplar *(Populus balsamifera*) and trembling aspen *(Populus tremuloides*), are dominant along the alluvial flats and contain diverse understories (Figure 9a). In these locations, late successional stands are white spruce dominant with herb-feather moss understories (Figure 9b). Stands consisting of jack pine (*Pinus banksiana*) and trembling aspen are found in dry, coarse-textured soils associated with beach ridges, and typically have sparse shrub, forb, and reindeer lichen (*Cladina mitis*) understories (Figure 10a). Cold, poorly drained sites are populated by black spruce *(Picea mariana*), tamarack *(Larix laricina*) and white birch *(Betula papyrifera*), with Labrador tea (*Ledum groenlandicum*) and mosses (*Sphagnum* spp., *Drepanocladus* spp.) understories (Figure 10b).

5.2.2. Data Collection

5.2.2.1. Imagery

To represent different stages of vegetative phenology within the study area region, a total of five Landsat-5 TM scenes were downloaded from the United States Geological Survey data archive using the GLOVIS interface (Table 14). The scenes were the most appropriate with respect to the year of the forest inventory data (± 1 year). All Landsat-5 TM radiance data were atmospherically corrected to surface reflectance using Fast Line-of-sight Atmospheric Analysis of Spectral Hypercubes (FLAASH) in ENVI 4.8 (Atmospheric model: Mid-Latitude Winter / Sub-arctic Summer, Aerosol model: Rural). To create the multi-temporal dataset, all scenes were subsequently layer-stacked.

Table 14: Processed Landsat-5 TM scenes.

Scene ID	Date	Year	Path/Row	Sun Elevation (°)
LT50480172006131PAC01	May 11	2006	48 / 17	45.6
LT50480172006163PAC02	June 12	2006	48 / 17	50.6
LT50480172004190PAC01	July 8	2004	48 / 17	49.1
LT50470172005233PAC01	August 21	2005	47 / 17	39.1
LT50470172005249PAC01	September 6	2005	47 / 17	33.7

Source: United States Geological Service (2013).

5.2.2.2. Forest Inventory Data

Forest inventory data was collected in July 2005 within the study area, whereby a plots (20 m x 20 m in size) were distributed in stands of jack pine, white spruce, black spruce, trembling aspen, and various mixed-woods (Hall & Skakun, 2007). Forest plots were located at least 100 m away from roads, cut lines, water bodies, and non-forested areas, and were generally within 500 m of the nearest road for ease of accessibility. Plot centres were established using a pigtail with flagging tape, after which the locations were recorded using a Trimble differentially corrected GPS system (UTM Zone 11, NAD83). Measuring tape and a compass were used to mark the cardinal (i.e., N, W, S, E) and

intercardinal (i.e., NW, SW, SE, NE) points of the plot with flagging tape and to determine plot boundaries. Every tree that was at least 1.3 m in height and 5 cm in diameter breast height was measured, whereby the species, diameter at breast height, and height were noted. Because northern boreal forest stands typically contain a very large number of small trees, the same measurements were recorded for a selection of small trees (i.e., diameter breast height less than 5 cm, and a height of 1.3 m or greater) although within a smaller 10-m x 10-m quadrant. The stand attribute estimations of small trees were subsequently multiplied by 4 to represent the entire contribution of the small trees within the plot. Crown closure estimates were obtained at the intercardinal corners of the plot (n = 4) and within the plot at mid-corner locations (n = 5) using a spherical densitometer. An ocular Alberta Vegetation Inventory (AVI) stand call attribute was also made to record the species, height, and crown closure of the stand following the Alberta Vegetation Inventory Interpretation Standards (Alberta Sustainable Resource Development, 2005). Fractional cover of understory species was visually estimated for the six most dominant species in 5-% increments for each plot.

5.2.3. Data Processing

5.2.3.1. Spectral Libraries

Spectral libraries, which contained image spectral endmembers, were required to meet the objectives of this study. Image endmember selection criteria were formulated to test whether the application of image endmembers was feasible and evaluate if their performance was dependent on the method used to develop spectral libraries using relevant forest inventory information. Representative sunlit canopy spectra were selected either by basal area of crown closure, while representative background spectra were

selected either outside or inside of forest cover (Table 15 and 16). Spectra for plots of relatively high species purity (e.g., Sw_9A_1) and mixed abundance (e.g., Pj_6Sb_4) were collected to meet the mapping needs of operational forest management, whereby plots lower than 80-% relative abundance for one species were designated as mixed.

Table 15: Criteria for the establishment of sunlit canopy spectral libraries.

Spectral library	Criteria
By basal area "*Basalarea*"	Pure: Plots selected where the relative abundance of a particular tree species exceeded 95 % of total basal area of the dominant trees above stand height Mixed: Plots of mixed abundance by total basal area of the dominant trees above stand height, where the leading species contributed between 50 % and 70 %.
By crown closure "*HighestCC*"	Pure: Plots selected that were relatively pure by species (> 80 %), and that had the highest crown closure estimates within each species group. Mixed: Plots of mixed abundance were selected that had the highest crown closure estimates within each mixed-species group.

Table 16: Criteria for the establishment of background spectral libraries.

Spectral library	Criteria
By spectral purity "*PurestBg*"	Using a *fishnet* vector file at the exact resolution and extent of the Landsat TM imagery, homogenous areas of low vegetation outside of forested areas were selected using the panchromatic QuickBird image as visual reference
By crown closure "*LowestCC*"	Pure: Plots selected that were relatively pure by species (> 80 %), and which had the lowest crown closure estimates within each species group. Mixed: Plots selected of mixed abundance were selected that had the lowest crown closure estimates within each mixed-species group.

The overall goal of the selection of image endmember spectra was to include the overall heterogeneity of the forest stands, but because many inventory plots met the selection criteria, an effort was made to reduce the number of endmember spectra to increase computational efficiencies and increase the number of independent plots used for validation. To select pure plots that met the basal area criterion, the spectra of the closest pixel that overlaid each of the 14 candidate plots were obtained and analyzed to derive a subset of candidate spectra using strategies highlighted in Roberts et al. (2007). A total of 7 coniferous plots were identified that were spectrally most similar to other

plots of the same species and most dissimilar with plots of other species (count-based endmember selection; Roberts et al., 2003), had the lowest average root-mean-square error in modeling all other spectra within their species class (endmember average RMSE; Dennison & Roberts, 2003b), and had the lowest average spectral angle in modeling all other spectra within their species class (minimum average spectral angle; Dennison et al., 2004). These 7 pure plots were therefore spectrally most similar for all other pure plots belonging to their species class and were most dissimilar with other species classes.

No semi-automated methods were used to select representative mixed stands, which were manually selected on the basis of the AVI data whereby the heterogeneity of the mixed plots for each species group was incorporate. The forest inventory data did not contain any pure aspen stands that met the criteria of the sunlit canopy, and as such, two 20-m by 20-m plots were manually drawn in ESRI ArcMap where dominant patches of aspen appeared using a panchromatic QuickBird scene as a visual aid. Once the optimal plots for species discrimination were known, image endmember spectra were acquired through the "Create Spectral Library from ROIs" module in the open-source software plugin VIPER Tools available for ENVI (Visualization and Image Processing for Environmental Research; Roberts et al., 2007). In cases where forest inventory polygons overlaid multiple pixels, all individual spectra were extracted without averaging to preserve the spectral variability. To test whether multi-temporal imagery improves species discrimination, the same optimized plots were used to extract multi-temporal spectral signatures.

5.2.3.2. Spectral Mixture Analysis

SMA quantifies the proportion of each pixel that is occupied by a set of pure features occurring in an image, whereby the output is a fraction image for each endmember along with the error of fit (Adams et al., 1993). For each pixel, this model can be derived as follows:

$$R'_i = \sum_{k=1}^{N} f_k R_{ik} + \varepsilon_i \quad , \tag{1}$$

where the spectral mixture R'_i is the encoded reflectance in band *i* for each pixel, and modeled as the sum of the reflectance in band *i* for N image endmembers *k*, whereby each endmember is weighted by fraction f_k. The ε_i term represents the remainder between the measured and modelled reflectance, and is expressed as a band residual. Model fitness can be assessed either by using this residual term, or via the root mean square error (RMSE; Roberts et al., 1998) over the total number of bands (v):

$$RMSE_{(\lambda)} = \sqrt{\sum_{i=1}^{v} (\varepsilon_i)^2 / N} \quad . \tag{2}$$

For this study, Multiple Endmember Spectral Mixture Analysis (MESMA; Roberts et al., 1998) was chosen as an alternative to conventional SMA, as MESMA is not constrained by a single set of endmembers and allows the number and types of endmembers to vary on a per-pixel basis to account for spatial heterogeneity. Because MESMA is not constricted by the number of spectral bands it has been successfully applied to obtain species abundance maps in vegetated areas in California (Dennison & Roberts, 2003b), Australia (Youngentob et al., 2011), and Hawaii (Somers & Asner, 2012). MESMA was facilitated by the open-source software plugin VIPER Tools, where it returns estimates of sub-pixel fractions of endmembers and a raster image of the

endmember model of best fit that represents a per-pixel land-cover classification. MESMA shares characteristics of both fully constrained and unconstrained unmixing, whereby the sum of the fractions must equal 1.00, but where the individual endmember fractions are allowed to be less than 0.00 and greater than 1.00). Minimum and maximum fractions of -10 % and 110 % were empirically determined to optimize vegetation class accuracies by permitting MESMA to consider models that fit the measured reflectance of a pixel despite physically unrealistic endmember fractions (Dennison & Roberts, 2003a; Thorp et al., 2013). A maximum RMSE criterion of 2.5 % was used to ensure that a candidate model was selected for the majority of pixels and to guarantee reasonable confidence in the accuracy of the candidate model selected (Roberts et al., 1998).

Both the July and multi-temporal dataset were unmixed using three-endmember models, whereby all possible combinations of sunlit canopy spectra and background spectra were iteratively computed, and whereby the best model based on RMSE was selected as a combination of sunlit canopy, background, and shadow components. A variety of spectral library combinations were tested in a three-endmember model setup (Table 17). The classification images produced by MESMA were regrouped to four pure species classes to compare the classification images derived through image endmember spectra and endmember spectra acquired with the spectroradiometer.

Table 17: Endmember model setup.

Source of spectra	**Spectral library**		
	Sunlit canopy	**Background**	**Shade**
Field [1]	Dominant tree spectra	Weighted average spectra	Yes
Image	*Basalarea*	*PurestBg*	Yes
Image	*Basalarea*	*LowestCC*	Yes
Image	*HighestCC*	*PurestBg*	Yes
Image	*HighestCC*	*LowestCC*	Yes

[1] This model represents the best combination of sunlit canopy and background endmember types using spectral data acquired by a spectroradiometer, as identified in Chapter 4.

5.2.4. Accuracy Assessment and Experimental Design

Because the Landsat TM imagery acquired in July showed highest sensitivity to the dominant species per fraction of total basal area of the dominant and co-dominant trees (Chapter 4), this field-based description of leading species was used for accuracy assessment purposes. In ENVI 4.8, contingency matrices were obtained to determine the overall accuracy, the producer and user accuracy, and the Kappa estimate using the 48 ground-reference plots. The overall accuracy of each classified image is the sum of the correctly classified points divided by the total number of points assessed (Congalton & Green, 2009). Individual class accuracies are represented by the producer accuracy (errors of omission) and user accuracy (errors of commission). The Kappa measure is an estimate derived through Kappa analysis (Cohen, 1960), which is a measure of the proportional improvement by the image classifier over a purely random assignment of pixels to classes (Congalton & Green, 2009). The Kappa estimate is recognized as a powerful accuracy measure, because it takes non-diagonal elements of the contingency matrix into account and addresses the probability of chance agreement. It can be used along with its variance to compare the accuracy of two classified images and determines if the contingency matrices are significantly different at a particular confidence level (CL) using the standard normal deviate (e.g., 95-% CL; Z-critical value = 1.96; Congalton & Green, 2009). To determine whether differences existed between image endmember selection criteria, the accuracy estimates were compared at a global level (i.e., all 48 ground-reference plots combined) and for plots grouped by crown closure using ground observations of crown closure and range definitions from the Alberta Vegetation Inventory (Table 18).

Table 18: Crown closure classes of the Alberta Vegetation Inventory.

Crown Closure (%)	Stand call class	Authors' Interpretation
6 - 30	A	Very open forest
31 - 50	B	Open forest
51 - 70	C	Medium dense forest
71 - 100	D	Dense forest

Source: Alberta Sustainable Resource Development (2005)

5.3. Results

5.3.1. Field Inventory Data

A total of 48 field-inventory plots were established in both compositionally pure (> 80 % abundance of one species) and mixed stands to take into account the heterogeneity of the forests in the study area (Table 9). The plots reflected a wide range of stand structural characteristics common in the region. The majority were established in very open (n = 14) to open stands (n = 27) with crown closure estimates ranging between 16 % and 61 % (mean = 35 %). The average stand height was 12 m, with a range between 6 m and 21 m. Stem density estimates also indicated that the field inventory plots were selected over a wide variety of stands, ranging between 875 stems/ha and 3,600 stems/ha.

Candidate endmember spectra were chosen using forest inventory information by either basal-area or crown-closure criteria, and captured the range of compositional and stand structure characteristics for both pure and mixed stands (Table 19). The landscape heterogeneity was to a certain degree less represented by the *HighestCC* spectral library because plots were selected by highest crown closure estimates within each species group (pure and mixed), regardless of composition. For example, the *Basalarea* spectral library represented mixed jack pine stands by both a PjSw spectra and a PjSb spectra, while the *HighestCC* spectral library contained two PjSw plots for this species class.

Table 19: Selected plots for image endmember spectra.

Species	By basal area *"Basalarea"* [1]					By crown closure *"HighestCC"* [1]				
	Plot ID	Species Composition	Crown closure	Stand height	Stem density	Plot ID	Species Composition	Crown closure	Stand height	Stem density
Jack pine	60	Pj_9Sw_1	27	12	1850	74	Pj_9Sb_1	42	13	2200
	64	Pj_{10}	34	15	1700	77	Pj_9Sb_1	38	13	2000
	84	Pj_{10}	34	14	1375	25	Pj_6Sw_4	40	9	2750
	26	Pj_7Sb_3	39	8	3550	91	Pj_7Sw_3	45	12	2325
	91	Pj_7Sw_3	45	12	2325					
White spruce	03	Sw_{10}	56	16	2525	01	Sw_9A_1	60	15	2875
	90	Sw_{10}	44	21	1275	48	Sw_{10}	61	18	2075
	52	Sw_5Sb_5	23	10	1825	59	Sw_8Sb_2	32	11	1575
	54	Sw_8Sb_2	22	9	1375	88	Sw_8Sb_2	33	17	875
Black spruce	51	Sb_{10}	16	8	1025	55	Sb_9Pj_1	27	9	1700
	55	Sb_9Pj_1	27	9	1700	73	Sb_9La_1	24	8	2450
	70	Sb_6Pj_4	28	7	2825	71	Sb_7Pj_3	32	10	1650
	75	$Sb_5Pj_3Sw_2$	38	9	2700	75	$Sb_5Pj_3Sw_2$	38	9	2700
Aspen	89	$A_6Sw_3Pj_1$	53	18	1825	89	$A_6Sw_3Pj_1$	53	18	1825
	Image	n/a	n/a	n/a	n/a	n/a	n/a	n/a	n/a	n/a
	Image	n/a	n/a	n/a	n/a	n/a	n/a	n/a	n/a	n/a

[1] Species composition by relative fraction of total basal area of the dominant trees above stand height, Stand height in metres, Crown closure in percentages, and stem density in stems per hectare.

5.3.2. Classification Accuracies for July Imagery

Classification accuracies were relatively low, with overall accuracies ranging between 44 % and 52 %, and Kappa ranging from 0.24 to 0.29 (Table 20). The results achieved using single-date image endmembers were similar to the results obtained using reference endmembers acquired with a spectroradiometer (i.e., 52 % accuracy). This suggests that endmember spectral impurity does not influence the discrimination between tree species, and that the image spectral endmembers identified using forest inventory information were viable alternatives to reference endmembers collected in the field. Together the low accuracies achieved highlight the considerable challenges to which the leading species can be identified in northern boreal forests using either field reflectance or image-derived endmember spectra.

When all 48 forest inventory plots were included in the accuracy assessment, it was evident that there were no considerable differences existed in overall accuracy and

Kappa between the combinations of sunlit canopy and background spectral libraries (Table 20). When individual class accuracies were compared, the differences in classification performance between different types of sunlit canopy libraries were generally less than 15 %. One notable difference was the 57 % improvement in the user accuracy of black spruce when the *Basalarea* sunlit spectral library was used instead of the *HighestCC* spectral library (43 % versus 100 %). In general, however, the results indicated that the criteria used to select candidate sunlit canopy spectral signatures were of minor influence to the overall classification accuracy. Except for the 60 % improvement in user accuracy of black spruce when the *PurestBg* background spectral library was used instead of the *LowestCC* library (40 % versus 100 %), the influence of candidate background spectral signatures to accuracy was minor.

Table 20: Overall classification accuracies and class accuracies (%) of July imagery per spectral library combination.

Species [1]	**Image endmember spectra**								**Field spectra**	
	Basalarea + PurestBg [2]		***Basalarea + LowestCC*** [2]		***HighestCC + PurestBg*** [2]		***HighestCC + Lowest CC*** [2]			
	PA[3]	UA[3]	PA	UA	PA	UA	PA	UA	PA	UA
Jack pine	35	75	54	70	19	83	35	69	42	79
Black spruce	56	100	44	40	67	43	56	26	56	42
White spruce	67	31	50	50	75	35	67	57	75	47
Aspen	100	20	100	17	100	50	100	50	0	0
OA [3]	48		52		44		48		52	
Kappa	0.26		0.29		0.24		0.26		0.31	

[1] Size of vegetation classes. Jack pine (n = 26), black spruce (n = 9), white spruce (n = 12), aspen (n = 1).
[2] Refer to Tables 15 and 16 for spectral library descriptions.
[3] OA: overall accuracy, PA: producer accuracy, UA: user accuracy.

Recognizing the influence of small sample sizes, only minor variations in overall accuracy existed among the different combinations of spectral libraries for each crown closure class, albeit that the small sample sizes precluded any meaningful patterns to be

observed (Table 21). The *HighestCC* sunlit canopy spectral library outperformed the *Basalarea* library for medium dense stands (+ 14 % improvement for both combinations), while the latter library outperformed the former library for very open stands (7 % and 14 % improvement). The field spectra performed similarly for open and medium dense stands, yet outperformed image endmember spectra when very open stands were unmixed. No patterns in classification accuracy were observed among spectral libraries representing the understory. Based on these results, the criteria used to select candidate spectra for the sunlit canopy and background endmembers were of little influence to classification accuracy.

Table 21: Overall accuracy (%) grouped per crown closure (July imagery).

Crown closure Class [1,2]	**Image endmember spectra**				**Field spectra**
	Basalarea + PurestBg [3]	***Basalarea + LowestCC*** [3]	***HighestCC + PurestBg*** [3]	***HighestCC + LowestCC*** [3]	
A	57	50	43	43	71
B	41	56	37	48	41
C	57	43	71	57	57

[1] Crown closure classes: A: 6 % to 30 %, B: 31 % to 50 %, C: 51 % to 70 %. None of the ground inventory plots had an estimated crown closure larger than 70 % (i.e., the D class).
[2] Sample size: A (n = 14), B (n = 27), C (n = 7).
[3] Refer to Tables 15 and 16 for spectral library descriptions.

5.3.3. Classification Accuracies for Multi-temporal Imagery

Multi-temporal imagery improved the discrimination of vegetation classes among all spectral library combinations as multi-temporal imagery increased spectral differences among tree species (Figure 20). However, the improvements in Kappa were only significant at the 95-% confidence level when the *Basalarea* sunlit canopy spectral library was used (Table 22). Greater differences in classification accuracy existed among the spectral library combinations using the multi-temporal imagery, whereby on average the *Basalarea* sunlit canopy spectral library performed better than the *HighestCC* sunlit

canopy spectral library, and whereby the *PurestBg* spectral library outperformed the *LowestCC* spectral library. Consequently, the best results were achieved using the *Basalarea* sunlit canopy spectral library in combination with the *PurestBg* background spectral library (overall accuracy: 79 %, Kappa: 0.67). The considerable differences in classification accuracy among spectral library combinations suggested that the criteria by which candidate image endmembers were selected definitely influenced the classification accuracy of multi-temporal imagery.

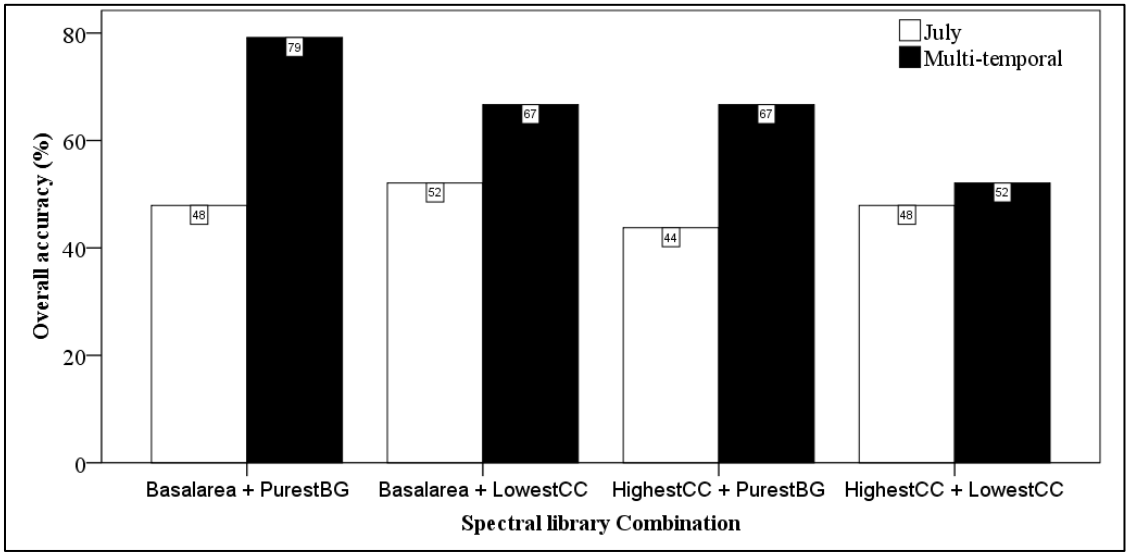

Figure 20: Classification accuracies for July and multi-temporal imagery.

Table 22: Pairwise comparison of Kappa estimates of July and multi-temporal imagery.

Spectral libraries	**Kappa**		**Z-score**
	July imagery	Multi-temporal imagery	
Basalarea + LowestCC	0.29	0.50	1.47
Basalarea + PurestBg	0.26	0.67	2.61 *
HighestCC + PurestBg	0.24	0.47	1.41
HighestCC + LowestCC	0.26	0.32	0.39

* Significant at 95-% confidence level (Z-score > 1.96).

Similar patterns in terms of overall accuracy per crown closure class were observed between the July and multi-temporal imagery (Tables 21 and 23). The *HighestCC* sunlit canopy spectral library outperformed the *Basalarea* library for medium

dense stands (+ 14 % improvement for *PurestBg* combination), while the latter library outperformed the former library for very open stands (21 % and 31 % improvement) and open stands (7 % and 11 % improvement). Given these larger differences among spectral libraries, it appears that the criteria used to select image endmembers influenced tree species classifications. Although the field spectra performed the best when very open stands were unmixed, they achieved worse results than image spectral endmembers for open and medium dense stands. This again highlighted that spectral impurity did not affect the discrimination between tree species.

Table 23: Overall accuracy (%) grouped per crown closure (multi-temporal imagery).

Crown closure Class [1,2]	**Image endmember spectra**				**Field spectra**
	Basalarea + PurestBg [3]	***Basalarea + LowestCC*** [3]	***HighestCC + PurestBg*** [3]	***HighestCC + LowestCC*** [3]	
A	64	64	43	33	71
B	85	70	74	63	41
C	86	57	100	57	57

[1] Crown closure classes: A: 6 % to 30 %, B: 31 % to 50 %, C: 51 % to 70 %. None of the ground inventory plots had an estimated crown closure larger than 70 % (i.e., the D class).
[2] Sample size: A (n = 14), B (n = 27), C (n = 7).
[3] Refer to Tables 15 and 16 for spectral library descriptions.

5.3.4. Fitness Metrics

The RMSE output of SMA is an indication of how well the modeled reflectance matches the measured reflectance of the pixels. The RMSEs achieved using July image endmembers were similar among spectral library combinations, and were comparable to the RMSE obtained when field spectral measurements were used for spectral unmixing (e.g., both 0.001 on average; Figure 21). No discernible differences among spectral library combinations were observed for the average RMSE when all plots were grouped together. Considerable increases in RMSE were observed when the multi-temporal imagery was unmixed, which average between 0.002 and 0.0025 of the measured pixel

reflectance (Figure 21). Among the different combinations of spectral libraries, combinations with the *PurestBg* background spectral library had the largest RMSE on average. Based on these results, spectral impurity did not influence the fitness of unmixing, and the criteria used to select candidate endmember spectra only affected the fitness of unmixing for the multi-temporal imagery.

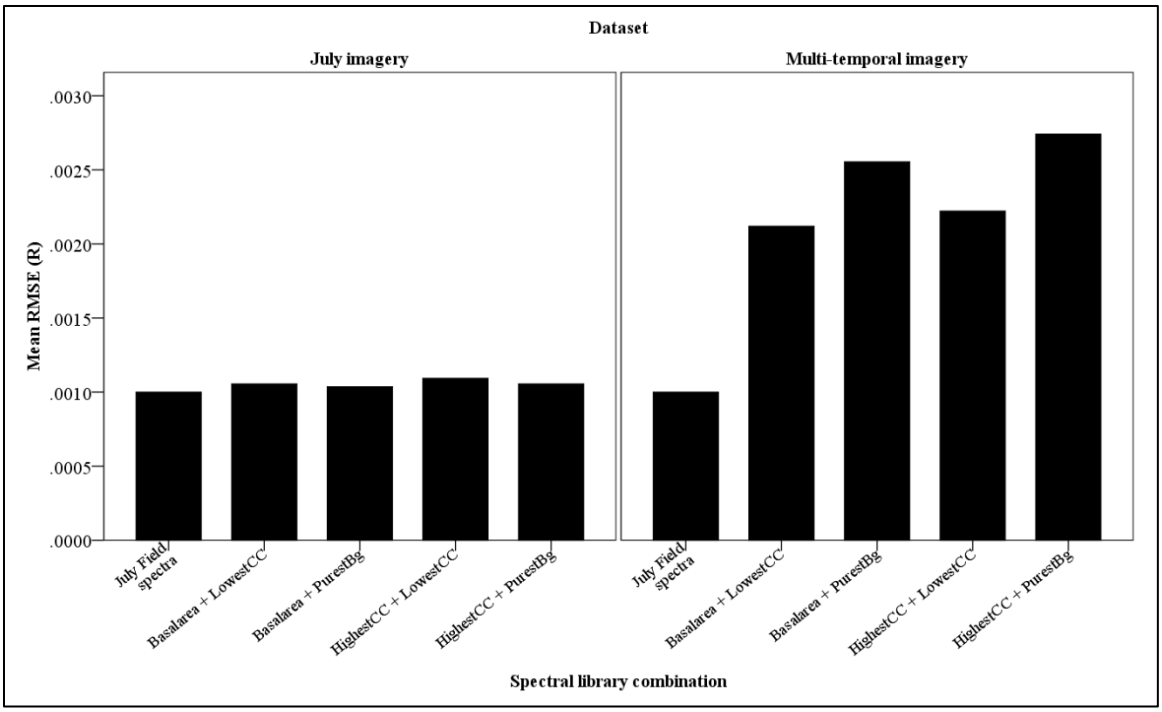

Figure 21: RMSE for July (4 bands) and multi-temporal imagery (36 bands).

An analysis of band residuals of the multi-temporal imagery indicated that seasonal patterns in SMA fitness occurred within this dataset (Figure 22). The band residuals in July were much smaller than the residuals in the other months as the locations for optimal candidate image endmembers (i.e., the forest inventory plots) were entirely based on the July dataset to maintain the same locations for image endmembers. It was also evident that residuals were predominantly positive earlier in the growing season and negative later in the growing season. A distinct pattern of residuals was

identified for the June 12 dataset (positive VIS, negative NIR and SWIR2) and September 6 dataset (negative VIS, positive NIR and SWIR2), as well as in the SWIR1 band (positive in May and June, negative in August and September). This suggests that residuals were wavelength dependent and were a result of phenological changes in the sunlit canopy and understory.

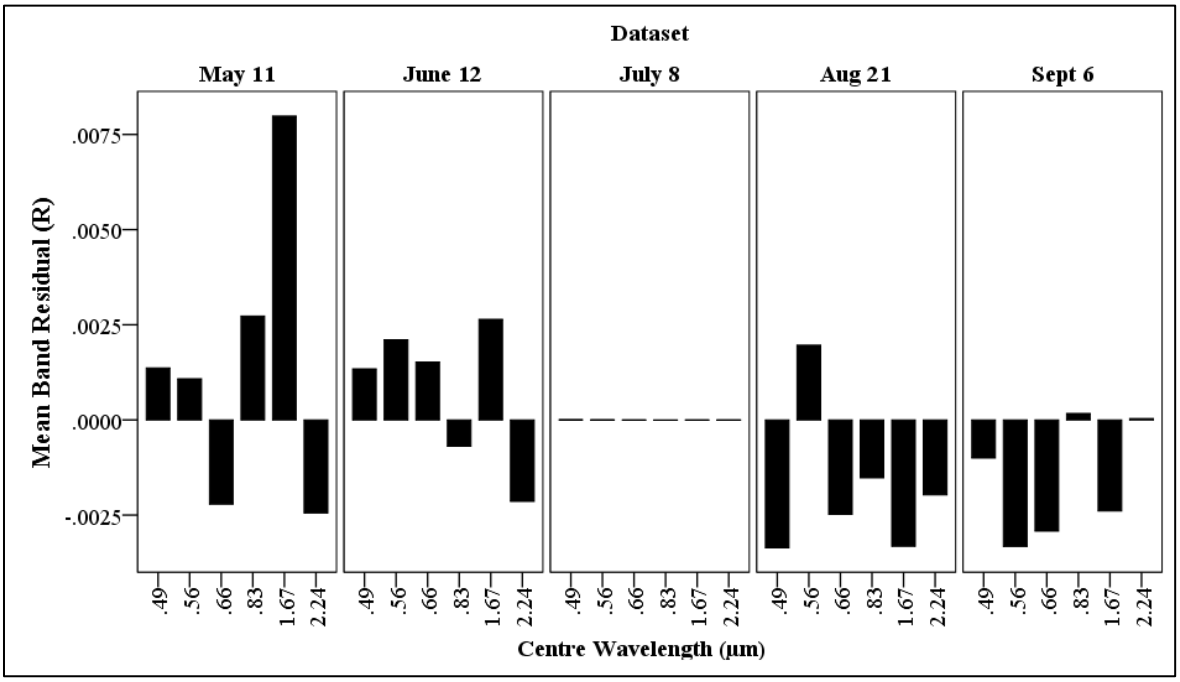

Figure 22: Average band residuals of the four spectral library combinations for each image date.

5.3.5. Distribution of Tree Species

Patterns of species distribution were not similar among datasets and spectral library combinations, with noticeable differences between the best July image classification (Figure 23a) and the best multi-temporal image classification (Figure 23b). The July dataset was classified with an overall accuracy of 52 % and Kappa of 0.29 when the *Basalarea* sunlit canopy and *LowestCC* background spectral libraries were used (Table 24; See Appendix 2 for other July matrices). A distinct pattern of aspen was observed, yet its low user accuracy of 17 % suggested that this vegetation class was over-

represented. This can be further highlighted through a comparison of its distribution in the multi-temporal classification. This dataset was classified with an overall accuracy of 79 % and a Kappa of 0.67 when the *Basalarea* sunlit canopy and *PurestBg* spectral libraries were used (Table 25; See Appendix 3 for other multi-temporal matrices). Relative to the July imagery, the distribution of aspen was much smaller and more closely agreed with the validation data (user accuracy improved from 17 % to 50 %).

Moreover, substantial improvements in producer and user accuracy were observed for jack pine (54 % to 77 % and 70 % to 87 %, respectively), white spruce (50 % to 83 % and 50 % to 91 %, respectively), and black spruce (44 % to 78 % and 40 % to 58 %, respectively) in compared to the July imagery (Tables 24 and 25). When the distributions of leading species between the multi-temporal classification and the classification based on field spectral measurements (Figure 23c) were compared, the significant increases in the producer accuracy of jack pine (42 % to 77 %) and black spruce (56 % to 78 %) as well as the user accuracy of white spruce (42 % to 91 %) were worth noting (Tables 12 and 25). On the basis of these results, multi-temporal image classifications are of definite benefit in the discrimination among leading species in northern boreal forests.

For the multi-temporal image classification, confusion between tree species occurred mainly between jack pine and black spruce (Table 25). This confusion was expected given that upland black spruce and jack pine often occur on the same well-drained sites with reindeer lichen understories (Figure 18). Among the field plots sampled for example, varying amounts of jack pine and black spruce was observed in 11 of the 26 jack pine dominant stands (Table 9), of which 5 stands were misclassified.

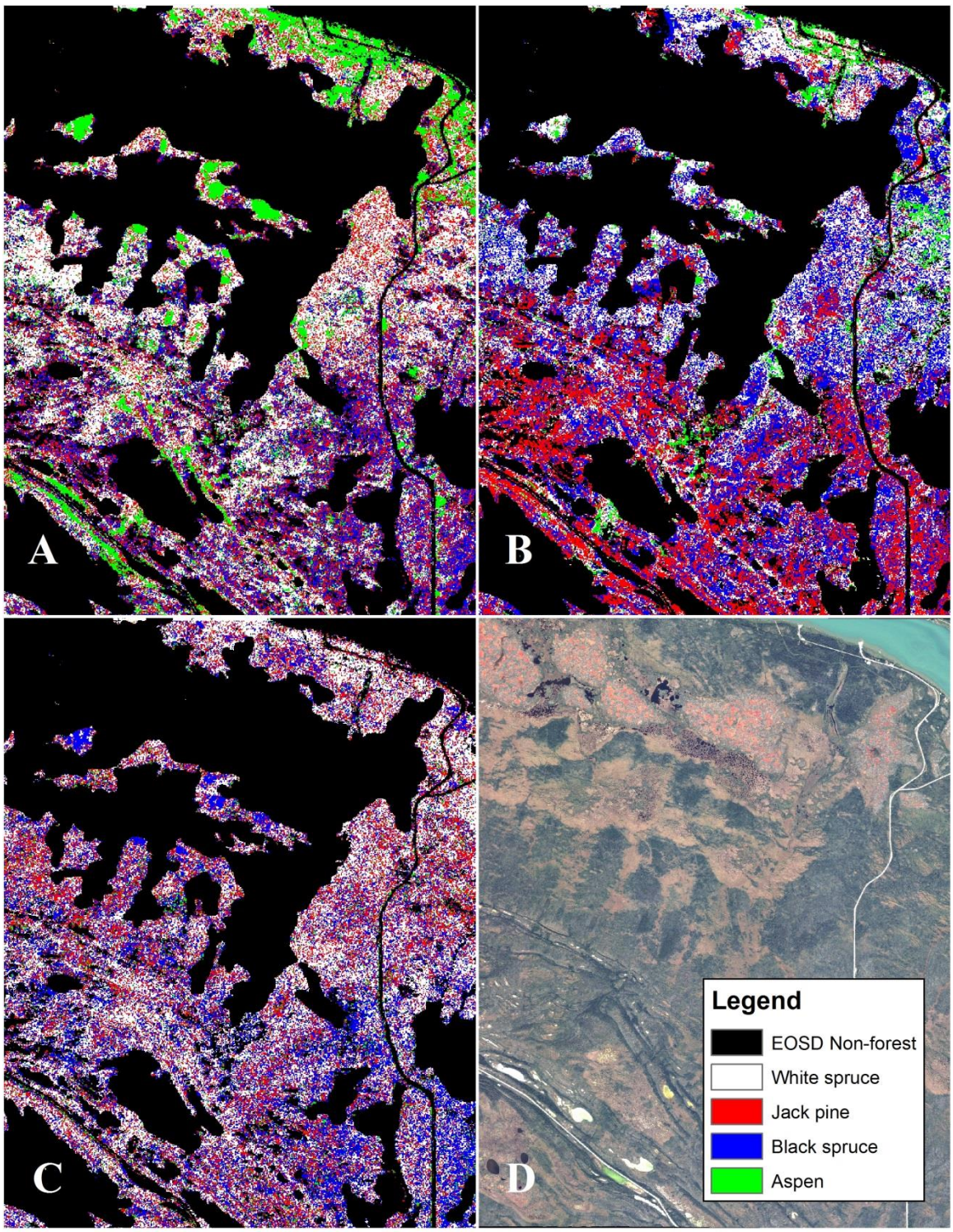

Figure 23: Tree species distribution maps generated using image and reference endmembers. (A) July image endmembers, (B) multi-temporal image endmembers, and (C) July reference endmembers. A multispectral QuickBird image is provided for spatial reference (D).

Table 24: Contingency matrix of the best July image classification.

Map prediction	**Ground reference (# of stands)** [1]				**Total**	**User accuracy**
	Aspen	Jack pine	White spruce	Black spruce		
Aspen	**1**	1	3	1	6	17 %
Jack pine	0	**14**	3	3	20	70 %
White spruce	0	5	**6**	1	12	50 %
Black spruce	0	6	0	**4**	10	40 %
Total	1	26	12	9	**48**	
Producer accuracy	100 %	54 %	50 %	44 %		
Overall accuracy = (25/48) 52 %						
Kappa = 0.29						

[1] The leading species was identified per fraction of total basal area of the dominant/co-dominant trees.

Table 25: Contingency matrix of the best multi-temporal image classification.

Map prediction	**Ground reference (# of stands)** [1]				**Total**	**User accuracy**
	Aspen	Jack pine	White spruce	Black spruce		
Aspen	**1**	0	1	0	2	50 %
Jack pine	0	**20**	1	2	23	87 %
White spruce	0	1	**10**	0	11	91 %
Black spruce	0	5	0	**7**	12	58 %
Total	1	26	12	9	**48**	
Producer accuracy	100 %	77 %	83 %	78 %		
Overall accuracy = (38/48) 79 %						
Kappa = 0.67						

[1] The leading species was identified per fraction of total basal area of the dominant/co-dominant trees.

5.4. Discussion

Three advancements were reported in this study. This study represented one of the first documented cases of tree-species classification using medium spatial resolution imagery in a northern boreal forest context. Second, impure, yet meaningful image endmember spectra selected through forest inventory information were compared with pure reference endmember spectra for mapping the leading species using spectral mixture analysis. Third, the benefits of multi-temporal imagery were assessed.

5.4.1. Impure Image Endmember Spectra for Classification Purposes

Because of the structural and compositional heterogeneity of northern boreal forests, EEAs which automatically select purest image endmembers of the sunlit canopy and background component are of limited use for species discrimination given that the assumptions of object and spectral purity cannot be met. Nevertheless, this study highlights that positive classification results can be obtained when impurity in representative sunlit canopy and background spectra is accepted and when meaningful endmember selection criteria are used based on *a priori* knowledge. There is a need to improve descriptions of the physical meaning of endmembers derived by methods which do not assume pixel purity (Plaza et al., 2012), which forest inventory information can provide. Because of the similarities in classification accuracy and unmixing fitness between image endmembers and reference endmembers, this study indicated that non-pure but meaningful endmember spectra can be appropriate even when field-based measurements of reflectance are not available. Although phenology, bi-directional reflectance, and solar zenith angles limit the portability of single-scene image endmembers between different images (Dennison & Roberts, 2003a), they are more easily obtained and unlike reference endmembers, are selected at the same scale and atmospheric conditions as the imagery (Drake et al., 1999).

5.4.2. Multi-temporal Imagery

Challenges regarding the similarity of reflectance spectra of differing tree species and the large intra-species variation in reflectance spectra often limit the capabilities of medium-spatial resolution sensors for discriminating among leading tree species (Treitz & Howarth, 1999; Cochrane, 2000). As a result, remote sensing approaches conducted

within the North American boreal zone have on average achieved only moderate success in approximating the information derived through ground inventories or aerial photo-interpretation (Tables 3, 4, and 5). Imagery acquired at key phenological periods can reduce spectral similarity among tree species, and when combined, could exploit phenological differences among tree species. In this study, multi-temporal imagery significantly improved the discrimination of leading species in northern boreal zones and reached a similar classification accuracy as achieved by Franklin (1994), Wolter et al. (1995), and Peddle et al. (2004) in other boreal forest settings. Even though Landsat TM has a limited spectral and spatial resolution relative to hyperspectral imagery, spectral mixture analysis and multi-temporal imagery could partially compensate for these limitations. For resource mapping purposes, the multi-temporal image classification corresponded better to ground-reference data than the black/white aerial photo interpretation for leading species (GNWT Forest Management Division) with significant improvements at the 95-% confidence level when all 48 plots were considered (79 % versus 56 %; Z-score = 2.01) as well as for a compositionally pure subset of plots at the 90-% confidence level (85 % versus 64 %; Z-score = 1.65). Much more detailed information about forest stands are collected through an aerial photo interpretation (e.g., the relative abundance of tree species to the nearest 10 percent, height, moisture regime) and, therefore, multi-temporal image classifications such as described in this study could supplement but not replace inventory approaches for operational forest management. For example, the information produced in this study could function as a stratification tool to aid forest inventories, highlight areas of interest, and provide opportunities to refine predictive models of specific stand parameters (sensu Gerylo et al., 2002).

5.4.3. Importance of Background Endmember Spectra

The best spectral library of the background component contained spectra acquired just outside of forest cover. Even though they may not be representative of the understory species typical of northern boreal forests (e.g., reindeer lichen), they are of value in the spectral mixture analysis approach. To differentiate between different vegetation types using MESMA, studies typically analyze the performance of two-endmember models whereby one forest vegetation class endmember is combined with a shade endmember (Dennison & Roberts, 2003a; Schaaf et al., 2011; Youngentob et al., 2011). For example, Roberts et al. (1999) achieved encouraging yet anecdotal results for mapping dominant vegetation types in the Canadian boreal forest using a two-endmember model. Two-endmember models are primarily used because of difficulties with the characterization of the understory, whereby it is assumed that the combined sunlit canopy and understory components are spectrally dissimilar among leading species classes. Some exploration between two-endmember models and three-endmember models was undertaken in this study, and highlighted that for the multi-temporal data in this study, two-endmember models underperform in overall classification accuracy, Kappa, and RMSE (not shown) in comparison to the most accurate three-endmember classification (Figure 24). These results emphasize the necessity of background spectra to discriminate among tree species, and that three-endmember models could improve classification results in areas where the understory component increased confusion among tree species (e.g., Cho et al., 2010).

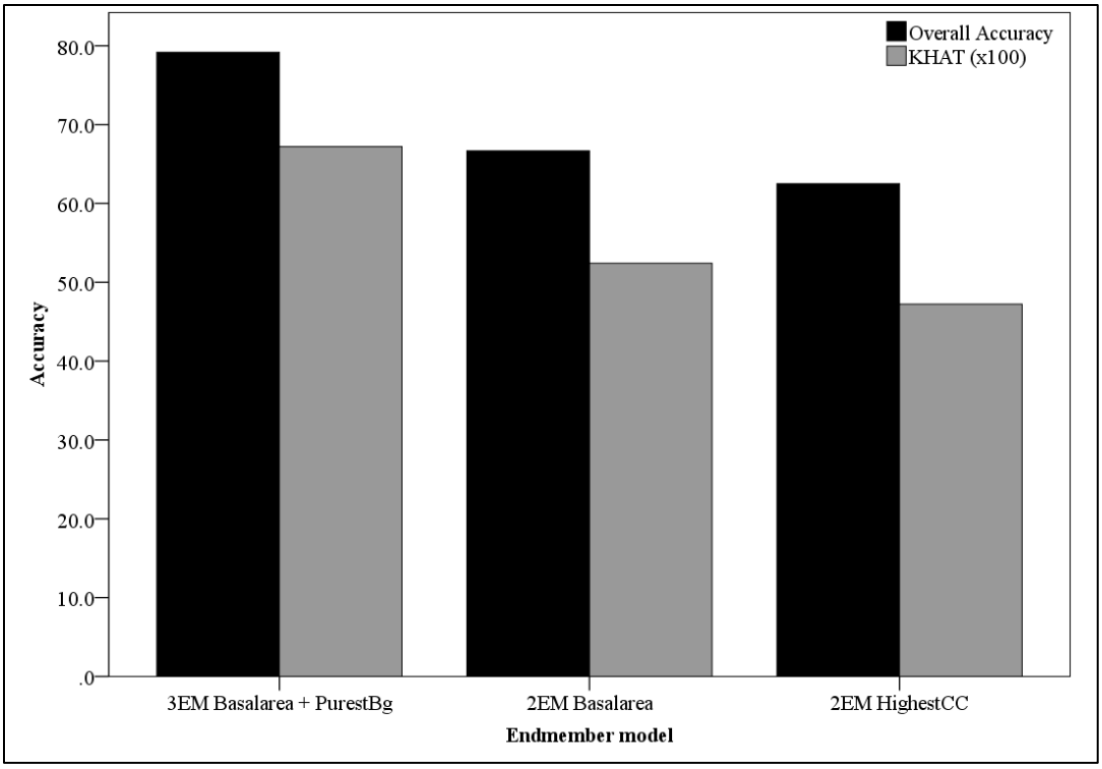

Figure 24: Classification accuracies of two- and three-endmember models.

5.4.4. Challenges

In the examination of unmixing fitness, it was evident that band residuals in July were much smaller than the residuals in the other months. This was likely because the locations for optimal candidate image endmembers were entirely based on the July dataset in order to make meaningful comparisons with the multi-temporal dataset. Positive and negative band residuals occurred early and late in the growing season, respectively, and highlighted that the best model fit had a reflectance higher/lower than the measured reflectance. These differences can be attributed to temporal changes in reflectance of the sunlit canopy and background components, of which the latter is spectrally brighter than the former and dominates the radiance signals received by medium-spatial resolution sensors (Bubier et al., 1997; Gerylo et al., 2002). Within

mature coniferous stands, the amount of photosynthetic active radiation and simple ratio (SR = red / near-infrared) of the background component steadily decreases throughout the growing season as a result of canopy development and foliar display early in the growing season and decreasing solar angle later in the growing season (Ross et al., 1986). As reported by Miller et al. (1997), seasonal phenology can be characterized by decreasing reflectance in the visible spectrum and increasing reflectance in the near-infrared wavelengths, which closely resembles the patterns of band residuals of the June and September imagery (Figure 18). As well, the positive residuals in the SWIR1 band early in the growing season were most likely a result of understory development where the foliage, due to its water content, absorbs radiance in the short-wave infrared portion of the electromagnetic spectrum (Carter, 1991; Gemmell et al., 2001). When these phenological changes are taken into account during the optimization process of the candidate image endmembers, smaller band residuals would be expected for the multi-temporal imagery, which could consequently lead to incremental improvements in RMSE and ultimately classification accuracy.

Within MESMA all spectral bands are weighted equally during model inversion, and as a result, the estimated cover fractions are mainly influenced by the high reflectance values which dominate the near-infrared spectrum. The visible spectrum, which have showed to be of great importance for discriminating among coniferous species (Peddle & Franklin, 1991; van Aardt & Wynne, 2007; Dalponte et al., 2013), is therefore of little influence in the image classification approach. A band weighting scheme may emphasize differences in reflectance at wavelengths that are characterized with low reflected energy (Somers et al., 2009b). An alternative to this solution would be

the creation of an integrated time-series spectral image that captures the seasonal phenology per spectral region in the most responsive months, which subsequently maximizes the spectral separability between tree species (Somers & Asner, 2012).

5.5. Conclusion

Northern boreal forests are characterized by open stands whereby understory ground vegetation and shadows are significant contributors to pixel-reflectance. In these forest settings, an accurate characterization of the sunlit canopy and background component is required for accurate modelling of the pixel reflectance through SMA, yet this is difficult to achieve if field-based spectral measurements are not available. Alternatively, the detection of image-derived endmembers is challenging because the canopy layer prohibits pure reflectance measurements from the understory vegetation to be made, and vice versa.

This study highlighted that satisfactory classification results of leading species can be obtained through the use of non-pure, but meaningful image endmember spectra. It was demonstrated that variability owing to surface heterogeneity can be tolerated, and may in fact be desirable in terms of providing SMA inputs that are more representative over larger areas. Although no clear differences in overall accuracy (± 50 %) and Kappa (± 0.30) were observed between reference and image-derived endmembers for single-date imagery, the improvements for multi-temporal imagery were significant at the 95-% confidence level (overall accuracy = 79 %, Kappa = 0.67). The criteria by which image endmembers of the sunlit canopy and background components were selected affected considerably the classification accuracy and unmixing fitness for multi-temporal imagery. The sunlit canopy endmember was best described through a basal-area purity criterion

whereby the compositional diversity of forest stands was most accounted for, whereas spectra obtained outside of the forest canopy best approximated the background endmember. These image-based endmember spectral protocols become viable alternatives when field-based measurements of reflectance are not available, and it was shown that these outperformed field-based spectral endmembers when multi-temporal imagery was used. In conclusion, image-derived spectral endmembers are suitable for leading tree-species classifications in these northern boreal forests using Landsat TM imagery, and imagery acquired throughout the growing season increased classification accuracies significantly to the extent that the information product is relevant to operational forest management.

CHAPTER 6

Discussion

This thesis described a study of mapping the leading species in an area representative of northern boreal forests, and investigated four aspects relevant to obtain this information through remote sensing: 1) the sensitivity of Landsat TM imagery to field-based descriptions of the leading species, 2) performance differences between field-based training spectra and spectra derived from the image itself, 3) the method used to obtain these representative field spectra (e.g., dominant understory species or an mixed understory spectra) and image spectra (e.g., by basal-area based species composition or by crown closure), and 4) the benefits of using multi-temporal imagery collected at various stages throughout the growing period. The basis for these investigations was a literature review, which provided an overview of the potential and limitations of remote sensing to derive tree-species information within a northern boreal forest context.

6.1. Key Findings

This study indicated that Landsat TM imagery is most sensitive to the indicator of leading species per fraction of total basal area of the dominant/co-dominant trees, and that this observation is consistent among crown closure ranges. The sensitivity of image classifications to field-based descriptions of leading species is typically not assessed in remote sensing studies due to general lack of multiple validation datasets. However, it is important to understand this sensitivity for operational forest management as it encourages relevance of the generated information product for professional foresters and promotes the integration of this information in existing forest inventory databases. For example, the findings of this study indicated that the Landsat TM image classification

labels the leading species of a forest stand consistent with forest inventories for operational-forest management in the Northwest Territories that focus on the dominant/co-dominant trees in a stand (Government of Northwest Territories, 2006a). Landsat TM also showed a strong agreement with the ocular calls of the overstory, which therefore can be used to identify the leading species when field measures of basal area and height are not available due to time and budget limitations. However, it was shown that some differences exist between the two validation datasets for highly mixed stands, and that Landsat TM is more sensitive to the leading species identified by quantitative measurements of basal area than by qualitative measurements in these cases. This finding was expected as ocular calls generally have an acceptable range of species composition of 85 % of the composition correctly identified (Government of Northwest Territories, 2006a). This indicates that a hybrid validation dataset, consisting of species information derived through basal-area ground measurements for highly mixed stands and ocular calls for relatively pure stands, could be formulated to increase the number of validation samples and improve the confidence in the derived information product.

For field-based spectra of the background component, this study indicated that the highest similarities with ground-reference data were obtained when the heterogeneity of the understory was approximated through the calculation of a weighted average of individual spectra at the stand level. Knowledge of understory compositions and relative abundances lead to a better characterization of the spectral response of the background endmember, with higher classification accuracies as a result. Because the composition of the understory in different forest types should be similar within ecologically similar units, general associations between the overstory of a stand and understory compositions can be

made (e.g., Beckingham & Archibald, 1996; Ecosystem Classification Group, 2007). Therefore large, a regionally representative spectral library could be developed through expert knowledge that contain weighted spectra of slightly different compositions and relative abundances. Such libraries could more easily accommodate the complexity of the understory at regional scales, and are less complicated to develop than the acquisition of new field spectra.

As a result of time, budget, site access, and data challenges, the usefulness of reflectance data collected with a spectroradiometer is limited for mapping large, remote forests in the Northwest Territories. Therefore, investigations with regards to the performance of image spectra selected using forest inventory information were conducted. Although these spectra are not pure due to the patchiness of the forest canopy, results indicate that impurity in representative sunlit canopy and background image endmembers is tolerated for leading species discrimination. These endmember spectra are appropriate when field-based measurements of reflectance are not available, and outperform the latter when multi-temporal imagery was used. However, forest inventory plots are required to identify optimal spectra for image classification. Because the availability of such forest inventory data is typically greater than ground-reflectance data, the need for forest inventory information is not necessarily a limiting factor, especially when only one or two pixels are required to characterize the image endmember spectra for each species class. The criteria to select representative image endmember spectra only influenced the classification performance of multi-temporal imagery. The best results were achieved when the representative sunlit canopy spectra of pure stands were selected using a basal area purity measure (> 95-% abundance), and representative spectra of

mixed stands were selected in a way that included highly mixed stands irrespective of crown closure. As the best understory spectral library contained spectra collected just outside forest stands using high-resolution QuickBird imagery as a visual aid, it suggests that image endmembers of the background component should not be affected by the sunlit canopy. When high-spatial resolution imagery is not available, Google Earth (Google Inc.) could potentially be used. Because three-endmember models (sunlit canopy + background + shade) improved classification results over two-endmember models (vegetation component + shade), the importance of background spectra was emphasized.

6.2. Future Research

This work presents incremental advances towards the overall goal of a partnership between Natural Resources Canada – Canadian Forest Service (NRCan-CFS) and the Government of the Northwest Territories (GNWT) to meet information needs regarding forest structure, stand volume, and aboveground biomass (Hall et al., 2012). The objective of the partnership is to develop a multi-sensor remote sensing inventory system within the framework of EOSD (Earth Observation for Sustainable Development of Forest) land cover maps, and integrate the derived information with the GNWT forest inventory into a combined Multisource Vegetation Inventory (MVI) in vector polygon format. EOSD characterizes forest cover in coniferous, deciduous, and mixed classes, and a more specific characterization of tree species is desired for polygon labelling.

This study needs to be repeated across a broad range of northern boreal forests (e.g., Fort Simpson, Fort Liard, Hay River) to increase confidence in the results and observations made in this study. Within the study area of this research, the raster-based leading species classification needs to be integrated into the existing MVI. Within the

existing MVI polygons, the leading species pixels should be enumerated to generate a species composition label for each polygon. These labels should be evaluated against independent field information to assess consistency among forest inventory methods.

To extend the work undertaken in this research, Landsat TM image classifications are required at much larger geographic extents to meet the objective of the NRCan-CFS and GNWT partnership (e.g., the southern most productive forests span more than 90,000 km^2; Hall et al., 2012). Due to the frequency of cloud cover at high latitudes (Rees et al., 2002), it was difficult to obtain cloud-free imagery that captured the phenological stages of the forests and that were appropriate with respect to the timing of the forest inventory data (2005 ± 1 year). Therefore, an assessment to find those phenological stages and image bands that maximize the spectral separability between tree species is a worthy investigation (e.g., Somers & Asner, 2012). Such data reduction facilitates easier data retrieval (i.e., less imagery needed to achieve similar classification results), pre-processing (e.g., atmospheric correction, image normalization) and faster spectral mixture analysis. When these optimal phenological stages are known, image mosaics are required that span the study area of the NRCan-CFS and GNWT partnership. These can be generated through a Landsat TM normalization to MODIS (Moderate Resolution Imaging Spectroradiometer) imagery (Hall et al., 2012). Once available, the MESMA approach highlighted in this study can be used to derive the leading species over larger areas. Because spectral weighing of image bands can emphasize differences in reflectance at visible and shortwave-infrared wavelengths (Somers et al., 2009b), it is worthwhile to investigate whether spectral differences between coniferous tree species can be increased to improve the image classification results reported in this study.

CHAPTER 7

Conclusions

There is a need for accurate information on the spatial distribution, composition, structure, and processes of forests. However, information regarding the spatial distribution of tree species is prohibitively expensive and a challenge to obtain over large, remote forests, such as the northern boreal forests in the Northwest Territories. Although an inventory approach based on remote sensing may be used to supplement current forest inventory data, the capabilities of such approaches to map the leading species of forest stands are unknown due to the absence of studies in these regions. A challenge is that the approach by which the leading species is determined differs among jurisdictions and in the scientific literature, and it is not known whether imagery is sensitive to how species composition is characterized in the field. Because the spectral response from these types of forests are noticeably mixed in 30-m Landsat TM images, an image classification based on Spectral Mixture Analysis may be a viable approach to identify the leading species using representative spectra of physically meaningful components (i.e., endmembers). The objectives of this thesis were to improve the understanding of the extent Landsat TM could be related to field-based descriptions of leading species, and determine whether differences in classification performance exist between: 1) field-based and image-derived endmember spectra, 2) endmember selection methods based on forest inventory information, and 3) single-date and multi-temporal imagery.

Interpretation of the results suggested that Landsat TM imagery is most sensitive to the indicator of leading species per fraction of total basal area of the dominant/co-dominant trees, and that this observation is consistent among crown closure ranges. This

finding is relevant as it indicates compliance to forest inventories for operational-forest management in the Northwest Territories which also focus on the dominant/co-dominant trees. With regards to the use of field spectra for classification purposes, the highest similarities with ground-reference data were obtained when the heterogeneity of the understory was approximated through the calculation of a weighted average of individual spectra and whereby individual cover fractions were known. Therefore, good knowledge of the understory leads to a better characterization of the spectral response of the background endmember and thereby improved classification results.

This study also highlighted that satisfactory classification results can be obtained when impurity in representative sunlit canopy and background image endmembers is accepted and when meaningful endmember selection criteria are selected based on forest inventory information. These image endmember spectra are appropriate when field-based measurements of reflectance are not available, and can outperform the latter using multi-temporal imagery. Although previous studies have classified leading species using two-endmember models, this study emphasizes the need for a separate background spectral component to improve the discrimination of tree species in open canopy forests. In this study, the image classification obtained with the MESMA approach are encouraging (overall accuracy = 79 %) and highlights its applicability for other areas in northern boreal forests. To use the generated information product for operational forest management, the raster-based image classification requires integration into the existing Multisource Vegetation Inventory (a NRCan-CFS and GNWT partnership) and subsequent validation at the vector polygon level before expanding the mapping area.

CHAPTER 8: REFERENCES

Adams, J. B., Smith, M. O., & Gillespie, A. R. (1993). Imaging spectroscopy: interpretation based on spectral mixture analysis. In C. M. Pieters & P. Englert (Eds.), *Remote geochemical analysis: elemental and mineralogical composition*. Cambridge, United Kingdom: Cambridge University Press. (pp. 145-166).

Aitken, S. N., Yeaman, S., Holliday, J. A., Wang, T., & Curtis-McLane, S. (2008). Adaptation, migration or extirpation: climate change outcomes for tree populations. *Evolutionary Applications, 1*(1): 95-111.

Alberta Environmental Protection. (1991). *Alberta vegetation inventory. Standards manual, version 2.1*. Edmonton, AB. (49 p.).

Alberta Sustainable Resource Development. (2005). *Alberta vegetation inventory interpretation standards, version 2.1.1*. Edmonton, AB, Canada. (73 p.).

Amos-Binks, L. J., MacLean, D. A., Wilson, J. S., & Wagner, R. G. (2010). Temporal changes in species composition of mixedwood stands in northwest New Brunswick: 1946-2008. *Canadian Journal of Forest Research, 40*(1): 115-137.

Amundson, R. (2001). The carbon budget in soils. *Annual Review of Earth and Planetary Sciences, 29*(1): 535-562.

Anderson, J. R., Hardy, E. E., Roach, J. T., & Witmer, R. E. (1976). A land use and land cover classification system for use with remote sensor data. Washington, DC. (pp. 1-41).

Asner, G. P. (1998). Biophysical and Biochemical Sources of Variability in Canopy Reflectance. *Remote Sensing of Environment, 64*: 234-253.

Bailey, R. G., Pfister, R. D., & Henderson, J. A. (1978). Nature of land and resource classification - a review. *Journal of Forestry, 76*(10): 650-655.

Bateson, A., & Curtiss, B. (1996). A method for manual endmember selection and spectral unmixing. *Remote Sensing of Environment, 55*(3): 229-243.

Beaubien, J., Cihlar, J., Simard, G., & Latifovic, R. (1999). Land cover from multiple thematic mapper scenes using a new enhancement-classification methodology. *Journal of Geophysical Research, 104*(D22): 27909-27920.

Beckingham, J. D., & Archibald, J. H. (1996). *Field guide to ecosites in northern Alberta*. Edmonton, AB, Canada. (336 p.).

Berg, E. E., Henry, J. D., Fastie, C. L., De Volder, A. D., & Matsuoka, S. M. (2006). Spruce beetle outbreaks on the Kenai Peninsula, Alaska, and Kluane National Park and Reserve, Yukon Territory: Relationship to summer temperatures and regional differences in disturbance regimes. *Forest Ecology and Management, 227*(3): 219-232.

Boardman, J. W. (1994). *Geometric mixture analysis of imaging spectrometry data.* Proceedings of International Geoscience and Remote Sensing Symposium, 1994. Surface and Atmospheric Remote Sensing: Technologies, Data Analysis and Interpretation. (pp. 2369-2371).

Boardman, J. W. (1998). *Leveraging the High Dimensionality of AVIRIS Data for Improved Sub-Pixel Target Unmixing and Rejection of False Positives: Mixture Tuned Matched Filtering*. Pasadena, CA, U.S.A: National Aeronautics and Space Administration. (1 p.).

Bond-Lamberty, B., Wang, C., Gower, S. T., & Norman, J. (2002). Leaf area dynamics of a boreal black spruce fire chronosequence. *Tree Physiology, 22*(14): 993-1001.

Borel, C. C., & Gerstl, S. A. W. (1994). Nonlinear spectral mixing models for vegetative and soil surfaces. *Remote Sensing of Environment, 47*(3): 403-416.

Boudewyn, P., Song, X., Magnussen, S., & Gillis, M. D. (2007). Model-based, volume-to-biomass conversion for forested and vegetated land in Canada. Victoria, BC, Canada. (pp. 1-106).

Brandt, J. P. (2009). The extent of the North American boreal zone. *Environmental Reviews, 17*: 101-161.

Brandt, J. P., Flannigan, M. D., Maynard, D. G., Thompson, I. D., & Volney, W. J. A. (2013). An introduction to Canada's boreal zone: ecosystem processes, health, sustainability, and environmental issues1. *Environmental Reviews, 21*(4): 207-226.

Brassard, B. W., & Chen, H. Y. H. (2006). Stand structural dynamics of North American boreal forests. *Critical Reviews in Plant Sciences, 25*(2): 115-137.

Brissette, J. C., & Barnes, B. V. (1984). Comparisons of phenology and growth of Michigan and western North American sources of Populustremuloides. *Canadian Journal of Forest Research, 14*(6): 789-793.

Bronge, B. L. (1999). Mapping boreal vegetation using Landsat-TM and topographic map data in a stratified approach. *Canadian Journal of Remote Sensing, 25*(5): 460-474.

Bubier, J. L., Rock, B. N., & Crill, P. M. (1997). Spectral reflectance measurements of boreal wetland and forest mosses. *Journal of Geophysical Research: Atmospheres, 102*(D24): 29483-29494.

Byrne, G. F., Crapper, P. F., & Mayo, K. K. (1980). Monitoring land-cover change by principal component analysis of multitemporal Landsat data. *Remote Sensing of Environment, 10*(3): 175-184.

Carroll, A. L., Taylor, S. W., Regniere, J., & Safranyik, L. (2003). *Effect of climate change on range expansion by the mountain pine beetle in British Columbia.* Proceedings of Mountain Pine Beetle Symposium: Challenges and Solutions, Kelowna, BC, Canada. (pp. 223-232).

Carter, G. A. (1991). Primary and Secondary Effects of Water Content on the Spectral Reflectance of Leaves. *American Journal of Botany, 78*(7): 916-924.

Chasmer, L., Hopkinson, C., Morrison, H., Petrone, R., & Quinton, W. (2011). *Fusion of airborne LiDAR and WorldView-2 MS data for classification of depth to permafrost within Canada's sub-arctic.* Proceedings of SilviLaser 2011 - 11th International Conference on LiDAR Applications for Assessing Forest Ecosystems, Hobart, Australia. (pp. 1-7).

Chavez, P. S. (1988). An improved dark-object subtraction technique for atmospheric scattering correction of multispectral data. *Remote Sensing of Environment, 24*(3): 459-479.

Chen, G., Wulder, M. A., White, J. C., Hilker, T., & Coops, N. C. (2012). Lidar calibration and validation for geometric-optical modeling with Landsat imagery. *Remote Sensing of Environment, 124*: 384-393.

Chen, H. Y. H., Vasiliauskas, S., Kayahara, G. J., & Ilisson, T. (2009). Wildfire promotes broadleaves and species mixture in boreal forest. *Forest Ecology and Management, 257*(1): 343-350.

Cho, M. A., Debba, P., Mathieu, R., Naidoo, L., van Aardt, J., & Asner, G. P. (2010). Improving Discrimination of Savanna Tree Species Through a Multiple-Endmember Spectral Angle Mapper Approach: Canopy-Level Analysis. *IEEE Transactions on Geoscience & Remote Sensing, 48*(11): 4133-4141.

Chubey, M. S., Franklin, S. E., & Wulder, M. A. (2006). Object-based analysis of Ikonos-2 imagery for extraction of forest inventory parameters. *Photogrammetric Engineering & Remote Sensing, 72*(4): 383-394.

Coburn, C. A., & Roberts, A. C. B. (2004). A multiscale texture analysis procedure for improved forest stand classification. *International Journal of Remote Sensing, 25*(20): 4287-4308.

Cochrane, M. A. (2000). Using vegetation reflectance variability for species level classification of hyperspectral data. *International Journal of Remote Sensing, 21*(10): 2075-2087.

Cogbill, C. V. (1985). Dynamics of the boreal forests of the Laurentian Highlands, Canada. *Canadian Journal of Forest Research, 15*(1): 252-261.

Cohen, J. (1960). A coefficient of agreement for nominal scales. *Educational of Psychological Measurement, 20*: 37-46.

Congalton, R. G., & Biging, G. (1992). A pilot study evaluating ground reference data collection efforts for use in forest inventory. *Photogrammetric Engineering & Remote Sensing, 58*(12): 1669-1671.

Congalton, R. G., & Green, K. (2009). *Assessing the Accuracy of Remotely Sensed Data: Principles and Practises* (2nd ed.). Boca Raton, Florida, U.S.A.: CRC/Taylor & Francis. (183 p.).

Cullingham, C. I., Cooke, J. E. K., Dang, S. O. P. H., Davis, C. S., Cooke, B. J., & Oltman, D. W. (2011). Mountain pine beetle host-range expansion threatens the boreal forest. *Molecular Ecology, 20*(10): 2157-2171.

Cumming, S., & Vernier, P. (2002). Statistical models of landscape pattern metrics, with applications to regional scale dynamic forest simulations. *Landscape Ecology, 17*(5): 433-444.

Dalponte, M., Bruzzone, L., & Gianelle, D. (2008). Fusion of Hyperspectral and LIDAR Remote Sensing Data for Classification of Complex Forest Areas. *IEEE Transactions on Geoscience & Remote Sensing, 46*(5): 1416-1427.

Dalponte, M., Orka, H. O., Gobakken, T., Gianelle, D., & Næsset, E. (2013). Tree species classification in boreal forests with hyperspectral data. *IEEE Transactions on Geoscience & Remote Sensing, 51*(5): 2632-2645.

Day, J. H. (1968). Soils of the Upper Mackenzie River Area - Northwest Territories. Canada Department of Agriculture, Research Branch. Ottawa, ON. (pp. 89).

de la Giroday, H., Carroll, A. L., & Aukema, B. H. (2012). Breach of the northern Rocky Mountain geoclimatic barrier: initiation of range expansion by the mountain pine beetle. *Journal of Biogeography, 39*(6): 1112-1123.

DeFries, R. S., Field, C. B., Fung, I., Justice, C. O., Los, S., Matson, P. A., Matthews, E., Mooney, H. A., Potter, C. S., Prentice, K., Sellers, P. J., Townsend, J. R. G., Tucker, C. J., Ustin, S. L., & Vitousek, P. M. (1995). Mapping the land surface for global atmosphere-biosphere models: Toward continuous distributions of vegetation's functional properties *Journal of Geophysical Research, 100*(D10): 20867-20882.

Dennison, P. E., Halligan, K. Q., & Roberts, D. A. (2004). A comparison of error metrics and constraints for multiple endmember spectral mixture analysis and spectral angle mapper. *Remote Sensing of Environment, 93*(3): 359-367.

Dennison, P. E., & Roberts, D. A. (2003a). The effects of vegetation phenology on endmember selection and species mapping in southern California chaparral. *Remote Sensing of Environment, 87*(2ΓÇô3): 295-309.

Dennison, P. E., & Roberts, D. A. (2003b). Endmember selection for multiple endmember spectral mixture analysis using endmember average RMSE. *Remote Sensing of Environment, 87*: 123-135.

Dorigo, W., Bachmann, M., & Heldens, W. (2006). AS Toolbox & Processing of field spectra: User's manual version 1.12. German Remote Sensing Data Center - German Aerospace Center. Wessling, Germany. (pp. 1-30).

Drake, N. A., Mackin, S., & Settle, J. J. (1999). Mapping Vegetation, Soils, and Geology in Semiarid Shrublands Using Spectral Matching and Mixture Modeling of SWIR AVIRIS Imagery. *Remote Sensing of Environment, 68*(1): 12-25.

Dymond, C. C., Mladenoff, D. J., & Radeloff, V. C. (2002). Phenological differences in Tasseled Cap indices improve deciduous forest classification. *Remote Sensing of Environment, 80*(3): 460-472.

Ecological Stratification Working Group. (1995). A national ecological framework for Canada. Ottawa, ON, Canada. (pp. 1-125).

Ecosystem Classification Group. (2007). Ecological Regions of the Northwest Territories - Taiga Plains. Yellowknife, NT. (pp. 1-173).

Environment Canada. (2011). Annual regional temperature departures Retrieved November 2, 2013, from http://www.ec.gc.ca/adsc-cmda/default.asp?lang=en&n=B49D9F0B-1

Falkowski, M. J., Wulder, M. A., White, J. C., & Gillis, M. D. (2009). Supporting large-area, sample-based forest inventories with very high spatial resolution satellite imagery. *Progress in Physical Geography, 33*(3): 403-423.

Fent, L., Hall, R. J., & Nesby, R. K. (1995). Aerial films for forest inventory: optimizing film parameters. *Photogrammetric Engineering & Remote Sensing, 61*(3): 281-289.

Forman, R. T. T. (1987). Conclusion: the ethics of isolation, the spread of disturbance, and landscape ecology. In M. G. Turner (Ed.), *Landscape heterogeneity and disturbance*. New York: Springer-Verlag. (pp. 220-226).

Fowells, H. A., & Means, J. E. (1990). The tree and its environment. In R. M. Burns & B. H. Honkala (Eds.), *Silvics of North America: 1. Conifers*. Washington DC: USDA Forest Service. (pp. 1-11).

Franklin, S. E. (1994). Discrimination of subalpine forest species and canopy density using digital CASI, SPOT PLA, and Landsat TM data. *Photogrammetric Engineering & Remote Sensing, 60*(10): 1233-1241.

Franklin, S. E. (2001). *Remote sensing for sustainable forest management*. Boca Raton, Fla.: Lewis. (407 p.).

Franklin, S. E., Hall, R. J., Moskal, L. M., Maudie, A. J., & Lavigne, M. B. (2000). Incorporating texture into classification of forest species composition from airborne multispectral images. *International Journal of Remote Sensing, 21*(1): 61-79.

Franklin, S. E., Hall, R. J., Smith, L., & Gerylo, G. R. (2003). Discrimination of conifer height, age and crown closure classes using Landsat-5 TM imagery in the Canadian Northwest Territories. *International Journal of Remote Sensing, 24*(9): 1823-1834.

Franklin, S. E., Maudie, A. J., & Lavigne, M. B. (2001). Using spatial co-occurance texture to increase forest structure and species composition classification accuracy. *Photogrammetric Engineering & Remote Sensing, 67*(7): 849-855.

Franklin, S. E., & Peddle, D. R. (1990). Classification of SPOT HRV imagery and texture features. *International Journal of Remote Sensing, 11*(3): 551-556.

Gamon, J. A., Huemmrich, K. F., Peddle, D. R., Chen, J., Fuentes, D., Hall, F. G., Kimball, J. S., Goetz, S., Gu, J., McDonald, K. C., Miller, J. R., Moghaddam, M., Rahman, A. F., Roujean, J. L., Smith, E. A., Walthall, C. L., Zarco-Tejada, P., Hu, B., Fernandes, R., & Cihlar, J. (2004). Remote sensing in BOREAS: Lessons learned. *Remote Sensing of Environment, 89*(2): 139-162.

Gemmell, F. (2000). Testing the Utility of Multi-angle Spectral Data for Reducing the Effects of Background Spectral Variations in Forest Reflectance Model Inversion. *Remote Sensing of Environment, 72*(1): 46-63.

Gemmell, F., Varjo, J., & Strandstrom, M. (2001). Estimating forest cover in a boreal forest test site using thematic mapper data from two dates. *Remote Sensing of Environment, 77*: 197-211.

Gerylo, G., Hall, R. J., Franklin, S. E., Roberts, A., & Milton, E. J. (1998). Hierarchical image classification and extraction of forest species composition and crown closure from airborne multispectral images. *Canadian Journal of Remote Sensing, 24*(3): 219-232.

Gerylo, G. R., Hall, R. J., Franklin, S. E., & Smith, L. (2002). Empirical relations between Landsat TM spectral response and forest stands near Fort Simpson, Northwest Territories, Canada. *Canadian Journal of Remote Sensing, 28*(1): 68-79.

Gillis, M. D., & Leckie, D. G. (1993). Forest inventory mapping procedures across Canada. Chalk River, ON, Canada. (pp. 1-78).

Girardin, M. P., & Mudelsee, M. (2008). Past and future changes in Canadian boreal wildfire activity. *Ecol.Appl.Ecological Applications, 18*(2): 391-406.

Goetz, A. F. H. (2012). Making Accurate Field Spectral Reflectance Measurements. Analytical Spectral Devices Inc. Boulder, CO, U.S.A. (pp. 16).

Goodenough, D. G., Dyk, A., Niemann, K. O., Pearlman, J. S., Chen, H., Han, T., Murdoch, M., & West, C. (2003). Processing Hyperion and ALI for forest classification. *IEEE Transactions on Geoscience & Remote Sensing, 41*(6): 1321-1331.

Gougeon, F. A. (1995a). Comparison of possible multispectral classification schemes for tree crowns individually delineated on high spatial resolution MEIS images. *Canadian Journal of Remote Sensing, 21*(1): 1-9.

Gougeon, F. A. (1995b). A crown-following approach to the automatic deliniation of individual tree crowns in high spatial resolution aerial images. *Canadian Journal of Remote Sensing, 21*(3): 274-284.

Gougeon, F. A., & Leckie, D. G. (2006). The individual tree crown approach applied to Ikonos images of a coniferous plantation area. *Photogrammetric Engineering & Remote Sensing, 72*(11): 1287-1297.

Gougeon, F. A., Leckie, D. G., Scott, I., & Paradine, D. (1999, 1999). *Individual tree crown species recognition: the Nahmint study.* Proceedings of Proceedings of a workshop held on February 10-12, 1998, Victoria, BC, Canada. (pp. 209-223).

Government of Northwest Territories. (2005). Spatial Data Warehouse - Ecological Land Classification - ELC Photos, from http://www.geomatics.gov.nt.ca/sdw.aspx

Government of Northwest Territories. (2006a). Northwest Territories forest vegetation inventory standards with softcopy supplements, version 3.0. Yellowknife, NT. (pp. 1-88).

Government of Northwest Territories. (2006b). Spatial Data Warehouse - Ecological Land Classification - ELC Photos, from http://www.geomatics.gov.nt.ca/sdw.aspx

Government of Northwest Territories. (2010a). Action plan for boreal woodland caribou conservation in the Northwest Territories 2010-2015. Yellowknife, NT. (pp. 1-24).

Government of Northwest Territories. (2010b). NWT Biomass Energy Strategy. Yellowknife, NT. (pp. 1-24).

Government of Northwest Territories. (2011a). Map of NWT Land Cover Types. Hay River, NT. (pp. 1).

Government of Northwest Territories. (2011b). Northwest Territories State of the Environment Report 2011 - Vegetation (online version). Yellowknife, NT. (pp.

Gray, L. K., & Hamann, A. (2012). Tracking suitable habitat for tree populations under climate change in western North America. *Climatic Change, 117*(1-2): 289-303.

Griesbauer, H. P., & Green, D. S. (2012). Geographic and temporal patterns in white spruce climate–growth relationships in Yukon, Canada. *Forest Ecology and Management, 267*: 215-227.

Guyot, G. D., Guyon, D., & Riom, J. (1989). Factors affecting the spectral response of forest canopies: a review. *Geocarto International, 4*(3): 3-18.

Hall, F. G., Knapp, D. E., & Huemmrich, K. F. (1997). Physically based classification and satellite mapping of biophysical characteristics in the southern boreal forest. *Journal of Geophysical Research, 102*(D24): 29567-29580.

Hall, F. G., Peddle, D. R., & LeDrew, E. F. (1996). Remote sensing of biophysical variables in boreal forest stands of Picea mariana. *International Journal of Remote Sensing, 17*(15): 3077-3081.

Hall, R. J. (2003). The roles of aerial photographs in forestry remote sensing image analysis. In M. A. Wulder & S. E. Franklin (Eds.), *Remote sensing of forest environments: concepts and case studies*. Norwell, MA: Kluwer Academic Publishers. (pp. 47-76).

Hall, R. J., & Skakun, R. S. (2007, October 28 - November 1, 2007). *Mapping Forest Inventory Attributes Across Coniferous, Deciduous and Mixedwood Stand Types in the Northwest Territories from High Spatial Resolution QuickBird Satellite Imagery.* Proceedings of Our Common Borders - Safety, Security, and the Environment Through Remote Sensing. CRSS/ASPRS 2007 Specialty Conference, Ottawa, Ontario, Canada. (pp. 6).

Hall, R. J., Skakun, R. S., Filiatrault, M., Gartell, M., Arsenault, E., & Voicu, M. (2012). Project Progress Report - Multi-sensor Remote Sensing Data for Forest Inventory: Extending the Value of Satellite land Cover Maps. Natural Resources Canada, Canadian Forest Service, Northern Forestry Centre. Edmonton, AB. (pp. 1-135).

Harsanyi, J. C., & Chein, I. C. (1994). Hyperspectral image classification and dimensionality reduction: an orthogonal subspace projection approach. *Geoscience and Remote Sensing, IEEE Transactions on, 32*(4): 779-785.

Hart, S. A., & Chen, H. Y. H. (2006). Understory Vegetation Dynamics of North American Boreal Forests. *Critical Reviews in Plant Sciences, 25*(4): 381-397.

Hinzman, L., Bettez, N., Bolton, W., Chapin III, F. S., Dyurgerov, M., Fastie, C., Griffith, B., Hollister, R., Hope, A., Huntington, H., Jensen, A., Jia, G., Jorgenson, T., Kane, D., Klein, D., Kofinas, G., Lynch, A., Lloyd, A., McGuire, A., Nelson, F., Oechel, W., Osterkamp, T., Racine, C., Romanovsky, V., Stone, R., Stow, D., Sturm, M., Tweedie, C., Vourlitis, G., Walker, M., Walker, D., Webber, P., Welker, J., Winker, K., & Yoshikawa, K. (2005). Evidence and implications of recent climate change in northern Alaska and other Arctic regions. *Climatic Change, 72*(3): 251-298.

Hogg, E. H., Brandt, J. P., & Michaelian, M. (2008). Impacts of a regional drought on the productivity, dieback, and biomass of western Canadian aspen forests. *Canadian Journal of Forest Research, 38*(6): 1373-1384.

Hu, B., Miller, J. R., Zarco-Tejada, P., Freemantle, J., & Zwick, H. (2008). Boreal forest mapping at the BOREAS study area using seasonal optical indices sensitive to plant pigment content. *Canadian Journal of Remote Sensing, 34*(S1): S158-S171.

Jensen, J. R. (2007). *Remote sensing of the environment: an earth resource perspective*. Upper Saddle River, NJ: Pearson Prentice Hall. (592 p.).

Johnstone, J., & Chapin III, F. S. (2006). Fire interval effects on successional trajectory in boreal forests of northwest Canada. *Ecosystems, 9*(2): 268-277.

Johnstone, J. F., Rupp, T. S., Olson, M., & Verbyla, D. (2011). Modeling impacts of fire severity on successional trajectories and future fire behavior in Alaskan boreal forests. *Landscape Ecology, 26*(4): 487-500.

Jorgenson, M. T., & Osterkamp, T. E. (2005). Response of boreal ecosystems to varying modes of permafrost degradation. *Canadian Journal of Forest Research, 35*(9): 2100-2111.

Keith, H., Mackey, B. G., & Lindenmayer, D. B. (2009). Re-evaluation of forest biomass carbon stocks and lessons from the world's most carbon-dense forests. *Proceedings of the National Academy of Sciences, 106*(28): 11635-11640.

Kimmins, J. P. (2003). *Forest ecology: a foundation for sustainable forest management and environmental ethics in forestry* (3rd ed.). Upper Saddle River, N.J.: Prentice Hall. (720 p.).

Krawchuk, M. A., & Cumming, S. G. (2010). Effects of biotic feedback and harvest management on boreal forest fire activity under climate change. *Ecological Applications, 21*(1): 122-136.

Kurz, W., & Apps, M. (2006). Developing Canada's national forest carbon monitoring, accounting and reporting system to meet the reporting requirements of the Kyoto Protocol. *Mitigation and Adaptation Strategies for Global Change, 11*(1): 33-43.

Kurz, W. A., Shaw, C. H., Boisvenue, C., Stinson, G., Metsaranta, J., Leckie, D., Dyk, A., Smyth, C., & Neilson, E. T. (2013). Carbon in Canada's boreal forest — A synthesis1. *Environmental Reviews, 21*(4): 260-292.

Lambin, E. F. (1999). Monitoring Forest Degredation in Tropical Regions by Remote Sensing: Some Methodological Issues. *Global Ecology and Biogeography, 8*(3/4): 191-198.

Landis, J. R., & Koch, G. G. (1977). The Measurement of Observer Agreement for Categorical Data. *Biometrics, 33*(1): 159-174.

Leckie, D. G. (1998). Forestry applications using imaging radar. In F. M. Henderson & A. J. Lewis (Eds.), *Principles and applications of imaging radar*. 3 ed., Vol. 2. New York, NY: Wiley and Sons. (pp. 435-509).

Leckie, D. G., & Gillis, M. D. (1995). Forest inventory in Canada with emphasis on map production. *The Forestry Chronicle, 71*(1): 74-88.

Leckie, D. G., Gougeon, F. A., Walsworth, N., & Paradine, D. (2003). Stand delineation and composition estimation using semi-automated individual tree crown analysis. *Remote Sensing of Environment, 85*(3): 355-369.

Lemprière, T. C., Bernier, P. Y., Carroll, A. L., Flannigan, M. D., Gilsenan, R. P., McKenney, D. W., Hogg, E. H., Pedlar, J. H., & BLAIN, D. (2008). The importance of forest sector adaptation to climate change. Edmonton, A.B., Canada. (pp. 1-57).

Lemprière, T. C., Kurz, W. A., Hogg, E. H., Schmoll, C., Rampley, G. J., Yemshanov, D., McKenney, D. W., Gilsenan, R., Beatch, A., Blain, D., Bhatti, J. S., & Krcmar, E. (2013). Canadian boreal forests and climate change mitigation. *Environmental Reviews, 21*(4): 293-321.

Lillesand, M., & Kiefer, R. W. (1994). *Remote sensing and image interpretation* (3rd ed.). New York: Wiley and Sons Inc. (750 p.).

Lindenas, D. G. (1985). Specifications for the interpretation and mapping of aerial photographs in the forest inventory section. Saskatoon, SK, Canada. (pp. 1-42).

Luther, J. E., Fournier, R. A., Piercey, D. E., Guindon, L., & Hall, R. J. (2006). Biomass mapping using forest type and structure derived from Landsat TM imagery. *International Journal of Applied Earth Observation and Geoinformation, 8*(3): 173-187.

MacLean, D. A., & MacKinnon, W. E. (1997). Effects of stand and site characteristics on susceptibility and vulnerability of balsam fir and spruce to spruce budworm in New Brunswick. *Canadian Journal of Forest Research, 27*: 1859-1871.

Malhi, Y., Baldocchi, D. D., & Jarvis, P. G. (1999). The carbon balance of tropical, temperate and boreal forests. *Plant, Cell & Environment, 22*(6): 715-740.

Marceau, D. J., Howarth, P. J., & Gratton, D. J. (1994). Remote sensing and the measurement of geographical entities in a forested environment. 1. The scale and spatial aggregation problem. *Remote Sensing of Environment, 49*(2): 93-104.

Martin, M. E., Newman, S. D., Aber, J. D., & Congalton, R. G. (1998). Determining forest species composition using high spectral resolution remote sensing data. *Remote Sensing of Environment, 65*(3): 249-254.

McCoy, R. M. (2005). *Field methods in remote sensing*. New York: Guilford Press. (159 p.).

McKenney, D. W., Pedlar, J. H., Rood, R. B., & Price, D. (2011). Revisiting projected shifts in the climate envelopes of North American trees using updated general circulation models. *Global Change Biology, 17*(8): 2720-2730.

McRoberts, R. E., & Tomppo, E. O. (2007). Remote sensing support for national forest inventories. *Remote Sensing of Environment, 110*(4): 412-419.

Michaelian, M., Hogg, E. H., Hall, R. J., & Arsenault, E. (2011). Massive mortality of aspen following severe drought along the southern edge of the Canadian boreal forest. *Global Change Biology, 17*(6): 2084-2094.

Michalak, R., Kelatwang, S., Velazquez, A., Mas, J.-F., Palacio-Prieto, J. L., & Bocco, G. (2002). Forest inventory and assessment: country experiences and needs. Food and Agriculture Organization of the United Nations. FAO Corporate Document Repository. (pp.

Mickelson, J. G., Jr., Civco, D. L., & Silander, J. A., Jr. (1998). Delineating Forest Canopy Species in the Northeastern United States Using Multi-Temporal TM Imagery. *Photogrammetric Engineering & Remote Sensing, 64*(9): 891-904.

Miller, J. R., White, H. P., Chen, J. M., Peddle, D. R., McDermid, G., Fournier, R. A., Shepherd, P., Rubinstein, I., Freemantle, J., Soffer, R., & LeDrew, E. (1997). Seasonal change in understory

reflectance of boreal forests and influence on canopy vegetation indices. *Journal of Geophysical Research: Atmospheres, 102*(D24): 29475-29482.

Mora, B., Wulder, M. A., & White, J. C. (2010). Identifying leading species using tree crown metrics derived from very high spatial resolution imagery in a boreal forest environment. *Canadian Journal of Remote Sensing, 36*(4): 332-344.

Mora, B., Wulder, M. A., & White, J. C. (2012). An approach using Dempster-Shafer theory to fuse spatial data and satellite image derived crown metrics for estimation of forest stand leading species. *Information Fusion, 14*(4): 384-395.

Naesset, E. (1997). Determination of mean tree height of forest stands using airborne laser scanner data. *ISPRS Journal of Photogrammetry and Remote Sensing, 52*: 49 - 56.

Nascimento, J. M. P., & Bioucas Dias, J. M. (2005). Vertex component analysis: a fast algorithm to unmix hyperspectral data. *Geoscience and Remote Sensing, IEEE Transactions on, 43*(4): 898-910.

Natural Resources Canada. (2013). The State of Canada's Forests: Annual Report 2013. Canadian Forest Service. Ottawa, Ontario. (pp. 56).

Neville, R. A., Staenz, K., Szeredi, T., Lefebvre, J., & Hauff, P. (1999). *Automatic endmember extraction from hyperspectral data for mineral exploration.* Proceedings of 21st Canadian Symposium on Remote Sensing, Ottawa, ON. (pp. 21-24).

Pan, Y., Birdsey, R. A., Fang, J., Houghton, R., Kauppi, P. E., Kurz, W. A., Phillips, O. L., Shvidenko, A., Lewis, S. L., Canadell, J. G., Ciais, P., Jackson, R. B., Pacala, S. W., McGuire, A. D., Piao, S., Rautiainen, A., Sitch, S., & Hayes, D. (2011). A large and persistent carbon sink in the world's forests. *Science, 333*(6045): 988-993.

Peddle, D. R. (1998). *Field spectroradiometer data acquisition and processing for spectral mixture analysis in forestry and agriculture.* Proceedings of International Conference on Geospatial Information in Agriculture and Forestry, Lake Buena Vista, Florida, USA. (pp. 645-652).

Peddle, D. R., & Franklin, S. E. (1991). Image Texture Processing and Data Integration for Surface Pattern Discrimination. *Photogrammetric Engineering & Remote Sensing, 57*(4): 413-420.

Peddle, D. R., Hall, F. G., & LeDrew, E. F. (1999). Spectral mixture analysis and geometric-optical reflectance modeling of boreal forest biophysical structure. *Remote Sensing of Environment, 67*(3): 288-297.

Peddle, D. R., Johnson, R. L., Cihlar, J., & Latifovic, R. (2004). Large area forest classification and biophysical parameter estimation using the 5-Scale canopy reflectance model in Multiple-Forward-Mode. *Remote Sensing of Environment, 89*(2): 252-263.

Peddle, D. R., Johnson, R. L., Cihlar, J., Leblanc, S. G., Chen, J. M., & Hall, F. G. (2007). Physically based inversion modeling for unsupervised cluster labeling, independent forest classification, and LAI estimation using MFM-5-Scale. *Canadian Journal of Remote Sensing, 33*(3): 214-225.

Peddle, D. R., & Smith, A. M. (2005). Spectral mixture analysis of agricultural crops: Endmember validation and biophysical estimation in potato plots. *International Journal of Remote Sensing, 26*(22): 4959-4979.

Peddle, D. R., White, H. P., Soffer, R. J., Miller, J. R., & LeDrew, E. F. (2001). Reflectance processing of remote sensing spectroradiometer data. *Computers & Geosciences, 27*: 203-213.

Peng, C., Ma, Z., Lei, X., Zhu, Q., Chen, H., Wang, W., Liu, S., Li, W., Fang, X., & Zhou, X. (2011). A drought-induced pervasive increase in tree mortality across Canada's boreal forests. *Nature Climate Change, 1*(9): 467-471.

Plaza, J., Hendrix, E. T., García, I., Martín, G., & Plaza, A. (2012). On Endmember Identification in Hyperspectral Images Without Pure Pixels: A Comparison of Algorithms. *Journal of Mathematical Imaging and Vision, 42*(2-3): 163-175.

Plourde, L. C., Ollinger, S. V., Smith, M., & Martin, M. E. (2007). Estimating species abundance in a northern temperate forest using spectral mixture analysis. *Photogrammetric Engineering & Remote Sensing, 73*(7): 829-840.

Pontius, J., Hallett, R., & Martin, M. (2005). Using AVIRIS to assess hemlock abundance and early decline in the Catskills, New York. *Remote Sensing of Environment, 97*(2): 163-173.

Power, K., & Gillis, M. D. (2006). Canada's Forest Inventory 2001. Natural Resources Canada, Canadian Forest Service, Pacific Forestry Centre. Victoria, BC. (pp. 140).

Prescott, C. E. (2002). The influence of the forest canopy on nutrient cycling. *Tree Physiology, 22*(15-16): 1193-1200.

Price, D. T., Alfaro, R. I., Brown, K. J., Flannigan, M. D., Fleming, R. A., Hogg, E. H., Girardin, M. P., Lakusta, T., Johnston, M., McKenney, D. W., Pedlar, J. H., Stratton, T., Sturrock, R. N., Thompson, I. D., Trofymow, J. A., & Venier, L. A. (2013). Anticipating the consequences of climate change for Canada's boreal forest ecosystems. *Environmental Reviews, 21*(4): 322-365.

Quackenbush, L. J., Hopkins, P. F., & Kinn, G. J. (2000). Developing forestry products from high resolution digital aerial imagery. *Photogrammetric Engineering & Remote Sensing, 66*(11): 1337-1346.

Quintano, C., Fernández-Manso, A., Shimabukuro, Y. E., & Pereira, G. (2012). Spectral unmixing. *International Journal of Remote Sensing, 33*(17): 5307-5340.

Rees, G., Brown, I., Mikkola, K., Virtanen, T., & Werkman, B. (2002). How can the dynamics of the tundra-taiga boundary be remotely monitored? *Ambio*: 56-62.

Roberts, D. A., Dennison, P. E., Gardner, M. E., Hetzel, Y., Ustin, S. L., & Lee, C. T. (2003). Evaluation of the potential of Hyperion for fire danger assessment by comparison to the Airborne Visible/Infrared Imaging Spectrometer. *Geoscience and Remote Sensing, IEEE Transactions on, 41*(6): 1297-1310.

Roberts, D. A., Gamon, J. A., Keightley, K., Prentiss, K., Reith, E., & Green, R. (1999). *AVIRIS land-surface mapping in support of the BOReal Ecosystem-Atmosphere Study (BOREAS).* Proceedings of Proceedings of the 8th AVIRIS Earth Science Workshop, Pasadena, CA. (pp. 355-364).

Roberts, D. A., Gardner, M., Church, R., Ustin, S., Scheer, G., & Green, R. O. (1998). Mapping chaparral in the Santa Monica Mountains using multiple endmember spectral mixture models. *Remote Sensing of Environment, 65*(3): 267-279.

Roberts, D. A., Halligan, K., & Dennison, P. (2007). VIPER Tools user manual - version 1.5. (pp. 1-91).

Roberts, D. A., Ustin, S. L., Ogunjemiyo, S., Greenberg, J., Dobrowski, S. Z., Chen, J., & Hinckley, T. M. (2004). Spectral and structural measures of northwest forest vegetation at leaf to landscape scales. *Ecosystems, 7*(5): 545-562.

Ross, M. S., Flanagan, L. B., & Roi, G. H. L. (1986). Seasonal and successional changes in light quality and quantity in the understory of boreal forest ecosystems. *Canadian Journal of Botany, 64*(11): 2792-2799.

Safranyik, L., Carroll, A. L., Régnière, J., Langor, D. W., Riel, W. G., Shore, T. L., Peter, B., Cooke, B. J., Nealis, V. G., & Taylor, S. W. (2010). Potential for range expansion of mountain pine beetle into the boreal forest of North America. *The Canadian Entomologist, 142*(5): 415-442.

Sandmeier, S., & Deering, D. W. (1999). Structure analysis and classification of boreal forests using airborne hyperspectral BRDF data from ASAS. *Remote Sensing of Environment, 69*(3): 281-295.

Sandvoss, M., McClymont, B., & Farnden, C. (2005). User's guide to the vegetation resources inventory. (pp. 1-73).

Saskatchewan Environment. (2004). Saskatchewan forest vegetation inventory, forest planning manual, version 4.0. Saskatoon, SK, Canada. (pp. 1-82).

Schaaf, A. N., Dennison, P. E., Fryer, G. K., Roth, K. L., & Roberts, D. A. (2011). Mapping Plant Functional Types at Multiple Spatial Resolutions Using Imaging Spectrometer Data. *GIScience & Remote Sensing, 48*(3): 324-344.

Schriever, J. R., & Congalton, R. G. (1995). Evaluating Seasonal Variability as an Aid to Cover-type Mapping from Landsat Thematic Mapper Data in the Northeast. *Photogrammetric Engineering & Remote Sensing, 61*(3): 321-327.

Shang, J., Neville, R., Staenz, K., Sun, L., Morris, B., & Howarth, P. (2008). Comparison of fully constrained and weakly constrained unmixing through mine-tailing composition mapping. *Canadian Journal of Remote Sensing, 34*: S92-S109.

Shippert, P. (2004). Why use hyperspectral imagery? *Photogrammetric Engineering & Remote Sensing, 70*: 377-380.

Smith, D. M. (1986). *The practise of silviculture* (8th ed.). New York, NY: John Wiley & Sons, Inc. (527 p.).

Smith, L. (2002). Forest resource inventory and analysis strategic plan - draft. Hay River, NWT. (pp. 1-43).

Smith, M. O., Ustin, S. L., Adams, J. B., & Gillespie, A. R. (1990). Vegetation in deserts: I. A regional measure of abundance from multispectral images. *Remote Sensing of Environment, 31*(1): 1-26.

Smith, S. L. (2011). Trends in permafrost conditions and ecology in northern Canada. (pp. 22).

Somers, B., & Asner, G. P. (2012). Invasive Species Mapping in Hawaiian Rainforests Using Multi-Temporal Hyperion Spaceborne Imaging Spectroscopy. *IEEE Journal of Selected Topics in Applied Earth Observations and Remote Sensing, 6*(2): 351-359.

Somers, B., Cools, K., Delalieux, S., Stuckens, J., Van der Zande, D., Verstraeten, W. W., & Coppin, P. (2009a). Nonlinear Hyperspectral Mixture Analysis for tree cover estimates in orchards. *Remote Sensing of Environment, 113*(6): 1183-1193.

Somers, B., Delalieux, S., Stuckens, J., Verstraeten, W. W., & Coppin, P. (2009b). A weighted linear spectral mixture analysis approach to address endmember variability in agricultural production systems. *Int. J. Remote Sens., 30*(1): 139-147.

Song, S., & Woodcock, C. E. (2003). Monitoring forest succession with multitemporal Landsat images: factors of uncertainty. *Geoscience and Remote Sensing, IEEE Transactions on, 41*(11): 2557-2567.

Sonnentag, O., Chen, J. M., Roberts, D. A., Talbot, J., Halligan, K. Q., & Govind, A. (2007). Mapping tree and shrub leaf area indices in an ombrotrophic peatland through multiple endmember spectral unmixing. *Remote Sensing of Environment, 109*(3): 342-360.

Spanner, M. A., Pierce, L. L., Peterson, D. L., & Running, S. W. (1990). Remote sensing of temperate coniferous forest leaf area index. The influence of canopy closure, understory vegetation and background reflectance. *International Journal of Remote Sensing, 11*(1): 95-111.

Spies, T. A. (1997). Forest stand structure, composition, and function. In K. A. Kohm & J. F. Franklin (Eds.), *Creating a forestry for the 21st Century, the science of ecosystem management*. Washington, DC: Island Press. (pp. 11-30).

Staenz, K., & Held, A. (2012, 22-27 July 2012). *Summary of current and future terrestrial civilian hyperspectral spaceborne systems.* Proceedings of Geoscience and Remote Sensing Symposium (IGARSS), 2012 IEEE International. (pp. 123-126).

Tang, G., Beckage, B., Smith, B., & Miller, P. A. (2010). Estimating potential forest NPP, biomass and their climatic sensitivity in New England using a dynamic ecosystem model. *Ecosphere, 1*(6): 1-20.

Thompson, I. D., Maher, S. C., Rouillard, D. P., Fryxell, J. M., & Baker, J. A. (2007). Accuracy of forest inventory mapping: Some implications for boreal forest management. *Forest Ecology and Management, 252*: 208-221.

Thorp, K. R., French, A. N., & Rango, A. (2013). Effect of image spatial and spectral characteristics on mapping semi-arid rangeland vegetation using multiple endmember spectral mixture analysis (MESMA). *Remote Sensing of Environment, 132*: 120-130.

Tompkins, S., Mustard, J. F., Pieters, C. M., & Forsyth, D. W. (1997). Optimization of Endmembers for Spectral Mixture Analysis. *Remote Sensing of Environment, 59*: 472-489.

Tomppo, E. O., Gschwantner, T., Lawrence, M., & McRoberts, R. E. (2010). *National Forest Inventories pathways for common reporting*. New York, U.S.A: Springer. (612 p.).

Treitz, P. M., & Howarth, P. J. (1999). Hyperspectral remote sensing for estimating biophysical parameters of forest ecosystems. *Progress in Physical Geography, 23*(3): 359-390.

Trumper, K. (2009). The natural fix? The role of ecosystems in climate mitigation: a UNEP rapid response assessment. Cambridge, U.K. (pp. 1-65).

Turner, W., Spector, S., Gardiner, N., Fladeland, M., Sterling, E., & Steininger, M. (2003). Remote sensing for biodiversity science and conservation. *Trends in Ecology and Evolution, 18*(6): 306-314.

United States Geological Service. (2013). Landsat 5 History, from http://landsat.usgs.gov/about_landsat5.php

Ustin, S. L., & Xiao, Q. F. (2001). Mapping successional boreal forests in interior central Alaska. *International Journal of Remote Sensing, 22*(6): 1779-1797.

van Aardt, J. A. N., & Wynne, R. H. (2007). Examining pine spectral separability using hyperspectral data from an airborne sensor: An extension of field-based results. *International Journal of Remote Sensing, 28*(2): 431-436.

Walker, X., Henry, G. H. R., McLeod, K., & Hofgaard, A. (2012). Reproduction and seedling establishment of Picea glauca across the northernmost forest-tundra region in Canada. *Global Change Biology, 18*(10): 3202-3211.

Weber, M. G., & Van Cleve, K. (2005). The boreal forests of North America. In F. Anderson (Ed.), *6 - Coniferous forests*. Amsterdam, The Netherlands: Elsevier B.V. (pp. 101-130).

Westfall, J., & Ebata, T. (2011). 2011 Summary of forest health conditions in British Columbia. (pp. 1-88).

Williamson, T., Colombo, S., Duinker, P., Gray, P., Hennessey, R., Houle, D., Johnston, M., Ogden, A., & Spittlehouse, D. (2009). Climate change and Canada's forests: from impacts to adaptation. Edmonton, A.B., Canada. (pp. 1-104).

Wilson, B. A., Ow, C. F. Y., Heathcott, M., Milne, D., McCaffrey, T. M., Ghitter, G., & Franklin, S. E. (1994). Landsat MSS Classification of Fire Fuel Types in Wood Buffalo National Park, Northern Canada. *Global Ecology and Biogeography Letters, 4*(2): 33-39.

Winter, M. E. (1999). *N-FINDR: an algorithm for fast autonomous spectral end-member determination in hyperspectral data.* Proceedings of SPIE 3753, Image Spectronomy V Conference, Denver, CO. (pp. 266-275).

Wolf, P. R., & DeWitt, B. A. (2000). *Elements of photogrammetry: with applications in GIS*. Boston, MA: McGraw-Hill. (624 p.).

Wolter, P., Townsend, P., Sturtevant, B., & Kingdon, C. (2008). Remote sensing of the distribution and abundance of host species for spruce budworm in Northern Minnesota and Ontario. *Remote Sensing of Environment, 112*(10): 3971-3982.

Wolter, P. T., Mladenoff, D. J., Host, G. E., & Crow, T. R. (1995). Improved forest classification in the Northern Lake States using multi-temporal Landsat imagery. *Photogrammetric Engineering & Remote Sensing, 61*(9): 1129-1143.

Wolter, P. T., & Townsend, P. A. (2011). Multi-sensor data fusion for estimating forest species composition and abundance in northern Minnesota. *Remote Sensing of Environment, 115*(2): 671-691.

Wulder, M., Niemann, K. O., & Goodenough, D. G. (2000). Local maximum filtering for the extraction of tree locations and basal area from high spatial resolution imagery. *Remote Sensing of Environment, 73*(1): 103-114.

Wulder, M. A., White, J. C., Cranny, M., Hall, R. J., Luther, J. E., Beaudoin, A., Goodenough, D. G., & Dechka, J. A. (2008). Monitoring Canada's forests. Part 1: Completion of the EOSD land cover project. *Canadian Journal of Remote Sensing, 34*(6): 549-562.

Youngentob, K. N., Roberts, D. A., Held, A. A., Dennison, P. E., Jia, X., & Lindenmayer, D. B. (2011). Mapping two Eucalyptus subgenera using multiple endmember spectral mixture analysis and continuum-removed imaging spectrometry data. *Remote Sensing of Environment, 115*(5): 1115-1128.

Zhou, L., Tucker, C. J., Kaufmann, R. K., Slayback, D., Shabanov, N. V., & Myneni, R. B. (2001). Variations in northern vegetation activity inferred from satellite data of vegetation index during 1981 to 1999. *Journal of Geophysical Research: Atmospheres, 106*(D17): 20069-20083.

APPENDICES

Appendix 1: Contingency matrices Chapter 4

Appendix 2: Contingency matrices Chapter 5 (July imagery)

Appendix 3: Contingency matrices Chapter 5 (Multi-temporal imagery)

APPENDIX 1: Contingency matrices Chapter 4

Ocular AVI-Call indicator used as ground-reference data.

Single spectral library

	Ground reference (# of stands)				
Map prediction	Aspen	Jack pine	Black spruce	White spruce	Total
Unclassified	0	0	0	0	0
Aspen	**0**	0	0	0	0
Jack pine	0	**8**	2	3	13
Black spruce	0	9	**2**	3	14
White spruce	0	8	5	**3**	16
Total	0	25	9	9	**43**
Overall accuracy = (13/43) 30 %					
Kappa = -0.03					

Integrated spectral library

	Ground reference (# of stands)				
Map prediction	Aspen	Jack pine	Black spruce	White spruce	Total
Unclassified	0	0	0	0	0
Aspen	**0**	0	0	0	0
Jack pine	0	**11**	1	4	16
Black spruce	0	8	**4**	6	18
White spruce	0	7	2	**1**	10
Total	0	26	7	11	**44**
Overall accuracy = (16/44) 36 %					
Kappa = 0.04					

Weighted spectral library

	Ground reference (# of stands)				
Map prediction	Aspen	Jack pine	Black spruce	White spruce	Total
Unclassified	0	0	0	0	0
Aspen	**0**	0	0	0	0
Jack pine	0	**10**	1	3	14
Black spruce	0	7	**4**	1	12
White spruce	0	9	5	**5**	19
Total	0	26	10	9	**45**
Overall accuracy = (19/45) 42 %					
Kappa = 0.15					

Note: the number of total plots used in the determination of classification accuracy was dependent on the number of species included in the reference dataset. If a species was not included in the reference dataset (e.g. aspen) but was labelled in the classification image, ENVI 4.8 Contingency matrix function only assessed the plots that belong to the species instead of assessing the mis-labelled plots as "Unclassified". The accuracies posted in Chapter 4 were adjusted accordingly and were based on a 48 plot sample size. This appendix reflects the original accuracies.

All trees indicator used as ground-reference data.

Single spectral library

	Ground reference (# of stands)				
Map prediction	Aspen	Jack pine	Black spruce	White spruce	Total
Unclassified	0	0	0	0	0
Aspen	**1**	2	1	1	5
Jack pine	0	**6**	5	2	13
Black spruce	0	6	**5**	3	14
White spruce	0	5	6	**5**	16
Total	1	19	17	11	**48**
Overall accuracy = (17/48) 35 %					
Kappa = 0.09					

Integrated spectral library

	Ground reference (# of stands)				
Map prediction	Aspen	Jack pine	Black spruce	White spruce	Total
Unclassified	0	0	0	0	0
Aspen	**0**	0	3	1	4
Jack pine	1	**6**	7	2	16
Black spruce	0	7	**4**	7	18
White spruce	0	6	3	**1**	10
Total	1	19	17	11	**48**
Overall accuracy = (11/48) 23 %					
Kappa = -0.12					

Weighted spectral library

	Ground reference (# of stands)				
Map prediction	Aspen	Jack pine	Black spruce	White spruce	Total
Unclassified	0	0	0	0	0
Aspen	**0**	2	0	1	3
Jack pine	1	**4**	7	2	14
Black spruce	0	6	**5**	1	12
White spruce	0	7	5	**7**	19
Total	1	19	17	11	**48**
Overall accuracy = (16/48) 33 %					
Kappa = 0.05					

Dominant/Co-dominant indicator used as ground-reference data.

Single spectral library

	Ground reference (# of stands)				
Map prediction	Aspen	Jack pine	Black spruce	White spruce	Total
Unclassified	0	0	0	0	0
Aspen	**1**	2	2	0	5
Jack pine	0	**10**	1	2	13
Black spruce	0	6	**6**	4	16
White spruce	0	8	3	**3**	14
Total	1	26	12	9	**48**
Overall accuracy = (20/48) 42 %					
Kappa = 0.18					

Integrated spectral library

	Ground reference (# of stands)				
Map prediction	Aspen	Jack pine	Black spruce	White spruce	Total
Unclassified	0	0	0	0	0
Aspen	**0**	1	1	2	4
Jack pine	1	**10**	1	4	16
Black spruce	0	7	**3**	0	10
White spruce	0	8	7	**3**	18
Total	1	26	12	9	**48**
Overall accuracy = (16/48) 33 %					
Kappa = 0.04					

Weighted spectral library

	Ground reference (# of stands)				
Map prediction	Aspen	Jack pine	Black spruce	White spruce	Total
Unclassified	0	0	0	0	0
Aspen	**0**	2	0	1	3
Jack pine	1	**11**	1	1	14
Black spruce	0	6	**5**	1	12
White spruce	0	7	3	**9**	19
Total	1	26	9	12	**48**
Overall accuracy = (25/48) 52 %					
Kappa = 0.31					

GNWT Photo indicator used as ground-reference data.

Single spectral library

	Ground reference (# of stands)				
Map prediction	Aspen	Jack pine	Black spruce	White spruce	Total
Unclassified	0	0	0	0	0
Aspen	**0**	0	0	0	0
Jack pine	0	**3**	7	2	12
Black spruce	0	4	**7**	2	13
White spruce	0	3	10	**2**	15
Total	0	10	24	6	**40**
Overall accuracy = (12/40) 30 %					
Kappa = -0.04					

Integrated spectral library

	Ground reference (# of stands)				
Map prediction	Aspen	Jack pine	Black spruce	White spruce	Total
Unclassified	0	0	0	0	0
Aspen	**0**	0	0	0	0
Jack pine	0	**2**	11	1	14
Black spruce	0	7	**5**	5	17
White spruce	0	2	7	**0**	9
Total	0	11	23	6	**40**
Overall accuracy = (7/40) 17.5 %					
Kappa = -0.32					

Weighted spectral library

	Ground reference (# of stands)				
Map prediction	Aspen	Jack pine	Black spruce	White spruce	Total
Unclassified	0	0	0	0	0
Aspen	**0**	0	0	0	0
Jack pine	0	**2**	10	1	13
Black spruce	0	2	**9**	0	11
White spruce	0	6	7	**4**	17
Total	0	10	26	5	**41**
Overall accuracy = (15/41) 37 %					
Kappa = 0.10					

APPENDIX 2: Contingency matrices Chapter 5 (July imagery)

Basalarea sunlit canopy library + PurestBg background library

	Ground reference (# of stands)				
Map prediction	Aspen	Jack pine	Black spruce	White spruce	Total
Unclassified	0	0	0	0	0
Aspen	**1**	1	2	1	5
Jack pine	0	**9**	2	1	12
Black spruce	0	16	**8**	2	26
White spruce	0	0	0	**5**	5
Total	0	26	12	9	**48**
Overall accuracy = (23/48) 48 %					
Kappa = 0.26					

Basalarea sunlit canopy library + LowestCC background library

	Ground reference (# of stands)				
Map prediction	Aspen	Jack pine	Black spruce	White spruce	Total
Unclassified	0	0	0	0	0
Aspen	**1**	1	3	1	6
Jack pine	0	**14**	3	3	20
Black spruce	0	5	**6**	1	12
White spruce	0	6	0	**4**	10
Total	1	26	12	9	**48**
Overall accuracy = (25/48) 52 %					
Kappa = 0.29					

HighestCC sunlit canopy library + PurestBg background library

	Ground reference (# of stands)				
Map prediction	Aspen	Jack pine	Black spruce	White spruce	Total
Unclassified	0	0	0	0	0
Aspen	**1**	0	1	0	2
Jack pine	0	**5**	1	0	6
Black spruce	0	14	**9**	3	26
White spruce	0	7	1	**6**	14
Total	1	26	12	9	**48**
Overall accuracy = (21/48) 44 %					
Kappa = 0.24					

HighestCC sunlit canopy library + LowestCC background library

	Ground reference (# of stands)				
Map prediction	Aspen	Jack pine	Black spruce	White spruce	Total
Unclassified	0	0	0	0	0
Aspen	**1**	0	1	0	2
Jack pine	0	**9**	2	2	13
Black spruce	0	4	**8**	2	14
White spruce	0	13	1	**5**	19
Total	1	26	12	9	**48**
Overall accuracy = (23/48) 48 %					
Kappa = 0.26					

APPENDIX 3: Contingency matrices Chapter 5 (Multi-temporal imagery)

Basalarea sunlit canopy library + PurestBg background library

	Ground reference (# of stands)				
Map prediction	Aspen	Jack pine	Black spruce	White spruce	Total
Unclassified	0	0	0	0	0
Aspen	**1**	0	1	0	2
Jack pine	0	**20**	1	2	23
Black spruce	0	1	**10**	0	11
White spruce	0	5	0	**7**	12
Total	1	26	12	9	**48**
Overall accuracy = (38/48) 79 %					
Kappa = 0.67					

Basalarea sunlit canopy library + LowestCC background library

	Ground reference (# of stands)				
Map prediction	Aspen	Jack pine	Black spruce	White spruce	Total
Unclassified	0	0	0	0	0
Aspen	**1**	0	3	0	4
Jack pine	0	**16**	1	2	19
Black spruce	0	5	**8**	0	13
White spruce	0	5	0	**7**	12
Total	1	26	12	9	**48**
Overall accuracy = (32/48) 67 %					
Kappa = 0.50					

HighestCC sunlit canopy library + PurestBg background library

	Ground reference (# of stands)				
Map prediction	Aspen	Jack pine	Black spruce	White spruce	Total
Unclassified	0	0	0	0	0
Aspen	**1**	0	0	0	1
Jack pine	0	**17**	4	2	23
Black spruce	0	2	**7**	0	9
White spruce	0	7	1	**7**	15
Total	1	26	12	9	**48**
Overall accuracy = (32/48) 67 %					
Kappa = 0.48					

HighestCC sunlit canopy library + LowestCC background library

	Ground reference (# of stands)				
Map prediction	Aspen	Jack pine	Black spruce	White spruce	Total
Unclassified	0	0	0	0	0
Aspen	**1**	0	3	2	6
Jack pine	0	**12**	1	2	15
Black spruce	0	5	**7**	0	12
White spruce	0	9	1	**5**	15
Total	1	26	12	9	**48**
Overall accuracy = (25/48) 52 %					
Kappa = 0.32					